# NOTE TO USERS

UNIVERSITY OF CALIFORNIA

Los Angeles

# Distributed and Predictive Control of Nonlinear Distributed Process Systems

A dissertation submitted in partial satisfaction of the

requirements for the degree Doctor of Philosophy

in Chemical Engineering

by

Stevan Dubljevic

2005

The dissertation of Stevan Dubljevic is approved.

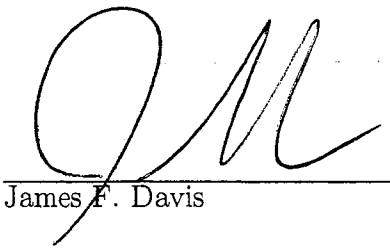

James F. Davis

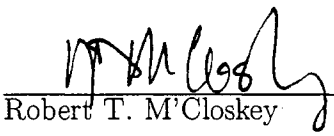

Robert T. M'Closkey

Gerassimos Orkoulas

Panagiotis D. Christofides, Committee Chair

University of California, Los Angeles

2005

# Contents

# List of Figures

## ACKNOWLEDGEMENTS

I would like to thank Dr. Panagiotis Christofides, chair of my graduate committee, for conceiving my project and giving the encouragement during the days of hardship. His support as friend always will be appreciated.

I would like to thank Professor James Davis, Professor Robert T. M'Closkey and Professor Gerassimos Orkoulas for agreeing to serve on my thesis committee and Professor Vasilios Manousiouthakis for giving me opportunity to be the part of graduate program at UCLA.

I would like to thank Dan Shi, Yiming Lou and Vladan Jankovic for bering with me through the days of hardship.

Financial support from NSF, CTS-0129571 and (ITR) CTS-0325246 is gratefully acknowledged.

Finally, I would like to express my gratitude to my parents, for their patients, understanding and love.

# VITA

1997 Bachelor, Chemical Engineering (with honors)
Belgrade University, Belgrade, Serbia

2001 M. S. , Chemical Engineering
Texas A&M University, College Station, TX

2001 present Ph.D student, Chemical Engineering
University of California, Los Angeles, CA

## Publications & Presentations

- Dubljevic, S., P. Mhaskar, N. H. El-Farra and P. D. Christofides, Predictive Control of Transport-Reaction Processes, *Comp. & Chem. Eng.*, in press, 2005.
- Dubljevic, S., P. Mhaskar, N. H. El-Farra and P. D. Christofides, Predictive Control of Parabolic PDEs with State and Control Constraints, *IEEE Trans. Automat. Contr.*, provisionally accepted, 2004.
- Dubljevic, S., P. D. Christofides and I. G. Kevrekidis, Distributed Nonlinear Control of Diffusion-Reaction Processes, *International Journal of Robust and Nonlinear Control*, **14**: 133 – 156, 2004.
- Dubljevic, S. and N. Kazantzis, A New Lyapunov Design Approach for Nonlinear Systems Based on Zubov's Method, *Automatica*, **38**:, 1999 – 2007, 2002.

Referred Conference Proceedings Papers:

- Dubljevic, S., P. Mhaskar, N. H. El-Farra and P. D. Christofides, Predictive Control of Diffusion-Reaction Processes, *Proceedings of American Control Conference*, to appear, Portland, Oregon, 2005.

- Dubljevic, S., P. D. Christofides and I. G. Kevrekidis, Distributed Nonlinear Control of Diffusion-Reaction Processes, *Proceedings of American Control Conference*, 1341 – 1348, Denver, Colorado, 2003.

- Armaou, A., S. Dubljevic and P. D. Christofides, Computation of Empirical Eigenfunctions and Order Reduction for Control of Parabolic PDEs with Time-Dependent Spatial Domains, *Proceedings of American Control Conference*, 2089 – 2096, Denver, Colorado, 2003.

- Kazantzis, N. and S. Dubljevic, Nonlinear Discrete-Time State Feedback Regulators with Assignable Closed-Loop Dynamics, *Proceedings of American Control Conference*, 3177 – 3182, Arlington, Virginia, 2001.

## ABSTRACT OF THE DISSERTATION

Distributed and Predictive Control of Nonlinear Distributed Process Systems

by

Stevan Dubljevic

Doctor of Philosophy in Chemical Engineering

University of California, Los Angeles, 2005

Professor Panagiotis D. Christofides, Chair

Key technological needs in growth areas such as semiconductor manufacturing, nanotechnology and biotechnology have motivated extensive research on the analysis and control of complex nonlinear distributed processes. Examples include temperature profile control in the Czochralski crystallization of high-purity crystals, deposition uniformity control in the chemical vapor deposition of thin films, as well as control of size distribution in the crystallization of proteins and the aerosol-based production of nanoparticles. From a control point of view, the distinguishing feature of complex distributed processes is that they give rise to nonlinear control problems that involve the regulation of highly distributed control variables by using spatially-distributed control actuators and measurement sensors. Thus, complex distributed processes cannot be effectively controlled with control methods which assume that the state, manipulated and to-be-controlled variables exhibit lumped behavior or with linear control algorithms derived on the basis of linear/linearized distributed models.

Motivated by these considerations, over the last decade, research has led to the development of a general framework for the synthesis of practically implementable nonlinear feedback controllers for complex distributed processes based on fundamental models that

accurately predict their behavior. However, the developed control methods do not address two important issues: a) the availability of actuation and sensing technologies which make possible the use of large numbers of actuators and sensors to control spatially distributed processes, and b) the direct incorporation of state variables and manipulated input constraints in the controller design.

Motivated by the possibility of using finely spatially distributed actuation/sensing, the first part of this thesis addresses the extension of the traditional control formulation for spatially-distributed processes to an 'infinite sensing' - 'infinite actuation' formulation. Under the assumption that the target complex spatio-temporal behavior is described by a "target nonlinear partial differential equation (PDE)", combination of Galerkin's method and nonlinear control techniques is used to design nonlinear state and static output feedback controllers that enforce the desired behavior in the closed-loop system. In the second part of the thesis, we focus on the development and application of predictive-based strategies for control of PDE systems, modeling transport-reaction processes, with state variable and manipulated input constraints. Both parabolic and hyperbolic PDE systems are considered. Throughout the thesis, we use numerous examples to illustrate the application and demonstrate the advantages of the new control methods.

# Chapter 1

# Introduction

Key technological needs in growth areas such as semiconductor manufacturing, nanotechnology, biotechnology and unmanned aerial vehicles have motivated extensive research on the analysis and control of complex nonlinear distributed processes. Examples include temperature profile control in the Czochralski crystallization of high-purity crystals, deposition uniformity control in the chemical vapor deposition of thin films, aerodynamic flow control for drag reduction and delay of separation, as well as control of size distribution in the crystallization of proteins and the aerosol-based production of nanoparticles. From a control point of view, the distinguishing feature of complex distributed processes is that they give rise to nonlinear control problems that involve the regulation of highly distributed control variables by using spatially-distributed control actuators and measurement sensors. Thus, complex distributed processes cannot be effectively controlled with control methods which assume that the state, manipulated and to-be-controlled variables exhibit lumped behavior or with linear control algorithms derived on the basis of linear/linearized distributed models.

Motivated by these trends, over the last decade, research has led to the development of a general framework for the synthesis of practically implementable nonlinear feedback controllers for complex distributed processes based on fundamental models that accurately predict their behavior. An important class of distributed parameter systems that

has received significant attention is parabolic PDE systems that arise naturally in the modelling of transport-reaction processes. Such systems exhibit significant spatial variations owing to the underlying diffusive and convective phenomena. The main feature of parabolic PDEs involve spatial differential operators whose spectrum can be partitioned into a finite (possibly unstable) slow part and an infinite stable fast complement. Therefore, the traditional approach to the control of parabolic PDEs involves the application of spatial discretization techniques (predominantly Galerkin's method) to the PDE system to derive large systems of ordinary differential equations (ODEs) that accurately describe the dynamics of the dominant (slow) modes of the PDE system. These are subsequently used as the basis for the synthesis of finite-dimensional controllers (e.g., [8, 50, 18]). A potential drawback of this approach is that the number of modes that should be retained to derive an ODE system that yields the desired degree of approximation may be very large, leading to complex controller design and high dimensionality of the resulting controllers (e.g., [9, 1]).

Motivated by this, recent work has focused on the synthesis of linear and nonlinear low-order controllers on the basis of ODE models obtained through Galerkin's method with data-based construction of the basis functions (empirical eigenfunctions) and combination of Galerkin's method with techniques for the construction of approximate inertial manifolds ( [9, 16, 53, 7, 4] and the recent book [14] for results in this area and references). The low-order models obtained through the Galerkin's method that is based on the Karhunen-Loeve decomposition is novel technique of obtaining the empirical eigenfunctions from the experimental or numerical simulation data of a system [32]. By employing empirical eigenfunctions as basis functions in a Galerkin's procedure, one can significantly decreased the large function space to the smallest linear subspace that is sufficient to describe the observed phenomena, and appropriately reduce the large set of ODE's to the finite small set of ODE's which describe the phenomena with desired degree of accuracy. The concept of inertial manifold (IM) has provided a natural framework for addressing this problem [58]. The IM is an appropriate tool for model reduction because if the tra-

jectories of the PDE system are on the IM, then this system is exactly described by a low-order ODE system (called inertial form). Unfortunately, even for PDE systems for which an IM is known to exist, the computation of the closed-form expression of the IM (and therefore the derivation of the corresponding inertial form) is a formidable task. Motivated by this, a novel procedure based on singular perturbations was proposed in [16] for the construction of approximate inertial manifolds (AIMs) which are used to derive low-dimensional ODE systems that accurately reproduce the solutions of the parabolic PDE system (see also [29, 28] for other approaches for the construction of AIMs). The theoretical development of the control methods has been accompanied by practical applications to several distributed chemical processes using high- fidelity simulated models to solve several industrially important distributed control problems. These applications include control of the wafer temperature profile in a chemical vapor deposition process and crystal thermal gradient profile in a crystal growth process.

In addition to this work, other notable advances in control of PDE systems have been made, including controller design based on the infinite-dimensional system and subsequent use of approximation theory to design and compute low-order finite dimensional compensators [12], results on distributed control using generalized invariants [47] and concepts from passivity and thermodynamics [62], and boundary backstepping control of a class of parabolic PDE systems [11]. Other recent results on model reduction and control of transport-reaction process include the use of wavelets as basis functions in Galerkin's method [44, 43].

While the above efforts have led to the development of a number of systematic approaches for distributed controller design, an underlying theme of the available approaches is to achieve stabilization of the process at a (possibly open-loop unstable) spatially non-uniform profile by using a finite (typically small) number of measurement sensors and control actuators, that are distributed along the spatial extent of the process. Significant recent advances in actuation and sensing technology make possible the use of large num-

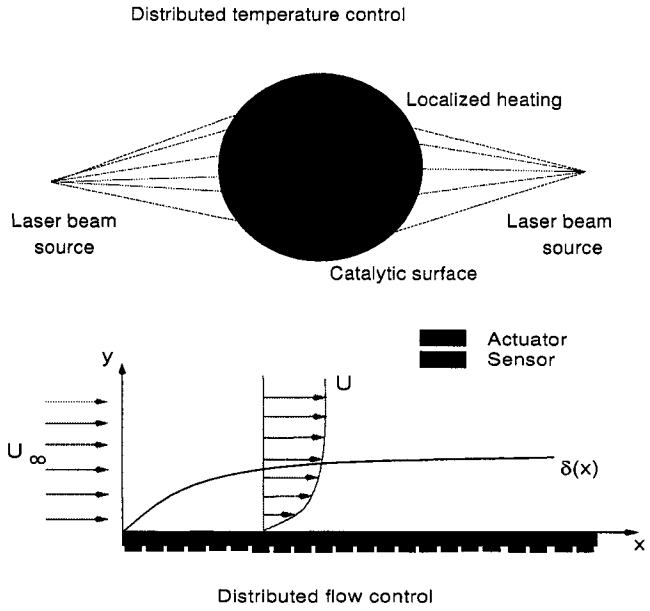


Figure 1.1: Example of distributed actuation for diffusion-reaction processes using a large number of computer-controlled focused laser beams.

bers of actuators and sensors to control spatially distributed processes. Examples include the manufacturing of arrays of micro-actuators/sensors for flow control (see, for example, the review article [38]) and the recent development of computer-controlled focused laser beams for temperature control of catalytic surfaces [41, 33, 42] (Figure 1.1). The advances in distributed actuation and sensing have motivated research on linear distributed control of linear spatially-invariant distributed parameter systems (e.g., [6]) and the discussion of the concept of inducing complex behavior in spatially-distributed systems using feedback (e.g., [61]). However, a systematic procedure for the design of nonlinear feedback laws that employ a large number of actuators and sensors to create a prespecified, yet complex, spatio-temporal behavior is currently not available.

Another limitation of the existing control methods for parabolic PDEs is the lack of direct incorporation of state variable and manipulated input constraints in the controller design. This is important because the operation of distributed chemical processes often requires respecting constraints on manipulated inputs and process states. Input constraints

typically reflect limits on the capacity of control actuators, such as valves or pumps, while state constraints represent desirable ranges of operation for the process state variables which reflect some safety or performance objectives. In transport-reaction processes, for example, safety requirements may require that the reactor temperature be maintained everywhere below a certain safety threshold, while product quality requirements may call for tight constraints on product purity. Appropriate control designs for spatially-distributed processes, therefore, need to take into account the spatial nature of the process, and enforce state variable constraints while respecting constraints on the manipulated inputs that arise due to physical limitations on the capacity of the control actuators.

In current industrial practice, the achievement of optimal performance, subject to input and state constraints, relies to a large extent on the use of model predictive control (MPC) policies which are well known for their ability to handle constraints, and optimization requirements, all in a consistent, systematic manner. Unlike open-loop model-based optimal control policies (where the optimal operating conditions are calculated off-line), in MPC, the control action is computed by solving repeatedly, on–line, a constrained optimization problem at each sampling time. Owing to this, MPC has the ability to suppress the influence of external disturbances and tolerate model inaccuracies (because of the use of feedback) and force the system to follow the optimal trajectory that respects constraints on the operating conditions. In general, an MPC control law does not admit an explicit analytic form, since an optimization problem should be solved numerically on-line. Having started as a linear, discrete-time control methodology [51], transparent connections between different versions of MPC were established using theoretical z-domain methods in the work presented in [34] through the internal model control (IMC) structure. Continuous-time linear versions of the (IMC) structure have been also developed [39]. Furthermore, continuous-time versions of IMC have been extended to nonlinear systems using appropriate operator formalism [25], and direct nonlinear generalization of traditional MPC methods have appeared in the literature as well [37, 46]. In the context of control of parabolic PDEs, few results are available on the development

of computationally-efficient predictive control algorithms. A potential drawback of using standard spatial discretization techniques (e.g., finite differences or finite elements) is that the number of equations that should be retained to derive an ODE system that yields the desired degree of approximation may be very large, leading to an MPC controller design that is highly computation-intensive.

Motivate by the above, the objectives of the present thesis are to:

- develop a systematic framework for distributed control of transport-reaction processes described by quasi-linear parabolic PDE systems,
- develop predictive control techniques for PDE systems with state and manipulated input constraints, and
- apply the proposed distributed and predictive control methods to transport-reaction processes.

This remainder of this doctoral thesis is structured as follows: Chapter 2 focuses on spatially-distributed processes described by quasi-linear parabolic PDE systems for which the control actuation and sensing spaces are infinite dimensional. For such systems, the control problem is formulated as the one of designing a feedback control system which makes the closed-loop system to exhibit a desired spatio-temporal behavior. Under the assumption that the target spatio-temporal behavior is described by a "target nonlinear PDE", combination of Galerkin's method and nonlinear control techniques is used to design nonlinear state and static output feedback controllers to address this problem. Several examples of diffusion-reaction processes are used to demonstrate the formulation of the control problem and the effectiveness of the proposed systematic approach to creating desirable spatio-temporal behavior.

Chapter 3 presents a technique for the construction of reduced-order models for a class of quasi-linear parabolic PDEs with spatially-varying coefficients and time-dependent spatial domain. The technique is applied to a diffusion-reaction process example.

In chapter 4, we consider linear parabolic PDEs with state and control constraints and we initially develop predictive control strategies on the basis of lower-order ODE models obtained through application of appropriate order reduction techniques to the infinite-dimensional system. Then, in order to account for the effect of both the slow and fast modes of the PDE in the cost function of the optimal control problem and the state constraints, we develop various MPC formulations which are distinct with respect to the number of modal states employed in the cost function and/or state constraints formulation. The developed predictive control algorithms are numerically validated using a linearized diffusion-reaction example.

Chapter 5 focuses on the development of computationally-efficient predictive control algorithms for nonlinear parabolic and hyperbolic PDEs with state and control constraints arising in the context of diffusion-reaction and convection-reaction processes, respectively. Specifically, we initially consider a diffusion-reaction process described by a nonlinear parabolic PDE and address the problem of stabilization of an unstable steady-state subject to input and state constraints. Galerkin's method is used to derive finite-dimensional systems that capture the dominant dynamics of the parabolic PDE, which are subsequently used for controller design. Various MPC formulations are constructed on the basis of the finite dimensional approximations that differ in the way the evolution of the fast eigenmodes is accounted for in the performance objective and state constraints. Finally, a predictive control scheme is developed for hyperbolic PDEs and applied to a convection-reaction process.

Finally, Chapter 6 concludes by summarizing the overall research contributions of this doctoral thesis.

# Chapter 2

# Distributed Nonlinear Control of Diffusion-Reaction Processes

## 2.1 Introduction

This chapter focuses on distributed control of quasi-linear parabolic PDEs and consider the problem of enforcing a prespecified spatio-temporal behavior in the closed-loop system using distributed nonlinear feedback control and a large number of actuators and sensors. Our control objectives go beyond the stabilization of unstable profiles to feedback laws that completely change the nonlinear vector field of the underlying PDE model when the loop is closed. Under the assumption that the desired spatio-temporal behavior is described by a "target parabolic PDE," we use a combination of Galerkin's method and nonlinear control techniques to design nonlinear state and static output feedback controllers to address this problem. To simplify our development, we consider "target parabolic PDEs" in which the structure of the spatial differential operator and boundary conditions is identical to the one of the original PDE model. We use examples of diffusion-reaction processes to demonstrate the formulation of the control problem and the effectiveness of the proposed systematic approach to creating prespecified spatio-temporal behavior. Using these illustrative examples, we demonstrate that both (a) a sufficiently

large number of actuators/sensors, and (b) nonlinear control laws are necessary to achieve this goal.

## 2.2 Preliminaries

In this work, we focus on quasi-linear parabolic PDE systems with the following state-space description:

$$\begin{aligned} \frac{\partial \bar{x}}{\partial t} &= B\frac{\partial^2 \bar{x}}{\partial z^2} + w\sum_{i=1}^{m} b_i(z)u_i + f(\bar{x}) \\ y_m^{\kappa} &= \int_0^{\pi} s^{\kappa}(z)\omega\bar{x}(z,t)dz \qquad \kappa = 1,\ldots,p \end{aligned} \tag{2.1}$$

subject to the boundary conditions:

$$\bar{x}(0,t) = 0, \;\; \bar{x}(\pi,t) = 0 \tag{2.2}$$

and the initial condition:

$$\bar{x}(z,0) = \bar{x}_0(z) \tag{2.3}$$

where $\bar{x}(z,t) = [\bar{x}_1(z,t) \;\cdots\; \bar{x}_n(z,t)]^T \in \mathbb{R}^n$ denotes the vector of state variables, $z \in [0,\pi] \subset \mathbb{R}$ is the spatial coordinate, $t \in [0,\infty)$ is the time, $u_i \in \mathbb{R}$ denotes the $i$-th manipulated input, and $y_m^{\kappa} \in \mathbb{R}$ denotes the $\kappa$-th measured output. $\frac{\partial^2 \bar{x}}{\partial z^2}$ denotes the second-order spatial derivative of $\bar{x}$, $f(\bar{x})$ is a sufficiently smooth nonlinear vector function, $w, \omega$ are constant vectors, $B$ is a positive-definite, constant matrix, and $\bar{x}_0(z)$ is the initial condition. $b_i(z)$ is a known smooth function of $z$ which describes how the control action $u_i(t)$ is distributed in the finite interval $[0,\pi]$, and $s^{\kappa}(z)$ is a known smooth function of $z$ which depends on the shape (point or distributed sensing) of the $\kappa$-th measurement sensors in the interval $[0,\pi]$. Whenever the control action enters the system at a single point $z_0$, with $z_0 \in [0,\pi]$ (i.e. point actuation), the function $b_i(z)$ is taken to be nonzero in a finite spatial interval of the form $[z_0-\mu, z_0+\mu]$, where $\mu$ is a small positive real number, and zero elsewhere in $[0,\pi]$.

To present the controller design method that we follow for enforcing complex spatio-temporal behavior in the closed-loop system, we formulate Eq.2.1 as an infinite dimensional system in the Hilbert space $\mathcal{H}([0,\pi];\mathbb{R}^n)$, with $\mathcal{H}$ being the space of measurable functions defined on $[0,\pi]$, with inner product and norm:

$$(\omega_1,\omega_2)=\int_0^{\pi}(\omega_1(z),\omega_2(z))_{\mathbb{R}^n}dz,\ ||\omega_1||_2=(\omega_1,\omega_1)^{\frac{1}{2}} \tag{2.4}$$

where $\omega_1,\omega_2$ are two elements of $\mathcal{H}([0,\pi];\mathbb{R}^n)$ and the notation $(\cdot,\cdot)_{\mathbb{R}^n}$ denotes the standard inner product in $\mathbb{R}^n$. Defining the state function $x$ on $\mathcal{H}([0,\pi];\mathbb{R}^n)$ as:

$$x(t)=\bar{x}(z,t),\quad t>0,\quad z\in[0,\pi], \tag{2.5}$$

the operator $\mathcal{A}$ in $\mathcal{H}([0,\pi];\mathbb{R}^n)$ as:

$$\begin{aligned}\mathcal{D}(\mathcal{A}) \;=\; \{\phi(z)\in L_2(0,\pi):\phi(z),\frac{d\phi(z)}{dz}&\text{ are absolutely continuous,}\\ \mathcal{A}\phi\in L_2(0,\pi),\phi(0)=0&\text{ and }\phi(\pi)=0\},\end{aligned} \tag{2.6}$$

and the input and measured output operators as:

$$\mathcal{B}u=\sum_{i=1}^{m}b_iu_i,\quad \mathcal{S}x=(s,x) \tag{2.7}$$

the system of Eqs.2.1-2.2-2.3 takes the form:

$$\begin{aligned}\dot{x} &= \mathcal{A}x+\mathcal{B}u+f(x),\quad x(0)=x_0\\ y_m &= \mathcal{S}x\end{aligned} \tag{2.8}$$

where $f(x(t))=f(\bar{x})$ and $x_0=x_0(z)$.

## 2.3 Problem formulation and solution method

To formulate the control problem, we assume that the target spatio-temporal profile, to be enforced in the closed-loop system, can be accurately captured by a "target parabolic PDE" system subject to boundary and initial conditions of the following form:

$$\begin{aligned}\frac{\partial\bar{x}}{\partial t} &= \bar{B}\frac{\partial^2\bar{x}}{\partial z^2}+\hat{f}(\bar{x},z,t)\\ \bar{x}(0,t) &= 0,\ \bar{x}(\pi,t)\ =\ 0,\ \bar{x}(z,0)=\bar{x}_0(z)\end{aligned} \tag{2.9}$$

where $\hat{f}(\bar{x}, z, t)$ is a nonlinear vector field and $\bar{B}$ is a positive-definite, constant matrix. It is assumed that $\hat{f}(\bar{x}, z, t)$ is a sufficiently smooth nonlinear vector function and satisfies $\hat{f}(0, 0, 0) = 0$. To simplify our development, the initial conditions of the original and "target PDE" are chosen to be the same.

The control problem is formulated as the one of determining a sufficient number of control actuators and measurements sensors and computing the corresponding explicit form of the control law that make the closed-loop system to be close (with respect to an appropriate norm) to the target spatio-temporal profile (Eq.2.9).

To address this problem, we employ the following methodology:

- Initially, Galerkin's method is used to derive nonlinear finite-dimensional approximations of the original (Eq.2.1) and target (Eq.2.9) parabolic PDE systems. The order of both finite-dimensional systems should be sufficiently high to ensure that the behavior of the original PDE system and of the "target PDE system" can be accurately captured by their finite-dimensional approximations (this is particularly important when the original and target PDEs involve complex spatiotemporal behavior and can be established by careful numerical simulation). Furthermore, to simplify the controller design, the order of both finite-dimensional systems is chosen here to be the same and equal to the smallest order needed to derive finite-dimensional approximations for both the original and target PDE systems that yield the desired accuracy.

- Once the order of the finite-dimensional approximations is fixed, the number of control actuators and measurement sensors is chosen to be equal to the order of the discretization (this requirement simplifies the controller design and can be relaxed), and nonlinear inversion-based control techniques are used to design nonlinear state and output feedback control laws that enforce the target behavior in the closed-loop finite-dimensional system. The design of the output feedback control laws involves a procedure proposed in [15] to obtain estimates for the states of the finite dimensional

system from the measurements.

- Finally, the closed-loop PDE system is analyzed to confirm that the target behavior is enforced in the infinite-dimensional system under appropriate convergence conditions of the finite-dimensional systems.

## 2.4 Controller design method

### 2.4.1 Galerkin's method

We apply Galerkin's method to the system of Eq.2.8 to derive an approximate finite-dimensional system. Let $\mathcal{H}_s$, $\mathcal{H}_f$ be two modal subspaces of operator $\mathcal{A}$, defined as, $\mathcal{H}_s = span\{\phi_1, \ldots, \phi_m\}$ and $\mathcal{H}_f = span\{\phi_{m+1}, \ldots, \}$ (the existence of $\mathcal{H}_s$, $\mathcal{H}_f$ follows from the properties of $\mathcal{A}$ and $\phi_j$ are eigenfunctions of $\mathcal{A}$). Defining the orthogonal projection operators $P_s$ and $P_f$ such that $x_s = P_s x$, $x_f = P_f x$, the state $x$ of the system of Eq.2.8 can be decomposed as:

$$x = x_s + x_f = P_s x + P_f x \tag{2.10}$$

Applying $P_s$ and $P_f$ to the system of Eq.2.8 and using the above decomposition for $x$, the system of Eq.2.8 can be equivalently written in the following form:

$$\begin{aligned} \frac{dx_s}{dt} &= \mathcal{A}_s x_s + \mathcal{B}_s u + f_s(x_s, x_f) \\ \frac{\partial x_f}{\partial t} &= \mathcal{A}_f x_f + \mathcal{B}_f u + f_f(x_s, x_f) \\ y_m &= \mathcal{S} x_s + \mathcal{S} x_f, \\ x_s(0) &= P_s x(0) = P_s x_0, \;\; x_f(0) = P_f x(0) = P_f x_0 \end{aligned} \tag{2.11}$$

where $\mathcal{A}_s = P_s\mathcal{A}$, $\mathcal{B}_s = P_s\mathcal{B}$, $f_s = P_s f$, $\mathcal{A}_f = P_f\mathcal{A}$, $\mathcal{B}_f = P_f\mathcal{B}$ and $f_f = P_f f$ and the notation $\frac{\partial x_f}{\partial t}$ is used to denote that the state $x_f$ belongs in an infinite-dimensional space. Note that due to the choice of $\mathcal{H}_s$ and $\mathcal{H}_f$ to be modal subspaces of $\mathcal{A}$, $P_s\mathcal{A}x_f = 0$ and $P_f\mathcal{A}x_s = 0$. In the above system, $\mathcal{A}_s$ is a diagonal matrix of dimension $m \times m$ of the form $\mathcal{A}_s = diag\{\lambda_j\}$ ($\lambda_j$ are eigenvalues of $\mathcal{A}_s$), $f_s(x_s, x_f)$ and $f_f(x_s, x_f)$ are Lipschitz vector functions, and $\mathcal{A}_f$ is an unbounded differential operator which is exponentially

stable (following from the fact that $\lambda_{m+1} < 0$ and the selection of $\mathcal{H}_s, \mathcal{H}_f$). Neglecting the fast and stable infinite-dimensional $x_f$-subsystem in the system of Eq.2.11, the following $m$-dimensional slow system is obtained:

$$\begin{aligned} \frac{d\tilde{x}_s}{dt} &= \mathcal{A}_s\tilde{x}_s + \mathcal{B}_s u + f_s(\tilde{x}_s, 0) \\ \tilde{y}_m &= \mathcal{S}\tilde{x}_s \end{aligned} \tag{2.12}$$

where the bar symbol in $\tilde{x}_s$ and $\tilde{y}_m$ denotes that these variables are associated with a finite-dimensional system.

In our development, we will also need to use a finite-dimensional approximation of the target parabolic PDE system of Eq.2.9. To this end, Eq.2.9 is formulated as an infinite-dimensional system in the Hilbert space $\mathcal{H}([0,\pi];\mathbb{R}^n)$ and Galerkin's method is used to obtain the following target finite-dimensional system:

$$\frac{d\tilde{x}_s}{dt} = \hat{\mathcal{A}}_s\tilde{x}_s + \hat{f}_s(\tilde{x}_s, 0, t) \tag{2.13}$$

Referring to the finite dimensional approximations of Eqs.2.12-2.13, we make the following assumptions: (a) both approximations converge uniformly to the solution of their corresponding infinite dimensional system as $m \to \infty$, and (b) the orders of both approximations are taken to be the same (equal to $m$) and sufficiently high to satisfy the desired accuracy with which the closed-loop behavior needs to be enforced. From these assumptions, the first one is standard and holds for most parabolic PDEs arising in the modeling of diffusion-convection-reaction processes (see also the example in section 4). The second assumption is made to simplify the controller design formulas and achieve the desired control objective, and it does not pose any limitations on the class of parabolic PDE systems for which the proposed method can be applied.

### 2.4.2 Nonlinear state feedback control

In this section, we consider the use of point control actuators and assume that measurements of the states of the system of Eq.2.12 are available. We first address the problem

of synthesizing nonlinear static state feedback control laws of the general form:

$$u = \mathcal{F}(\tilde{x}_s) \tag{2.14}$$

where $\mathcal{F}(\tilde{x}_s)$ is a nonlinear vector function that force the closed-loop finite-dimensional system to be identical to the target finite-dimensional system of Eq.2.13. To address this problem and simplify our development, we need to impose the following assumption.

**Assumption 2.1:** *$l = m$ (i.e., the number of control actuators is equal to the order of the finite-dimensional approximations), and the inverse of the matrix $\mathcal{B}_s$ exists.*

The requirement $l = m$ is sufficient and not necessary, and it is made to simplify the synthesis of the controller and the solution of the optimal placement problem (see also discussion in remark 2.2 below).

Proposition 2.1 that follows provides the explicit formula for the state feedback controller that achieves the control objective.

**Proposition 2.1:** *Consider the finite-dimensional system of Eq.2.12 for which assumption 1 holds. Then, under the state feedback controller:*

$$u = \mathcal{B}_s^{-1}\left((\hat{\mathcal{A}}_s - \mathcal{A}_s)\tilde{x}_s + \hat{f}_s(\tilde{x}_s, 0, t) - f_s(\tilde{x}_s, 0)\right) \tag{2.15}$$

*the closed-loop finite dimensional system is identical to the one of Eq.2.13.*

**Remark 2.1:** The proof of proposition 2.1 can be obtained by substituting the controller of Eq.2.15 in Eq.2.12 and performing several algebraic manipulations to show that the resulting closed-loop finite-dimensional system is identical to the one of Eq.2.13.

**Remark 2.2:** It is important to note that the requirements $l = m$ and existence of $\mathcal{B}_s^{-1}$ are sufficient to design a state feedback law that enforces the behavior of Eq.2.13 in the closed-loop finite dimensional system. To ensure (approximate) controllability and invertibility of the matrix $\mathcal{B}_s$, we impose that $rank(\mathcal{B}_s) = m$ by appropriate selection of actuator locations $z_j$, this requirement excludes several point actuator locations for which $rank < m$, see [21] for discussion on this issue. For certain classes of systems, it may be

possible to use coordinate changes and nonlinear feedback to achieve the desired control objective with a smaller number of control actuators.

### 2.4.3 Output feedback control

The nonlinear controller of Eq.2.15 was derived under the assumption that measurements of the states $\tilde{x}_s$ are available, which implies that measurements of the state variable, $x(z,t)$, are available at all positions and times. However, from a practical point of view, measurements of the state variables are only available at a finite number of spatial positions. Motivated by this, we address in this section the synthesis of nonlinear output feedback controllers that use measurements of the process outputs, $y_m$, that make the closed-loop finite-dimensional system to be identical to the "target" finite-dimensional system of Eq.2.13.

Specifically, we consider output feedback control laws of the general form:

$$u = \mathcal{F}(y_m) \tag{2.16}$$

where $\mathcal{F}(y_m)$ is a nonlinear vector function and $y_m$ is the vector of measured outputs. The synthesis of the controller of Eq.2.16 will be achieved by combining the state feedback controller of Eq.2.15 with a procedure proposed in [15] for obtaining estimates for the states of the approximate ODE model of Eq.2.12 from the measurements. To this end, we need to impose the following requirement on the number of measured outputs in order to obtain estimates of the states $x_s$ of the finite-dimensional system of Eq.2.12, from the measurements $y_m^\kappa$, $\kappa = 1, \ldots, p$.

**Assumption 2.2:** *$p = m$ (i.e., the number of measurements is equal to the order of the finite-dimensional approximations), and $\mathcal{S}^{-1}$ exists, so that $\hat{x}_s = \mathcal{S}^{-1} y_m$.*

We note that the requirement that the inverse of the operator $S$ exists can be achieved by appropriate choice of the location of the measurement sensors (i.e., functions $s^\kappa(z)$). When point measurement sensors are used, this requirement can be verified by checking the invertibility of a matrix (see example in the next section).

Theorem 2.1 presents the proposed output feedback controller which enforces the target behavior in the closed-loop system.

**Theorem 2.1:** *Consider the system of Eq.2.11, and the finite-dimensional system of Eq.2.12, for which assumptions 2.1 and 2.2 hold, under the nonlinear output feedback controller:*

$$\begin{aligned} \hat{x}_s &= \mathcal{S}^{-1} y_m \\ u &= \mathcal{B}_s^{-1} \left( (\hat{\mathcal{A}}_s - \mathcal{A}_s)\hat{x}_s + \hat{f}_s(\hat{x}_s, 0, t) - f_s(\hat{x}_s, 0) \right) \end{aligned} \tag{2.17}$$

*Then, the closed-loop infinite-dimensional system under the output feedback controller (Eq.2.1-Eq.2.17) converges to the "target" parabolic PDE system of Eq.2.9 as $m \to \infty$.*

**Proof:** Under the output feedback controller of Eq.2.17, the infinite-dimensional closed-loop system takes the following form:

$$\begin{aligned} \hat{x}_s &= \mathcal{S}^{-1} y_m \\ \dot{x} &= \mathcal{A}x + f(x) \\ &\quad + \mathcal{B}\mathcal{B}_s^{-1} \left( (\hat{\mathcal{A}}_s - \mathcal{A}_s)\hat{x}_s + \hat{f}_s(\hat{x}_s, 0, t) - f_s(\hat{x}_s, 0) \right), \\ &\quad x(0) = x_0 \\ y_m &= \mathcal{S}x \end{aligned} \tag{2.18}$$

or equivalently:

$$\begin{aligned} \hat{x}_s &= \mathcal{S}^{-1}\mathcal{S}x \\ \dot{x} &= \mathcal{A}x + f(x) \\ &\quad + \mathcal{B}\mathcal{B}_s^{-1} \left( (\hat{\mathcal{A}}_s - \mathcal{A}_s)\hat{x}_s + \hat{f}_s(\hat{x}_s, 0, t) - f_s(\hat{x}_s, 0) \right), \\ &\quad x(0) = x_0 \end{aligned} \tag{2.19}$$

Taking the limit as $m \to \infty$, we have that $\hat{x}_s \to x$, $\mathcal{B}_s \to \mathcal{B}$, $\hat{\mathcal{A}}_s \to \hat{\mathcal{A}}$, $\mathcal{A}_s \to \mathcal{A}$, $\hat{f}_s \to \hat{f}$ and $f_s \to f$, and thus Eq.2.19 takes the form:

$$\begin{aligned} \dot{x} &= \mathcal{A}x + f(x) \\ &\quad + \mathcal{B}\mathcal{B}^{-1} \left( (\hat{\mathcal{A}} - \mathcal{A})x_s + \hat{f}(x, t) - f(x) \right), \\ &\quad x(0) = x_0 \end{aligned} \tag{2.20}$$

or after some algebraic manipulations:

$$\dot{x} = \hat{\mathcal{A}}x + \hat{f}(x, t), \quad x(0) = x_0 \tag{2.21}$$

which is the infinite-dimensional representation of the "target" parabolic PDE system of Eq.2.9; this completes the proof.

**Remark 2.3:** Even though static output feedback is more sensitive to measurement noise than dynamic output feedback, we prefer to use static feedback of $y_m$ in the controller of Eq.2.17 because the use of a state observer to obtain estimates of the finite-dimensional state variables would significantly increase the computational demand for the computation of the control action, thereby impacting on the practical applicability of the proposed method. Note that in such a formulation, an $m$-th order nonlinear ODE system (with $m$ potentially a large number depending on the complexity of the spatio-temporal profile to be enforced in the closed-loop system) would have to be integrated in real-time in order to compute the control action.

**Remark 2.4:** To understand the essence of the result of theorem 1 and the structure of the controller, it is useful to put the control problem in question into perspective with respect to existing controller design methods whose objective is to make the process output to track a reference signal produced by an exogenous system. Under state feedback control, this problem is known as the state feedback regulator problem and was solved by Francis [30] for linear multivariable finite-dimensional systems. When only error measurements are available, this problem is known as the error (output) feedback regulator problem for which it was shown, in the context of linear finite-dimensional systems, by Francis and Wonham [31] that any controller (regulator) that solves this problem has to incorporate a model of the exogenous system generating the reference signal which is to be tracked (a property known as the internal model principle). More recently, the complete solution to the error (output) regulation problem for linear distributed parameter systems with bounded input/output operators was presented [13] and was shown that the resulting regulator incorporates a model of the exogenous system generating the tracking signal. With this in mind, it is easy to see why the controller of Eq.2.15 incorporates the entire vector field of the finite-dimensional approximation of the "target parabolic PDE" (which captures the desired closed-loop behavior); in this sense, the controller of Eq.2.15 obeys

the internal model principle. Our result also shows that it is possible by using a large number of control actuators and sensors to force not only the output (tracking error in the regulation problem) but the entire distributed state to behave according to a "target" behavior; this is not unexpected since a large number of actuators and sensors provides large number of degrees of freedom to shape the process dynamics according to a known "target PDE system". We also note that the notion of "target PDE system" was recently used in [11] in the context of backstepping boundary control of parabolic PDEs with the objective of stabilization.

**Remark 2.5:** Referring to the requirement that the initial condition of the original (Eq.2.1) and "target" (Eq.2.9) parabolic PDEs are identical, it is important to note that this is sufficient to ensure that the "target" spatio-temporal profile is enforced in the closed-loop system as $m \rightarrow \infty$ for all times. This requirement can be relaxed for initial conditions $\hat{x}_0(z)$ for which the solution of the "target" parabolic PDE asymptotically converges to the target spatiotemporal profile. This can be seen from the proof of Theorem 1 since for $m \rightarrow \infty$, the resulting closed-loop system would take the form of Eq.2.21 with $x(0) = \hat{x}_0 \neq x_0$. So for $\hat{x}_0$, for which the solution of the "target" parabolic PDE converges asymptotically ($t \rightarrow \infty$) to the "target" spatio-temporal profile, the desired behavior can be asymptotically ($t \rightarrow \infty$) enforced in the closed-loop system, provided that a sufficiently large number of control actuators and measurement sensors is employed.

The case studies of several representative models of diffusion-reaction processes described by the parabolic PDEs will be explored in order to determine a sufficiently large number of actuators/sensors necessary to be employed in order to force "target parabolic PDE" behavior, and appropriate control law that would achieve desired objectives. The proposed control methodology will be applied to a one-dimensional diffusion-reaction process example to enforce desired spatio-temporal behavior in the closed-loop system. The control is assumed to be implemented on the process by using spatially-distributed arrays consisting of large numbers of control actuators and measurement sensors, which will be

placed at equidistant positions. Through all case studies we consider point actuation and point sensing.

Specifically, we consider a diffusion-reaction process described by a quasi-linear parabolic PDE of the form:

$$\frac{\partial \bar{x}}{\partial t} = \mathcal{D}\frac{\partial^2 \bar{x}}{\partial z^2} + \beta_T e^{-\frac{\gamma}{1+\bar{x}}} + \beta_U(b(z)u(t) - \bar{x}) - \beta_T e^{-\gamma} \tag{2.22}$$

subject to the boundary and initial conditions:

$$\bar{x}(0,t) = 0, \quad \bar{x}(\pi,t) = 0, \quad \bar{x}(z,0) = \bar{x}_0(z) \tag{2.23}$$

where $\bar{x}$ denotes the state of the process, $\beta_T$ denotes a dimensionless heat of reaction, $\gamma$ denotes a dimensionless activation energy, $\beta_U$ denotes a dimensionless heat transfer coefficient, $\mathcal{D}$ denotes dimensionless diffusion coefficient, $u(t)$ denotes the vector of manipulated inputs (control actions) and $b(z)$ is the vector of the actuator distribution functions. The following typical values are given to the process parameters: $\beta_T = 50.0$, $\beta_U = 2.0$, $\gamma = 4.0$, and $\mathcal{D} = 1$ . For these, it was verified that the spatially-uniform steady state $\bar{x}(z,t) = 0$ is an unstable one. Specifically, the linearization of the PDE of Eq.2.22 around $\bar{x}(z,t) = 0$ has the following form:

$$\frac{\partial \bar{x}}{\partial t} = \mathcal{D}\frac{\partial^2 \bar{x}}{\partial z^2} + (\beta_T e^{-\gamma}\gamma - \beta_U)\bar{x} + \beta_U b(z)u(t) \tag{2.24}$$

To demonstrate the applicability and investigate the effect of various process and controller parameters on the ability of the proposed method to enforce desired spatio-temporal behavior in the closed-loop system, we will consider a set of three "target parabolic PDEs". Note that in an engineering application, the desired closed-loop behavior should be obtained from the solution of an optimization problem whose objective is to maximize process performance; in such a case the "target PDE" can be subsequently constructed using a closed-form approximation of the optimal spatio-temporal profile. Specifically, we consider the following "target parabolic PDEs": (1) a linear parabolic

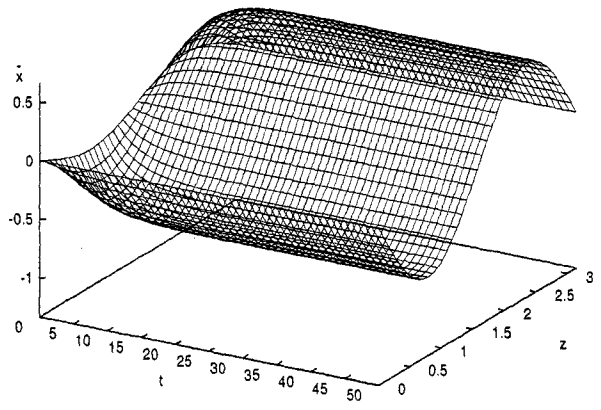


Figure 2.1: Spatio-temporal profile of linear parabolic PDE of Eq.2.25 with $b = 1.5$.

PDE with spatially-dependent additive term of the form:

$$\begin{aligned} \frac{\partial \bar{x}}{\partial t} &= b\frac{\partial^2 \bar{x}}{\partial z^2} - 4sin(2z) \\ \bar{x}(0,t) &= 0, \;\; \bar{x}(\pi,t) = 0, \;\; \bar{x}(z,0) = \bar{x}_0(z) \end{aligned} \tag{2.25}$$

where $b$ is a positive constant parameter, with the value $b = 1.5$, (2) the so-called Chafee-Infante diffusion-reaction equation:

$$\begin{aligned} \frac{\partial \bar{x}}{\partial t} &= b\frac{\partial^2 \bar{x}}{\partial z^2} + \alpha\bar{x} - \beta\bar{x}^3 \\ \bar{x}(0,t) &= 0, \;\; \bar{x}(\pi,t) = 0, \;\; \bar{x}(z,0) = \bar{x}_0(z) \end{aligned} \tag{2.26}$$

where $\alpha$, $\beta$ and $b$ are constant positive parameters, with the following values $\alpha = 2$, $\beta = 2$ and $b = 1.5$, and (3) a nonlinear time-varying parabolic PDE of the following form:

$$\frac{\partial \bar{x}}{\partial t} = b\frac{\partial^2 \bar{x}}{\partial z^2} + \hat{f}(\bar{x},t) \tag{2.27}$$

where $\hat{f}(\bar{x},t) = \alpha\bar{x} - \beta\bar{x}^3 + 2.5sin(0.5t)\beta_T e^{-\frac{\gamma}{1+\bar{x}}}$, and $\alpha$, $\beta$, $\beta_T$, $\gamma$ are constant positive parameters with the following values $\alpha = 2$, $\beta = 2$, $\beta_T = 50.0$ and $\gamma = 4.0$.

In the first set of simulation runs, we consider the linear PDE of Eq.2.24 (which results from the linearization of Eq.2.22 around $\bar{x}(z,t) = 0$, and thus, it has an unstable solution)

and focus on linear state feedback control. The "target PDE" is Eq.2.25 with $b = 1.5$. The reason for considering the linear PDE of Eq.2.24 as the starting point is to show that the desire to enforce a spatially-varying profile necessitates the use of a large number of control actuators and cannot be enforced, with the desired accuracy, when a restricted number of control actuators is available. A 40-th order Galerkin discretization of Eq.2.25 is computed and used in the simulation (higher order discretizations led to identical results). Figure 2.1 shows the target spatio-temporal behavior described by Eq.2.25 with $b = 1.5$.

The control problem is to compute the sufficient number of actuators and the corresponding state feedback law so that the solution of a 40-th order discretization of the closed-loop PDE system (linear PDE of Eq.2.24 under the state feedback law) is very close to the solution of the 40-th order discretization of the "target PDE" of Eq.2.25. The closeness of the two solutions is achieved after a short time needed for the fast transients associated with the modes of the high-order discretization, which are not included in the model used for controller design, to die out (note that this is possible because the initial conditions of the original and "target PDE" are chosen to be the same). To solve this problem, we derive several finite-dimensional approximations of Eq.2.24 and use them to design state feedback laws that make the vector fields of the corresponding closed-loop systems to be identical to the ones of the finite-dimensional approximations of the "target PDE" of Eq.2.25 of the same dimension. At this point, it is important to note that (a) closeness of the solutions of the closed-loop system and of the target PDE can be defined by using various norms; in this work, the closeness is evaluated by checking the discrepancy between the two solutions at all positions and times, and (b) the fast decay of the modes which are not included in the model used for controller design is a consequence of the highly dissipative behavior of parabolic PDEs.

Specifically, we construct second-, fifth- and tenth-order Galerkin approximations of the PDEs of Eq.2.24 and Eq.2.25 and design three state feedback control laws that exactly enforce the target behavior in the corresponding finite-dimensional closed-loop systems.

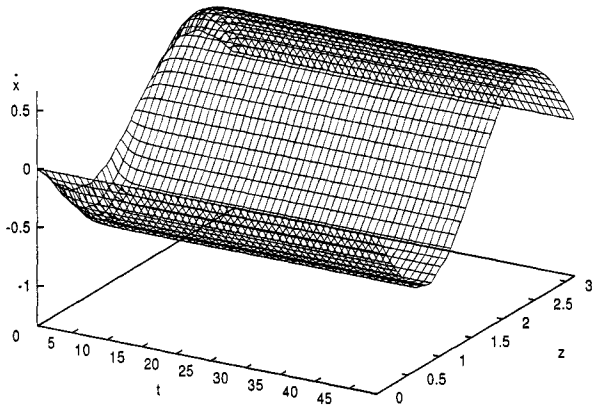


Figure 2.2: Closed-loop spatio-temporal profile of linearized diffusion-reaction equation (Eq.2.24) under linear state feedback control with 10 equidistant control actuators - Target behavior: Linear parabolic PDE of Eq.2.25 with $b = 1.5$.

Following our approach, the developed control laws require two, five and ten control actuators to be implemented. Figures 2.2, 2.3 and 2.4 show the spatio-temporal profile of the closed-loop system (simulated by the 40-th order Galerkin approximation) in the case of using ten, five and two control actuators, respectively. The use of ten and five control actuators suffices to enforce the desired target behavior in the closed-loop system after a short time needed for the transients associated with the higher-order modes to die out; the use of two control actuators is not adequate to enforce the desired behavior with the desired accuracy, see Figure 2.16 for the profiles of the error between the solution of the "target PDE" and the solution of the closed-loop system under ten, five and two control actuators.

The control problem is to compute the sufficient number of actuators and the corresponding state feedback law so that the solution of a 40-th order discretization of the closed-loop PDE system (linear PDE of Eq.2.24 under the state feedback law) is very close to the solution of the 40-th order discretization of the "target PDE" of Eq.2.25. The

closeness of the two solutions is achieved after a short time needed for the fast transients associated with the modes of the high-order discretization, which are not included in the model used for controller design, to die out (note that this is possible because the initial conditions of the original and "target PDE" are chosen to be the same). To solve this problem, we derive several finite-dimensional approximations of Eq.2.24 and use them to design state feedback laws that make the vector fields of the corresponding closed-loop systems to be identical to the ones of the finite-dimensional approximations of the "target PDE" of Eq.2.25 of the same dimension. At this point, it is important to note that (a) closeness of the solutions of the closed-loop system and of the target PDE can be defined by using various norms; in this work, the closeness is evaluated by checking the discrepancy between the two solutions at all positions and times, and (b) the fast decay of the modes which are not included in the model used for controller design is a consequence of the highly dissipative behavior of parabolic PDEs.

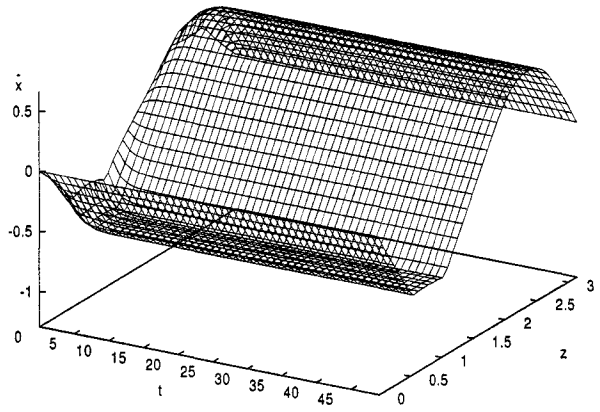


Figure 2.3: Closed-loop spatio-temporal profile of linearized diffusion-reaction equation (Eq.2.24) under linear state feedback control with 5 equidistant control actuators - Target behavior: Linear parabolic PDE of Eq.2.25 with $b = 1.5$.

Specifically, we construct second-, fifth- and tenth-order Galerkin approximations of the PDEs of Eq.2.24 and Eq.2.25 and design three state feedback control laws that exactly

enforce the target behavior in the corresponding finite-dimensional closed-loop systems. Following our approach, the developed control laws require two, five and ten control actuators to be implemented. Figures 2.2, 2.3 and 2.4 show the spatio-temporal profile of the closed-loop system (simulated by the 40-th order Galerkin approximation) in the case of using ten, five and two control actuators, respectively. The use of ten and five control actuators suffices to enforce the desired target behavior in the closed-loop system after a short time needed for the transients associated with the higher-order modes to die out; the use of two control actuators is not adequate to enforce the desired behavior with the desired accuracy.

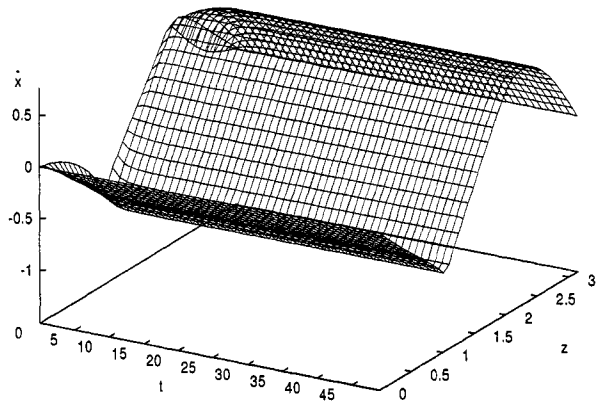


Figure 2.4: Closed-loop spatio-temporal profile of linearized diffusion-reaction equation (Eq.2.24) under linear state feedback control with 2 equidistant control actuators - Target behavior: Linear parabolic PDE of Eq.2.25 with $b = 1.5$.

In the second set of simulation runs, we consider the nonlinear parabolic PDE of Eq.2.22 as the starting point and the target PDE is Eq.2.25. The objective of this set of simulations is to study the ability of linear feedback control, which uses a large number of control actuators, to enforce (in the sense discussed above for the first set of simulation runs) the desired behavior. A 40-th order Galerkin's discretization of Eq.2.25 with $b = 1.5$ is computed and used in the simulation (higher order discretizations led to identical results).

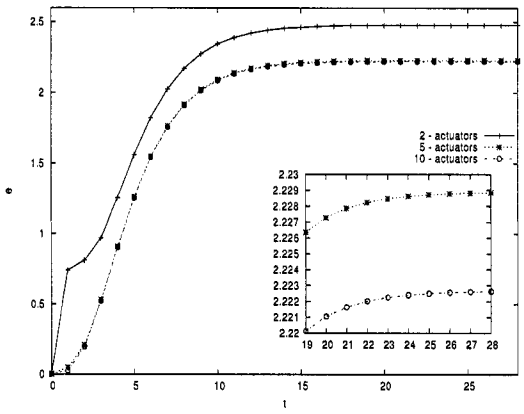


Figure 2.5: Time profiles of the error, $e(t)$ is defined as $e_{(t)} = \int_0^\pi (\bar{x} - \bar{x}_{target})^2 dz$, between the solution of the closed-loop system under two, five and ten control actuators and the solution of the "target" PDE - Original PDE - linearized diffusion-reaction equation PDE (Eq.2.24) - Target behavior: Linear parabolic PDE of Eq.2.25 with $b = 1.5$.

We apply the method of section 2.4.1 to construct second-order, fifth-order and twentieth-order Galerkin approximations of the PDEs of Eq.2.22 and Eq.2.25 and to design three nonlinear state feedback control laws that exactly enforce the target behavior to the finite-dimensional closed-loop systems. Then, the nonlinear state feedback laws are linearized around the steady-state $\bar{x}(z,t) = 0$ to obtain three linear state feedback laws. The developed control laws are implemented on a 40-th order Galerkin approximation of the nonlinear parabolic PDE of Eq.2.22 using two, five and twenty control actuators, respectively. Figures 2.6, 2.7 and 2.8 show the spatio-temporal profile of the closed-loop system in the case of using twenty, five and two control actuators, respectively. It is clear that linear control cannot satisfactorily compensate for the presence of nonlinear terms in Eq.2.22, and thus, the behavior of Eq.2.25 cannot be enforced in the closed-loop system. We note that when nonlinear control is implemented, the use of ten control actuators suffices to enforce the desired closed-loop behavior. This set of simulations demonstrates that linear feedback control may not be adequate to enforce a desired behavior in a quasi-linear parabolic PDE system (even though a large number of control actuators is used).

In the third set of simulation runs, we consider the nonlinear parabolic PDE of Eq.2.22

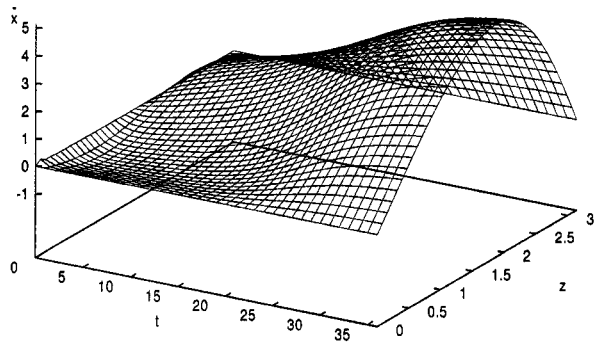


Figure 2.6: Closed-loop spatio-temporal profile of nonlinear diffusion-reaction equation (Eq.2.22) under linear state feedback control with 20 equidistant control actuators - Target behavior: Linear parabolic PDE of Eq.2.25 with $b = 1.5$.

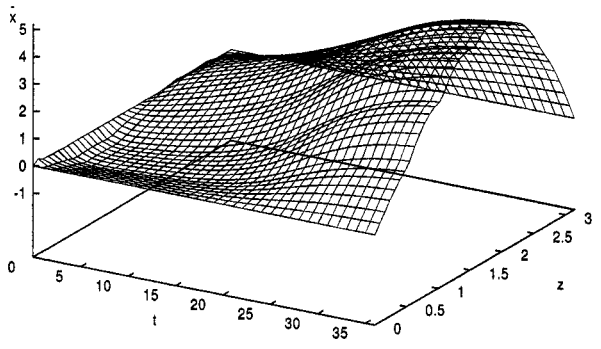


Figure 2.7: Closed-loop spatio-temporal profile of nonlinear diffusion-reaction equation (Eq.2.22) under linear state feedback control with 5 equidistant control actuators - Target behavior: Linear parabolic PDE of Eq.2.25 with $b = 1.5$.

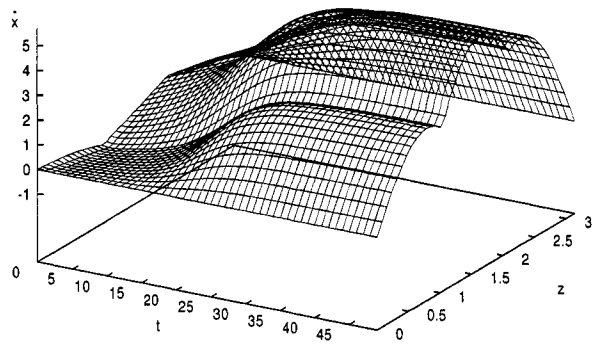


Figure 2.8: Closed-loop spatio-temporal profile of nonlinear diffusion-reaction equation (Eq.2.22) under linear state feedback control with 2 equidistant control actuators - Target behavior: Linear parabolic PDE of Eq.2.25 with $b = 1.5$.

as the starting point and the target PDE is the Chafee-Infante diffusion-reaction equation of Eq.2.26. The objective of this set of simulations is to show that it is possible to enforce (in the sense discussed above for the first set of simulations) a desired behavior in the closed-loop which is described by a "target nonlinear PDE".

We use the methodology of section 2.4.1 to construct second- and fifth-order Galerkin approximations of the PDEs of Eq.2.22 and Eq.2.26 and to design two nonlinear state feedback control laws that exactly enforce the target behavior to the finite-dimensional closed-loop systems. The developed control laws are implemented on a 40-th order Galerkin approximation of Eq.2.22 using two and five control actuators, respectively. Figures 2.9 and 2.10 show the spatio-temporal profile of the closed-loop system in the case of using two and five control actuators, respectively. Clearly, the use of five control actuators and nonlinear feedback enforces (in the sense discussed above for the first set of simulation runs) the desired closed-loop behavior.

In the fourth set of simulation runs, we consider the nonlinear parabolic PDE of Eq.2.22 as the starting point and the target PDE is the nonlinear time-dependent PDE

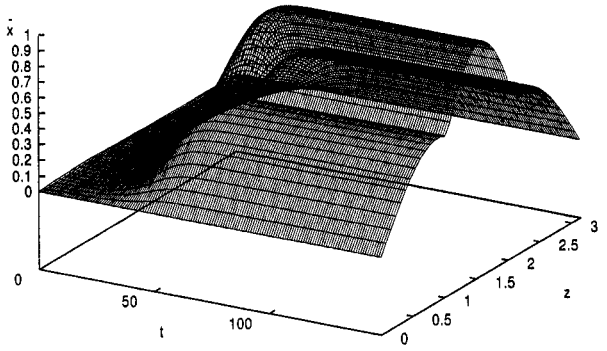


Figure 2.9: Closed-loop spatio-temporal profile of nonlinear diffusion-reaction equation (Eq.2.22) under nonlinear state feedback control with 2 equidistant control actuators - Target behavior: Chafee-Infante diffusion-reaction equation of Eq.2.26 with $\alpha = 2$, $b = 1.5$ and $\beta = 2$.

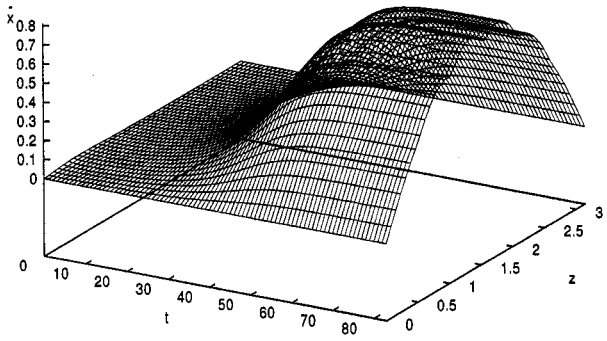


Figure 2.10: Closed-loop spatio-temporal profile of nonlinear diffusion-reaction equation (Eq.2.22) under nonlinear state feedback control with 5 equidistant control actuators - Target behavior: Chafee-Infante diffusion-reaction equation of Eq.2.26 with $\alpha = 2$, $b = 1.5$ and $\beta = 2$.

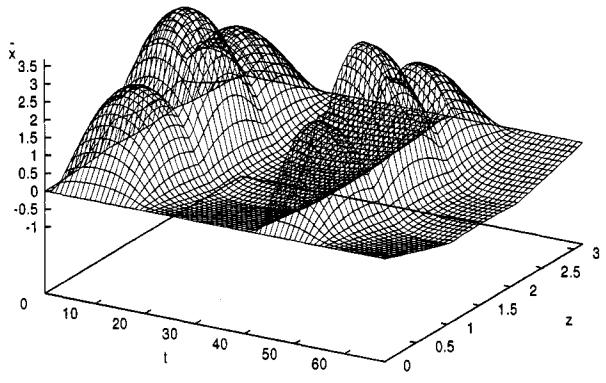


Figure 2.11: Closed-loop spatio-temporal profile of nonlinear diffusion-reaction equation (Eq.2.22) under nonlinear state feedback control with 2 equidistant control actuators - Target behavior: Nonlinear parabolic time-varying PDE of Eq.2.27 with $\alpha = 2$, $\beta = 2$, $\beta_T = 50.0$ and $\gamma = 4.0$.

of Eq.2.27. The objective is to show that is possible to use the proposed method to enforce time-varying behavior in the closed-loop system. We use the methodology of section 2.4.1 to construct second- and tenth-order Galerkin approximations of the PDEs of Eq.2.22 and Eq.2.27 and to design two nonlinear state feedback control laws that enforce the time dependent behavior described by the "target" nonlinear PDE of Eq.2.27 in the closed-loop finite dimensional system. The two control laws are implemented on the 40-th order Galerkin approximation of Eq.2.22 using two and ten control actuators, respectively. Figures 2.11 and 2.12 show the spatio-temporal profile of the closed-loop system in the case of using two and ten control actuators, respectively. It can be seen that while the use of two control actuators is not adequate to enforce the requested behavior in the closed-loop system, the use of ten control actuators and nonlinear feedback suffices to enforce the desired time-varying behavior in the closed-loop system (compare Figure 2.12 and Figure 2.13).

In the fifth set of simulation runs, the objective is to investigate the effect of the coefficient of the diffusion term on the ability of the proposed method to enforce a desired

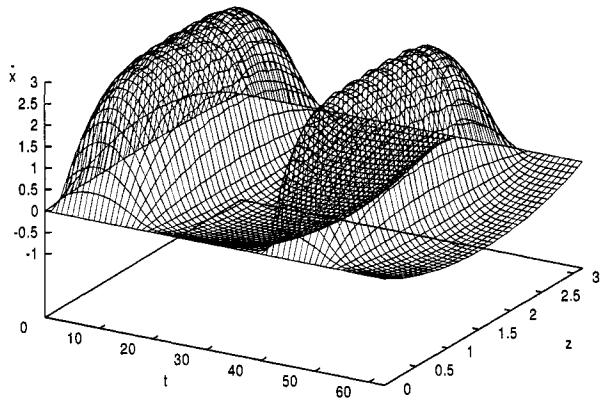


Figure 2.12: Closed-loop spatio-temporal profile of nonlinear diffusion-reaction equation (Eq.2.22) under nonlinear state feedback control with 10 equidistant control actuators - Target behavior: Nonlinear parabolic time-varying PDE of Eq.2.27 with $\alpha = 2$, $\beta = 2$, $\beta_T = 50.0$ and $\gamma = 4.0$.

spatio-temporal behavior in the closed-loop system. We consider the nonlinear PDE of Eq.2.22 as the starting point and the target PDE is Eq.2.25. We also consider the following two values for the coefficient of the diffusion term in the original PDE (a) $\mathcal{D} = 0.4$ and (b) $\mathcal{D} = 0.06$. In the first simulation run $\mathcal{D} = 0.4$, we consider two control actuators and design a nonlinear state feedback control law; Figure 2.14 shows the state of the resulting closed-loop system.

We can see that the use of two control actuators is not sufficient to enforce the behavior of Eq.2.25 (note that when the value of diffusion coefficient $\mathcal{D} = 1$ the use of two control actuators is sufficient to achieve the same control objectives).

This result is expected since when $\mathcal{D} = 0.4$ the effect of the higher-order (residual) modes (modes which are not included in the model used for controller design) increases and leads to poor performance. Of course this effect can be suppressed by increasing the number of control actuators and number of modes used in the controller design model.

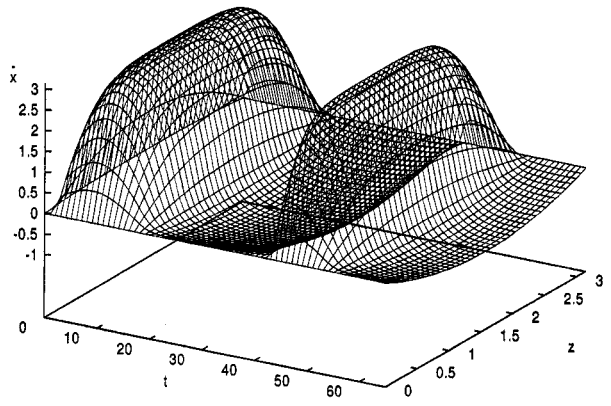


Figure 2.13: Evolution of the state of nonlinear time-varying parabolic PDE of Eq.2.27 with $\alpha = 2$, $\beta = 2$, $\beta_T = 50.0$ and $\gamma = 4.0$.

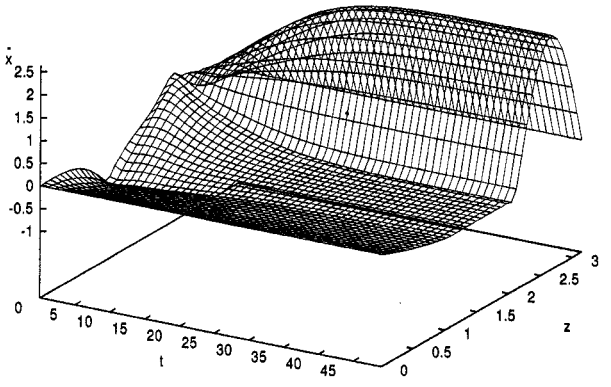


Figure 2.14: Closed-loop spatio-temporal profile of nonlinear diffusion-reaction equation (Eq.2.22) with $\mathcal{D} = 0.4$ under nonlinear state feedback control with 2 equidistant control actuators - Linear parabolic PDE of Eq.2.25 with $b = 1.5$.

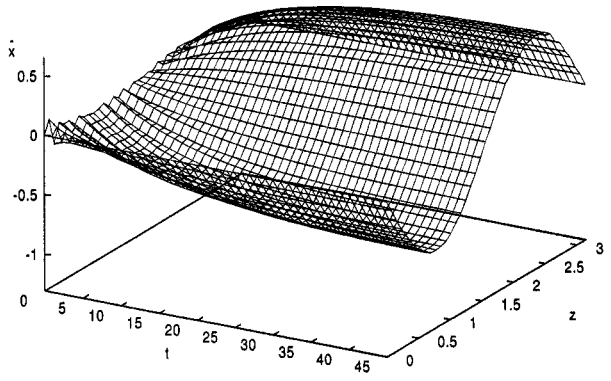


Figure 2.15: Closed-loop spatio-temporal profile of nonlinear diffusion-reaction equation (Eq.2.22) with $\mathcal{D} = 0.06$ under nonlinear state feedback control with 20 equidistant control actuators - Linear parabolic PDE of Eq.2.25 with $b = 1.5$.

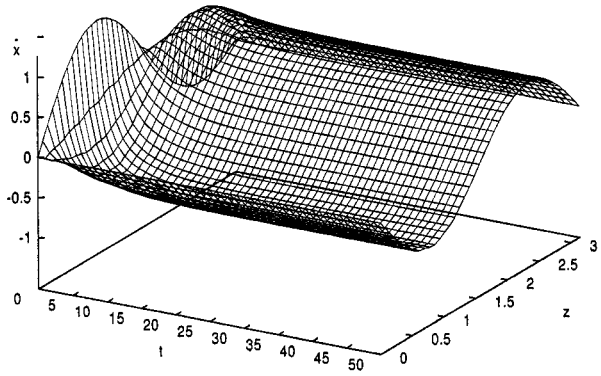


Figure 2.16: Closed-loop spatio-temporal profile of nonlinear diffusion-reaction equation (Eq.2.22) under nonlinear state feedback control with 10 equidistant control actuators - Target behavior: Linear parabolic PDE of Eq.2.25 with $b = 1.5$. Effect of variation on the initial condition.

To clearly demonstrate this point, we also considered the case of $\mathcal{D} = 0.06$ and used 20 control actuators and a nonlinear state feedback law to enforce the behavior of Eq.2.25 in the closed-loop system (in order to preserve numerical stability, the order of the Galerkin approximation of the original PDE, where the controller is implemented is taken to be 80). Figure 2.15 shows the state of the closed-loop system. We can see that, even though the effect of the residual modes is stronger, the use of 20 control actuators and nonlinear feedback suffices to enforce the desirable behavior in the closed-loop system.

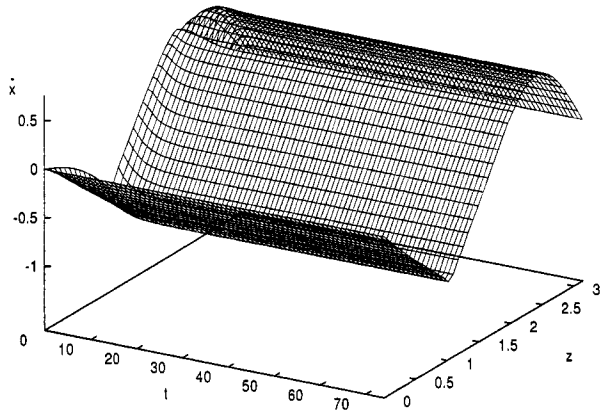


Figure 2.17: Closed-loop spatio-temporal profile of nonlinear diffusion-reaction equation (Eq.5) under nonlinear output feedback control with 2 equidistant control actuators and measurement sensors - Target behavior: Diffusion-reaction equation with spatially-dependent additive term (Eq.8 with $b = 1.5$)

In the sixth set of simulation runs, we consider relaxing the requirement that the initial conditions of the original (Eq.2.12) and "target" (Eq.2.13) parabolic PDEs are identical. Specifically, the initial condition for the original PDE is taken to be $\hat{x}_0(z) = 0.9sin(z) + 1.5sin(2z)$. Figure 2.16 shows the profile of the closed-loop system under a nonlinear state feedback control law (designed using the proposed method) which uses ten control actuators. As expected, the "target" spatio-temporal profile is asymptotically $(t \rightarrow \infty)$ enforced in the closed-loop system.

Finally, we consider the case where state measurements are not available and we focus

on output feedback controller design. Under the assumption that the number of measurements is equal to the number of control actuators (note that the number of control actuators should be chosen so that the target behavior is enforced in the closed-loop system, with the desired accuracy, under state feedback control), we employ a procedure proposed in [15] for obtaining estimates for the states of the finite-dimensional system from the measurements. The nonlinear parabolic PDE of Eq.2.22 is taken to be as the starting point and the target PDE is the linear parabolic PDE of Eq.2.25. Two nonlinear output feedback control laws are derived on the basis of second- and fifth-order finite-dimensional approximations. Figure 2.17 shows the evolution of the state of Eq.2.22 under a nonlinear output feedback control law which uses two control actuators and two measurement sensors; Figure 2.18 shows the evolution of the state of Eq.2.22 under a nonlinear state feedback control law which uses two control actuators. Clearly, there is some discrepancy between the closed-loop systems under state and output feedback control which is due to the estimation error. Figure 2.19 shows the evolution of the state of Eq.2.22 under a nonlinear output feedback control law which uses five control actuators and five measurement sensors; the target behavior has been enforced (in the sense discussed previously under state feedback control) which implies that five actuators/sensors suffice to achieve the desired control objective. We note that similar results have been obtained in the case of enforcing the spatio-temporal profiles of Eq.2.26-2.27 in the closed-loop system using output feedback control.

### 2.4.4 Application to a 2D diffusion-reaction process

In this subsection, the proposed control methodology is applied to a two-dimensional diffusion-reaction process example to enforce a desired spatio-temporal behavior in the closed-loop system. The control is assumed to be implemented on the process by using spatially-distributed arrays with large numbers of point control actuators which are placed

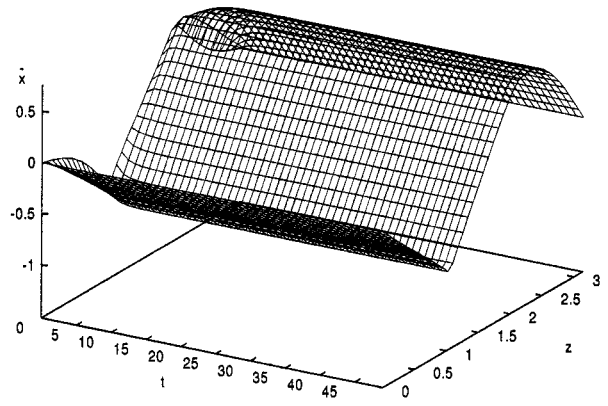


Figure 2.18: Closed-loop spatio-temporal profile of nonlinear diffusion-reaction equation (Eq.2.22) under nonlinear state feedback control with 2 equidistant control actuators - Target behavior: Linear parabolic PDE of Eq.2.25 with $b = 1.5$.

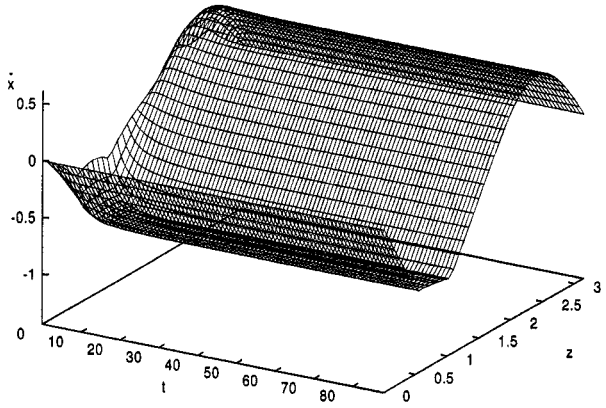


Figure 2.19: Closed-loop spatio-temporal profile of nonlinear diffusion-reaction equation (Eq.2.22) under nonlinear output feedback control with 5 equidistant control actuators and measurement sensors - Target behavior: Linear parabolic PDE of Eq.2.25 with $b = 1.5$.

at equidistant positions. Specifically, we consider a parabolic PDE of the form:

$$\frac{\partial \bar{x}}{\partial t} = \frac{\partial^2 \bar{x}}{\partial z^2} + \frac{\partial^2 \bar{x}}{\partial y^2} + \hat{f}(\bar{x}, t) \tag{2.28}$$

where $\hat{f}(\bar{x}, t)$ is a possibly nonlinear vector field, which is defined in a two-dimensional spatial domain $\Omega = [-\pi, \pi] \times [-\pi, \pi]$ (i.e., $z \in [-\pi, \pi]$ and $y \in [-\pi, \pi]$). Dirichlet boundary conditions are considered throughout the boundary of the domain, $\Gamma$, of the form $\bar{x}(z, y, t) = 0$ for all $(z, y)$ on $\Gamma$.

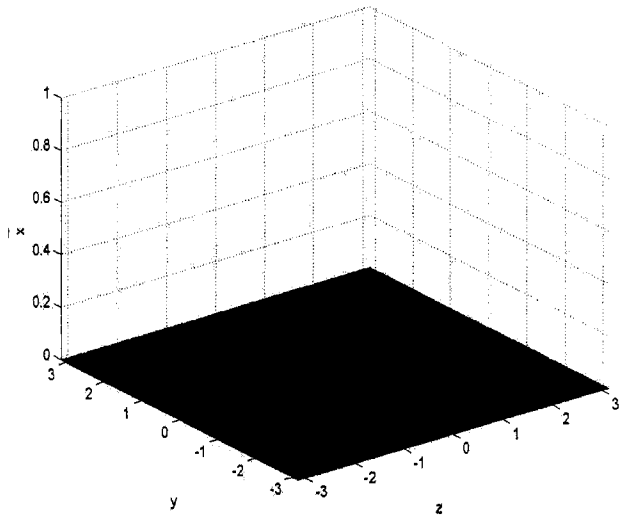


Figure 2.20: Steady-state of the two-dimensional parabolic PDE of Eq.2.28 with $\hat{f}(\bar{x}, t) = 0$.

To demonstrate the application of our method, we assume that the vector field of the "original" PDE is given by $\hat{f}(\bar{x}, t) = 0$, whereas the vector field of the "target PDE" is of the form $\hat{f}(\bar{x}, t) = \alpha\bar{x} - \beta\bar{x}^3$, where $\alpha$, $\beta$ are constant positive parameters with the following values $\alpha = 2$ and $\beta = 2$. A 1600-th order Galerkin discretization of Eq.2.28 is computed and used in the simulation (higher order discretizations led to identical results). Figure 2.20 shows the steady-state profile of the "original" PDE.

Figures 2.21, 2.22, 2.23 and 2.24 show profiles of the closed-loop *two*-dimensional parabolic PDE (simulated by the 1600-th order Galerkin approximation) under state feedback control, which employs one hundred control actuators, for $t$=1.7, 2.2, 3.0 and 5.0, respectively. The target behavior given by Eq.2.28 with $\hat{f}(\bar{x}, t) = 2\bar{x} - 2\bar{x}^3$ is asymp-

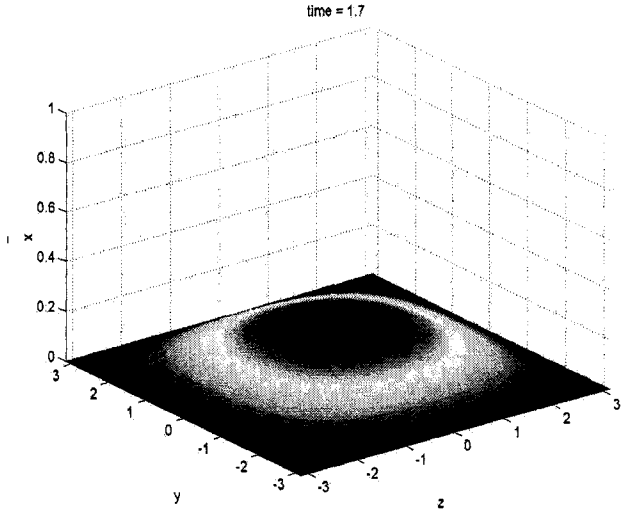


Figure 2.21: Closed-loop profile of the two-dimensional parabolic PDE under nonlinear state feedback control for t=1.7 - - Target behavior: Two-dimensional parabolic PDE of Eq.2.28 with $\hat{f}(\bar{x},t) = 2\bar{x} - 2\bar{x}^3$.

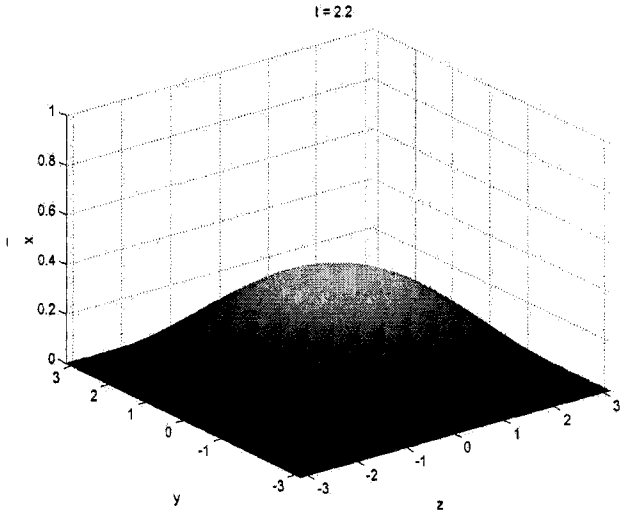


Figure 2.22: Closed-loop profile of the two-dimensional parabolic PDE under nonlinear state feedback control for t=2.2 - Target behavior: Two-dimensional parabolic PDE of Eq.2.28 with $\hat{f}(\bar{x},t) = 2\bar{x} - 2\bar{x}^3$.

totically enforced in the closed-loop system.

## 2.5 Conclusions

In this chapter, we focused on spatially-distributed processes described by quasi-linear parabolic PDE systems for which the control actuation and sensing spaces are infinite dimensional. For such systems, the control problem was formulated as the one of designing a feedback control system which provides the link between actuation and sensing, so that the closed-loop system exhibits a desirable spatio-temporal behavior. Under the assumption that the target complex spatio-temporal behavior is described by a "target nonlinear PDE," we used a combination of Galerkin's method and nonlinear control techniques to design nonlinear state and static output feedback controllers to address this problem. We used several examples of diffusion-reaction processes to demonstrate the formulation of the control problem and the effectiveness of the proposed systematic approach to creating desirable spatio-temporal behavior.

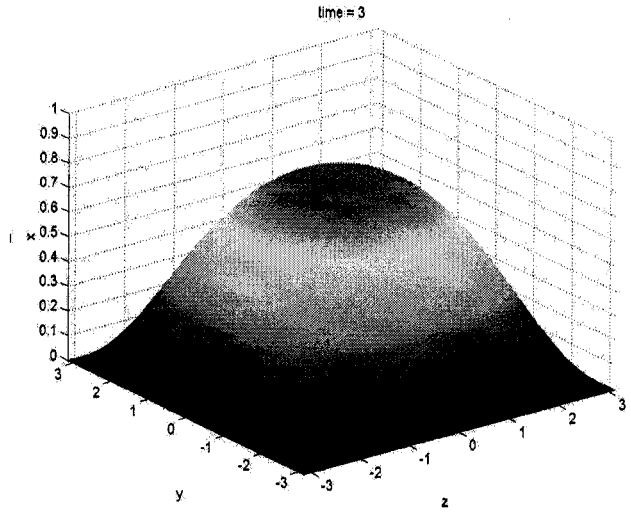


Figure 2.23: Closed-loop profile of the two-dimensional parabolic PDE under nonlinear state feedback control for t=3.1 - Target behavior: Two-dimensional parabolic PDE of Eq.2.28 with $\hat{f}(\bar{x},t) = 2\bar{x} - 2\bar{x}^3$.

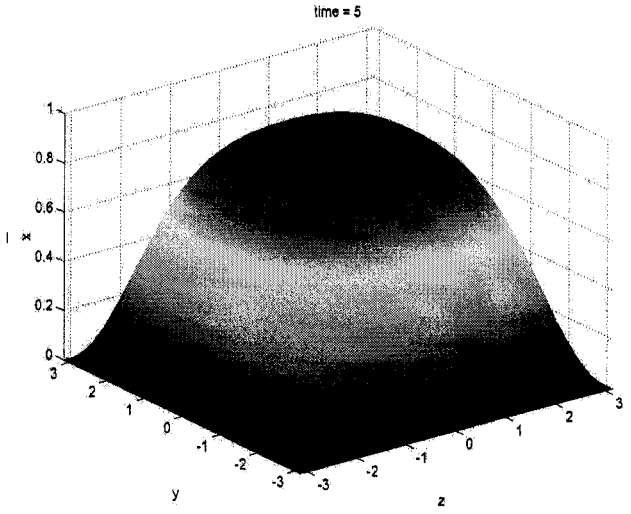


Figure 2.24: Closed-loop profile of the two-dimensional parabolic PDE under nonlinear state feedback control for t=5.0 - Target behavior: Two-dimensional parabolic PDE of Eq.2.28 with $\hat{f}(\bar{x},t) = 2\bar{x} - 2\bar{x}^3$.

# Chapter 3

# Order Reduction of Parabolic PDEs with Time-Dependent Spatial Domains

## 3.1 Introduction

The large number of industrially important transport-reaction processes which involve significant nonlinearities and time-dependent spatial domains are described by the nonlinear parabolic partial differential equations (PDEs). The main feature of the parabolic PDEs systems is that the eigenspectrum of the spatial differential operator can be partitioned into a finite-dimensional slow one and an infinite dimensional stable fast complement. This implies that dominant dynamics of such a system can be approximately described by the finite dimensional systems. Therefore, the standard approach to the derivation of low-dimensional models for linear/quasi-linear parabolic PDE systems (e.g., [8]) involves the application of standard Galerkin's method with the eigenfunctions of the spatial differential operator as basis functions, to the parabolic PDE system to derive ODE systems that accurately describe the dominant dynamics of the PDE system.

However, the standard model reduction techniques for parabolic PDE systems with

linear spatial differential operators can not be utilized directly for the construction of low-dimensional controllers for systems that include nonlinear spatial differential operators and spatially varying coefficients. Namely, the eigenvalue problems for nonlinear spatially differential operator can not be in general solved analytically, and therefore, it is difficult to a priori choose an optimal basis to expand the solution of the PDE system. An approximate way to address this problem [50] is to linearize the nonlinear spatial differential operator around the steady state and address the controller design problem on the basis of the resulting quasi-linear system. Hence, this approach is only valid in a small neighborhood of the steady states where linearization takes place. An alternative approach that is not based on a linearization is to utilize detailed finite-difference or finite-element simulations of the PDE systems to compute a set of empirical eigenfunctions (dominant spatial patterns) of the system through Karhunen-Loéve expansion (also known as proper orthogonal decomposition and principal component analysis), using the method of snapshots [54, 55, 56]. The use of empirical eigenfunctions as a basis functions in Galerkin's method has been shown to lead to the derivation of accurate nonlinear low-dimensional approximations of dissipative PDE systems arising in the modelling of diffusion-reaction processes (e.g.,[48, 9, 59]). In the area of control, linear feedback controllers were synthesized in [53, 60] for specific diffusion reaction systems on the basis of low-dimensional models obtaining using empirical eigenfunctions as basis functions in Galerkin's method, and a method for design of nonlinear output feedback controllers for nonlinear parabolic PDE systems was developed in [7] (see also [14]) by combining Galerkin's method with the empirical eigenfunctions. Other results include order reduction and control using wavelets as basis functions in Galerkin's method [43].

Motivated by the above considerations, we focus, in this chapter, on the computation of empirical eigenfunctions and construction of accurate low-dimensional approximations for control of nonlinear and time dependent parabolic PDE systems. The objective is to present a methodology for the computation of empirical eigenfunctions and the construction of accurate low-dimensional approximations for control of nonlinear and time-

dependent parabolic PDE systems. The method is applied to a diffusion-reaction process with nonlinearities, spatially-varying coefficients and time-dependent spatial domain, and is shown to lead to the construction of accurate low-order models and the synthesis of low-order controllers. The robustness of the predictions of the low-order models with respect to variations in the model parameters and different initial conditions, as well as the comparison of their performance with respect to low-order models which were constructed by using off-the-shelf basis function sets are successfully shown through computer simulations.

## 3.2 Time-dependent parabolic PDE systems and order reduction

We consider nonlinear parabolic PDE systems in one spatial dimension with the following state-space description:

$$\frac{\partial \bar{x}}{\partial t} = L(\bar{x}) + f(t, \bar{x}, u(t)) \tag{3.1}$$

subject to the boundary conditions:

$$\begin{aligned} C_1 \bar{x}(0,t) + D_1 \frac{\partial \bar{x}}{\partial z}(0,t) &= R_1 \\ C_2 \bar{x}(l(t),t) + D_2 \frac{\partial \bar{x}}{\partial z}(l(t),t) &= R_2 \end{aligned} \tag{3.2}$$

and the initial condition:

$$\bar{x}(z,0) = \bar{x}_0(z) \tag{3.3}$$

where the rate of change of the length of the domain, $l(t)$, is typically governed by an ordinary differential equation of the following general form:

$$\frac{dl}{dt} = \mathcal{G}(t, l, \int_0^{l(t)} \bar{a}(z, t, l, \bar{x}, \frac{\partial \bar{x}}{\partial z}) dz) \tag{3.4}$$

where $\bar{x}(z,t) = [\bar{x}_1(z,t) \ \cdots \ \bar{x}_n(z,t)]^T$ denotes the vector of state variables, $[0, l(t)] \subset \mathbb{R}$ is the domain of definition of the process, $z \in [0, l(t)]$ is the spatial coordinate and $t \in [0, \infty)$ is the time. $L(\bar{x})$ is a nonlinear differential operator which involves first- and

second-order spatial derivatives, $f(t, \bar{x}, u(t))$ is a nonlinear vector function, $u(t)$ is the manipulated input (to be used for the construction of the ensemble and the control of the system), $\mathcal{G}(t, l, \int_0^{l(t)} \bar{a}(z, t, l, \bar{x}, \frac{\partial \bar{x}}{\partial z})dz)$, $\bar{a}(z, t, l, \bar{x}, \frac{\partial \bar{x}}{\partial z})$ are nonlinear scalar functions, $C_1, D_1, C_2, D_2$ are constant matrices, $R_1, R_2$ are column vectors, and $\bar{x}_0(z)$ is the initial condition. In order to simplify the notation of this manuscript, we assume that $l(t)$ is a known, bounded and smooth function of time.

The main obstacles in developing a general model reduction method for systems of the form of Eq.3.1 are: a) the spatial differential operator is nonlinear, and b) the domain of definition of the process is generally time varying. These issues do not allow the computation of analytic expressions for the eigenvalues and eigenfunctions of the system, and thus, they prohibit the direct use of Galerkin's methods or orthogonal collocation methods with standard basis function sets, to derive finite dimensional approximations of the PDE system. To overcome the above problems, we employ the following methodology for the computation of empirical eigenfunctions and the construction of accurate low-dimensional approximations of systems of Eq.3.1.

1. Initially, the nonlinear parabolic PDE system is expressed with respect to an appropriate time-invariant spatial coordinate and a representative (with respect to different initial conditions and input perturbations) ensemble of solutions of the resulting time-varying PDE system is constructed by computing and solving a high-order discretization of the PDE.

2. Then, the Karhunen-Loéve expansion is directly applied to the ensemble of solutions to derive a small set of empirical eigenfunctions (dominant spatial patterns) that capture almost all the energy of the ensemble of solutions.

3. Finally, the empirical eigenfunctions are used as basis functions within a Galerkin's model reduction framework to derive low-order ordinary differential equation ODE systems that accurately describe the dominant dynamics of the PDE system.

### 3.2.1 Karhunen-Loéve expansion

For the simplicity of the presentation, we describe the K-L expansion in the context of the system of equation 3.19 and we assume that there is available a sufficiently large set of solutions of this system for different values of spatially dependent coefficients $k(z)$,$\{\bar{v}_\kappa\}$, consisting of K sampled states,$\bar{v}_\kappa(z)$, usually denoted as "snapshots". We assume that the snapshots are linearly independent [32]. We define the ensemble average of snapshots as $\langle \bar{v}_\kappa \rangle := (1/K) \sum_{\kappa=1}^{K} \bar{v}_\kappa(z)$ (we note that nonuniform sampling of the snapshots and weight ensemble average can be also considered [36]). Moreover, the ensemble average snapshots $\langle \bar{v}_\kappa \rangle$ is subtracted out from the snapshots, i.e.,

$$v_\kappa = \bar{v}_\kappa - \langle \bar{v}_\kappa \rangle \tag{3.5}$$

so that only fluctuations are analyzed. The issue is now how to obtain the most typical or characteristic structure $\phi(z)$ among these snapshots $\bar{v}_\kappa$. This problem mathematically can be posed as the one of obtaining a function $\phi(z)$ that maximizes the following objective function:

$$\begin{array}{ll} max. & \dfrac{\langle (\phi, v_\kappa)^2 \rangle}{(\phi, \phi)} \\ s.t. & (\phi, \phi) = 1, \;\; \phi \in L^2([\omega]) \end{array} \tag{3.6}$$

The constraint given by $(\phi, \phi) = 1$ is imposed to ensure that the function, $\phi(z)$, computed as a solution of the above maximization problem, is unique. The Lagrangian functional corresponding to this constrained optimization problem is

$$\bar{L} = \langle (\phi, v_\kappa)^2 \rangle - \lambda((\phi, \phi) - 1) \tag{3.7}$$

Necessary condition for extrema is that the functional derivative vanishes for all variations $\phi + \delta\phi \in L^2[\Omega]$, where $\delta$ is a real number:

$$\frac{\bar{L}(\phi + \delta\phi)}{d\delta}(\delta = 0) = 0, \;\; (\phi, \phi) = 1. \tag{3.8}$$

Using the definitions of inner product and ensemble average, $(d\bar{L}(\phi+\delta\phi)/d\delta)(\delta=0)$ can be computed from the following expression:

$$\frac{\bar{L}(\phi+\delta\phi)}{d\delta}(\delta=0)=\int_{\Omega}\left(\left\{\int_{\Omega}\langle\upsilon_{\kappa}(z)\upsilon_{\kappa}(\bar{z})\rangle\phi(z)dz\right\}-\lambda\phi(\bar{z})\right)\psi(\bar{z})d\bar{z} \tag{3.9}$$

As $\psi(\bar{z})$ is an arbitrary function, the necessary conditions for optimality take the form,

$$\int_{\Omega}\langle\upsilon_{\kappa}(z)\upsilon_{\kappa}(\bar{z})\rangle\phi(z)dz=\lambda\phi(\bar{z}),\quad(\phi,\phi)=1. \tag{3.10}$$

Introducing the two point correlation function

$$K(z,\bar{z})=\langle\upsilon_{\kappa}(z)\upsilon_{\kappa}(\bar{z})\rangle=\frac{1}{K}\sum_{\kappa=1}^{K}\langle\upsilon_{\kappa}(z)\upsilon_{\kappa}(\bar{z})\rangle \tag{3.11}$$

and the linear operator,

$$R:=\int_{\Omega}K(z,\bar{z})d\bar{z} \tag{3.12}$$

the optimality condition of Equation 3.10 reduces to the following eigenvalue problem of the integral equation:

$$R\phi=\lambda\phi\Rightarrow\int_{\Omega}K(z,\bar{z})\phi(\bar{z})d\bar{z}=\lambda\phi(z) \tag{3.13}$$

The computation of the solution of the above integral eigenvalue problem is computationally expensive task. To circumvent this problem, Sirovich introduced the method of snapshots [54]. The central idea of this technique is to assume that the requisite eigenfunction, $\phi(z)$, can be expressed as a linear combination of the snapshots, i.e.,

$$\phi(z)=\sum_{k}c_{k}\upsilon_{k}(z) \tag{3.14}$$

Substituting the above expression for $\phi(z)$ on Equation 3.13, we obtain the following eigenvalue problem:

$$\int_{\Omega}\frac{1}{K}\sum_{\kappa=1}^{K}\upsilon_{k}(z)\upsilon_{k}(\bar{z})\sum_{k=1}^{K}c_{k}\upsilon_{k}(\bar{z})d\bar{z}=\lambda\sum_{k=1}^{K}c_{k}\upsilon_{k}(z) \tag{3.15}$$

Defining

$$B^{\kappa k}:=\frac{1}{K}\int_{\Omega}\upsilon_{\kappa}(\bar{z})\upsilon_{k}(\bar{z})d\bar{z}) \tag{3.16}$$

the eigenvalue problem of Equation 3.15 can be equivalently written as

$$Bc = \lambda c \tag{3.17}$$

The solution of the above eigenvalue problem (which can be obtained by utilizing standard methods from matrix theory) yields the eigenvectors $c = [c_1\ c_2\ \ldots\ c_K]$ which can be used in Equation 3.14 to construct the eigenfunction $\phi(z)$. from the structure of the matrix B, it follows that it is symmetric and positive semi-definite, and therefore, its eigenvalues, $\lambda_\kappa$, $\kappa = 1, \ldots, K$ are real and non-negative. Furthermore, the resulting eigen-functions form an orthonormal set, i.e.:

$$\int_\Omega \phi_i(z)\phi_j(z)dz = 0, \quad i \neq j \tag{3.18}$$

## 3.3 Application to a diffusion-reaction process

We consider a diffusion-reaction process with moving domain which is described by the following parabolic PDE:

$$\begin{aligned} \frac{\partial \bar{x}}{\partial t} &= \frac{\partial}{\partial z}(k(z)\frac{\partial \bar{x}}{\partial z}) \\ &\quad +\beta_T(z)(e^{-\frac{\gamma}{1+\bar{x}}} - e^{-\gamma}) + \beta_U(b(z,t)u(t) - \bar{x}) \end{aligned} \tag{3.19}$$

subject to the Dirichlet boundary conditions:

$$\bar{x}(0,t) = 0, \quad \bar{x}(l(t),t) = 0 \tag{3.20}$$

and the initial condition:

$$\bar{x}(z,0) = 0.5 \tag{3.21}$$

where $\bar{x}$ is the state of the system, $\gamma, \beta_u$ are dimensionless process parameters (which will be assumed to be constant), $\beta_T(z), k(z)$ are dimensionless process parameters (which will be assumed to be explicit functions of the spatial coordinate $z$), $u(t) = [u_1(t)\ u_2(t)]^T$ is the vector of the inputs (which will be used in the construction of the ensemble of solutions), and $b(z,t) = [b_1(z,t)\ b_2(z,t)]$ is the vector function which determines how the inputs $u_1(t), u_2(t)$ are distributed in space.

Regarding the values of the process parameters, the following typical values were given to:

$$\beta_U = 2.0, \quad \gamma = 4.0 \tag{3.22}$$

while $\beta_T(z)$ and $k(z)$ were assumed to have the following expressions:

$$\beta_T = 45(1.5 - e^{-0.5\,z}), \quad k = e^{-0.5\,z} \tag{3.23}$$

Furthermore, the spatial domain was assumed to change according to the relation:

$$l(t) = \pi(1.4 - 0.4e^{(-0.02t^{2.7})}) \tag{3.24}$$

(it can be easily seen that the above function satisfies the requirements of assumption 1).

Introducing the spatial coordinate $\zeta = \frac{z}{l(t)}$ whose domain of definition is time-invariant, we can express the parabolic PDE system of Eq.3.19-3.20 in the following form:

$$\begin{aligned} \frac{\partial \bar{x}}{\partial t} &= \frac{1}{l^2}\frac{\partial}{\partial \zeta}(k(\zeta)\frac{\partial \bar{x}}{\partial \zeta}) + \frac{\dot{l}}{l(t)}\zeta\frac{\partial \bar{x}}{\partial \zeta} \\ &\quad +\beta_T(\zeta)(e^{-\frac{\gamma}{1+\bar{x}}} - e^{-\gamma}) + \beta_U(b(\zeta,t)u(t) - \bar{x}) \end{aligned} \tag{3.25}$$

subject to the boundary conditions:

$$\bar{x}(0,t) = 0, \quad \bar{x}(1,t) = 0 \tag{3.26}$$

The time-varying system of Eq.3.25 was used to construct the desirable set of empirical eigenfunctions for the PDE system of Eq.3.19. To this end, Galerkin's method with the following set of basis functions:

$$\phi_j(z,t) = \sqrt{\frac{2}{l(t)}}sin(j\,\pi\,\zeta), \quad j = 1, \ldots, \infty \tag{3.27}$$

was used to construct an accurate high-order discretization of the PDE of Eq.3.25 that was employed in the construction of the ensemble of solutions. It was found that a 30-th order Galerkin truncation of the system of Eq.3.19 using the above basis functions leads to an accurate solution of the PDE (it was verified that further increase of the order of the

Galerkin model provided no substantial improvement on the accuracy of the simulation results).

Figure 3.1 shows the evolution of the state of the PDE for $u(t) = 0$ starting from initial conditions which are very close to the steady-state $x(z,t) = 0$. We observe that the system moves to another steady-state which is characterized by a maximum at $z = 0.375\ l(t)$. This implies that the steady state $\bar{x}(z,t) = 0$ is an unstable one, and thus, the system moves to a stable spatially non-uniform steady state.

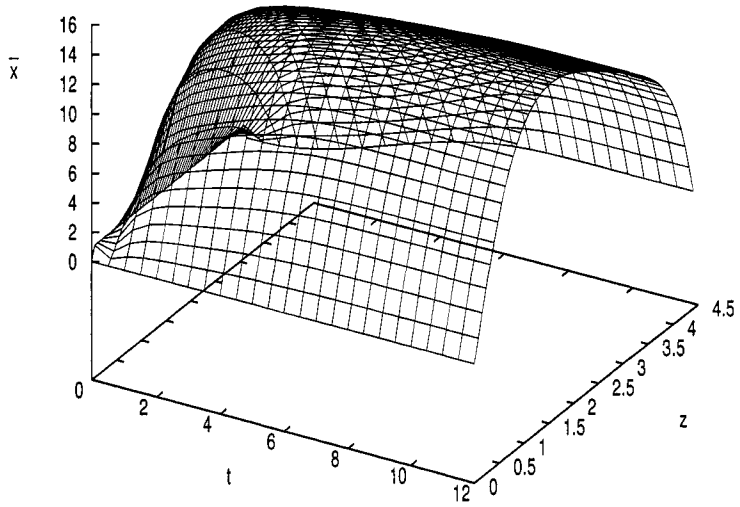


Figure 3.1: Profile of $\bar{x}$ for spatially varying $\beta_T$, $k$; $u(t) = 0$.

In order to compute a set of empirical eigenfunctions, we initially constructed an ensemble of 820 solutions (profiles of the state of the system as a function of the spatial coordinate, $\zeta$, for fixed time instants at different lengths of the spatial domain) of the high-order discretization of the PDE of Eq.3.25 by varying the initial conditions and the inputs to the system. The Karhunen-Loéve expansion was then applied to the developed ensemble of solutions to compute seven empirical eigenfunctions that describe the dominant solution patterns embedded in the ensemble (they account for more than 99.9% of the energy included in the entire ensemble). The first three of these empirical eigenfunctions are presented in Figure 3.2.

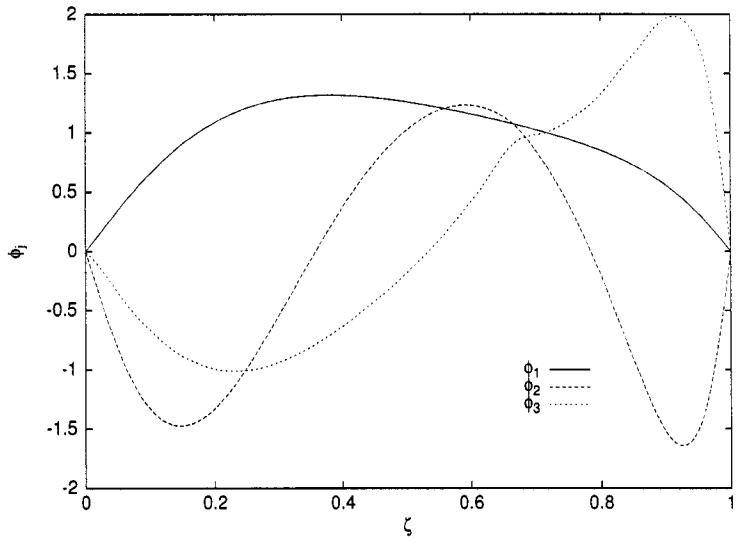


Figure 3.2: First three empirical eigenfunctions.

We now proceed with the use of the empirical eigenfunctions for the construction of accurate low-dimensional ODE approximations of the PDE. We initially applied Galerkin's method with the first two of the seven empirical eigenfunctions as basis functions to the PDE of Eq.3.25 to construct a second-order model. Figure 3.3 shows the deviation between the spatiotemporal profiles of the state of the system computed by the second-order ODE model and high-order discretization of the PDE; we observe a very good agreement between the two models for all times (the maximum deviation is lower than 3.4%).

To further improve the accuracy of the second-order model, we note that the spatial pattern of the error in Figure 3.3 resembles the shape of the third empirical eigenfunction (see Figure 3.2), and thus, we apply Galerkin's method with the first three empirical eigenfunctions as basis functions to the PDE of Eq.3.25 to construct a third-order model. Figure 3.3 shows the discrepancy between the third-order model and the high-order discretization of the PDE; it is clear that the addition of the third eigenfunction has greatly improve the accuracy of the low-order approximation (the maximum deviation in this case is less than 0.5%).

For the sake of comparison, we also constructed a third-order approximation of the

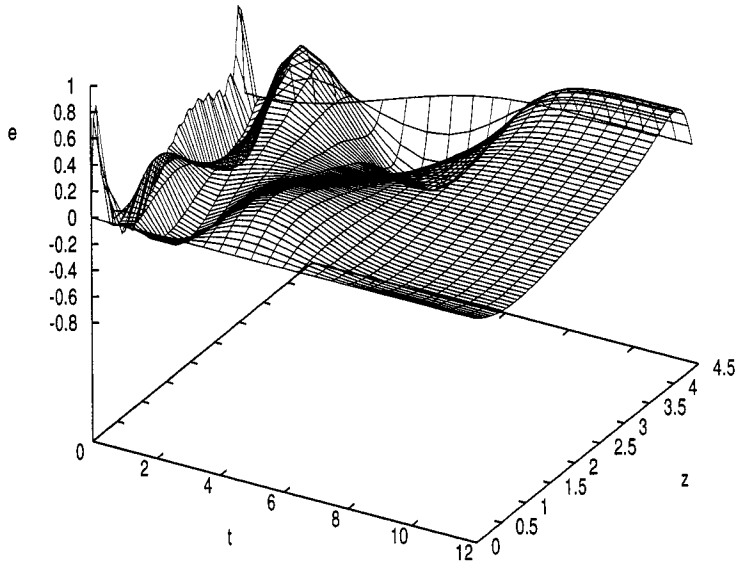


Figure 3.3: Deviation between the second-order model and the high-order discretization of the PDE (nominal case).

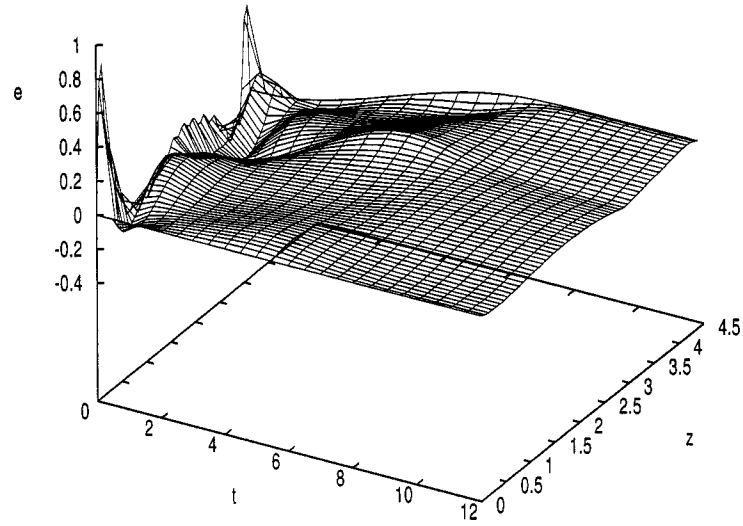


Figure 3.4: Deviation between the third-order model and the high-order discretization of the PDE (nominal case).

PDE by using Galerkin's method with the first three eigenfunctions of Eq.3.27 as basis functions (this set of eigenfunctions is the result of the solution of the eigenvalue problem of the spatial operator for constant values of $k$). We observe that the error (Figure 3.5) between this third-order model and the high-order discretization of the PDE is significant (about 11%), which is mainly a result of the fact that this approach does not account for the spatial distribution of the diffusion coefficient $k(z)$. We note that higher-order approximations computed by using this approach result in more accurate models; specifically, we found that a 7th order model was needed in order to produce the same error of 3.4% as the second order model based on empirical eigenfunctions, and a 10th order model was needed to have the same error of 0.5% as the third order model based on empirical eigenfunctions.

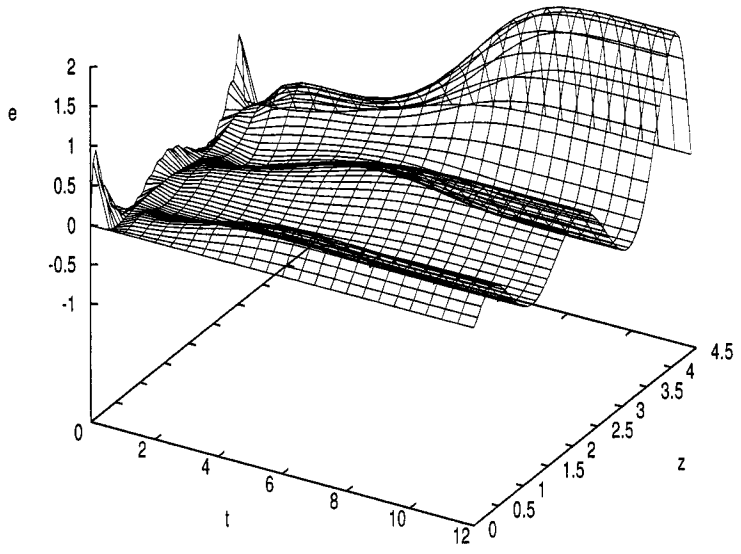


Figure 3.5: Deviation between the third-order model and the high-order discretization of the PDE (sinusoidal functions used as basis functions).

We also tested the ability of the third-order model to give accurate predictions when the process parameters have values which different from the ones used in the construction of the ensemble of solutions used in the computation of the empirical eigenfunctions. Specifically, for $\beta_T = 55(1.5 - e^{-0.5\,z})$ (which corresponds to an about +20% variation

with respect to the nominal value of $\beta_T$), the maximum error between the third-order model and the high-order discretization of the PDE is less than 0.5% for all times as can be seen in Figure 3.6. On the other hand, for $\beta_T = 45(1.5 - e^{-0.4\,z})$ (which corresponds to an about $-20\%$ variation with respect to the nominal value of $\beta_T$), the error between the these two models remains under 0.7% for all times as can be seen in Figure 3.7. We also tested the robustness of the third-order model for a $+20\%$ ($k = e^{-0.4\,z}$) and $-20\%$ ($k = e^{-0.6\,z}$) variation in the spatial dependence of $k$. The corresponding errors between the third-order model and the high-order discretization of the PDE are shown in Figures 3.8 and 3.9 respectively; they remain small for all times under 0.6% in the first and 1.6% in the second case.

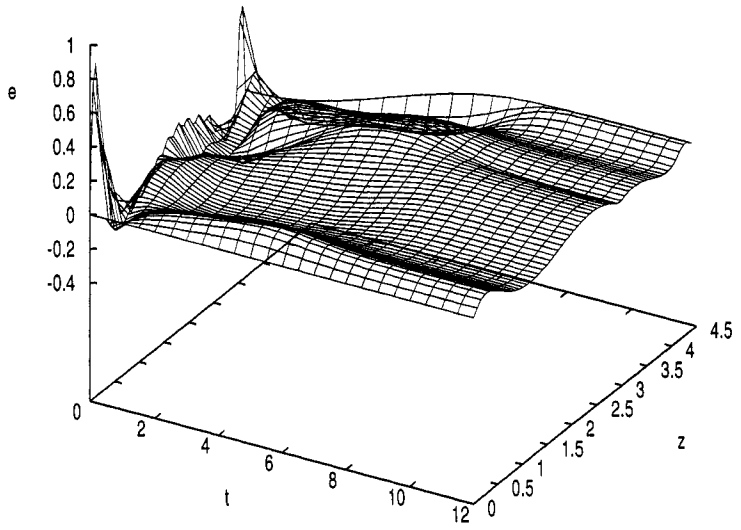


Figure 3.6: Deviation between the third-order model and the high-order discretization of the PDE ($\beta_T(z) = 55(1.5 - e^{-0.5\,z})$).

Finally, we tested the robustness of the third-order for two initial conditions which are different from the ones used for the construction of the empirical eigenfunctions. Specifically, for the initial condition $\bar{x}_0(z) = 0.5 + 0.5sin(z)$, the deviation between the third-order model and the high-order discretization of the PDE is presented in Figure 3.10, while for $\bar{x}_0(z) = 0.4 + 0.6sin(3\ z)$, the same deviation is shown in Figure 3.11.

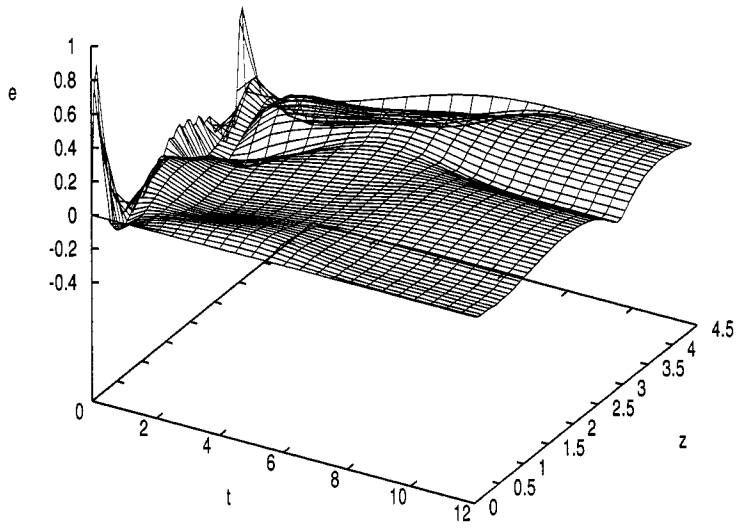


Figure 3.7: Deviation between the third-order model and the high-order discretization of the PDE ($\beta_T(z) = 45(1.5 - e^{-0.4\,z})$).

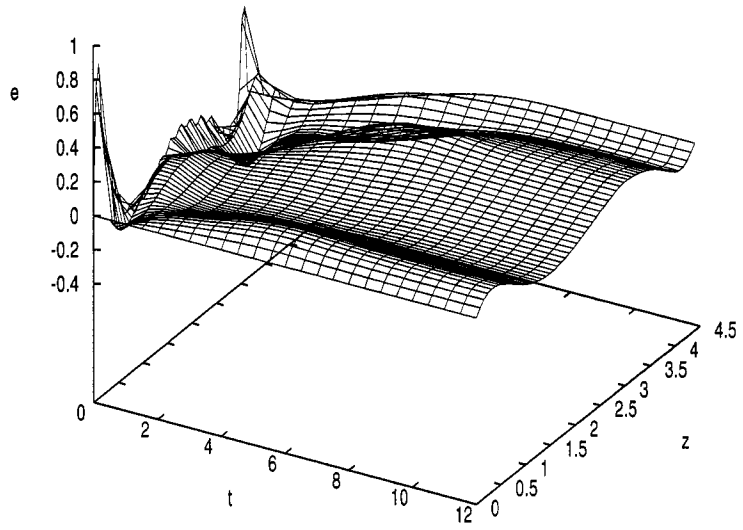


Figure 3.8: Deviation between the third-order model and the high-order discretization of the PDE ($k(z) = e^{-0.4\,z}$).

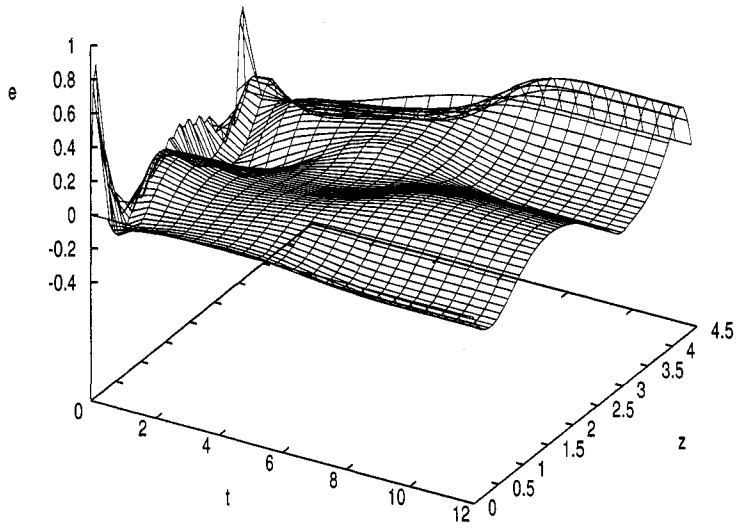


Figure 3.9: Deviation between the third-order model and the high-order discretization of the PDE ($k(z) = e^{-0.6\,z}$).

In both case, the maximum error between the two models is less than 1.6%, implying the robustness of the proposed model reduction procedure with respect to significant variations in the initial conditions.

Finally, we used the reduced-order models to synthesize nonlinear output feedback controllers using geometric methods; see [3] for details on controller design. Specifically, a second-order controller was synthesized on the basis of a second-order model obtained using Galerkin's method with the first two empirical eigenfunctions as basis functions. The control objective is to stabilize the system at the unstable steady state $\bar{x}(z,t) = 0$, using one point measurement of the state at $z = \dfrac{l(t)}{3}$ (i.e., moving sensor with $s(z,t) = \delta(z - \dfrac{1}{3}l(t))$, where $\delta(\cdot)$ is the Dirac function). Performing a linearization of the PDE system around the spatially uniform steady-state, we found that the first two modes are

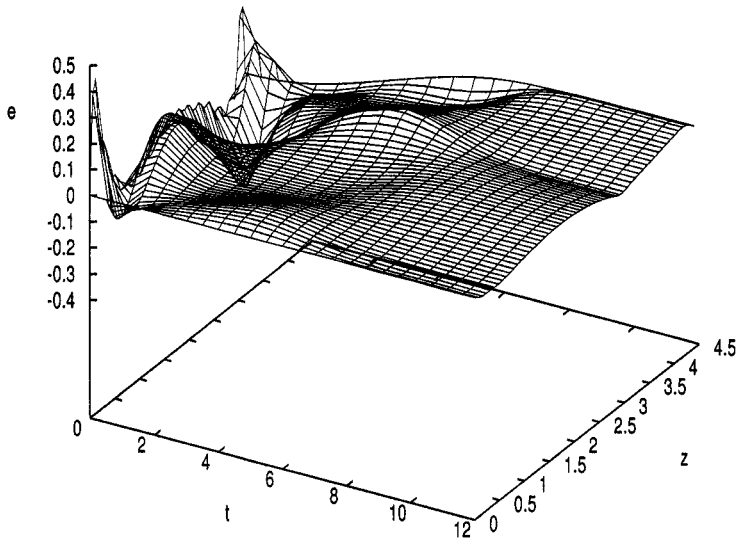


Figure 3.10: Deviation between the third-order model and the high-order discretization of the PDE ($\bar{x}_0(z) = 0.5 + 0.5sin(z)$).

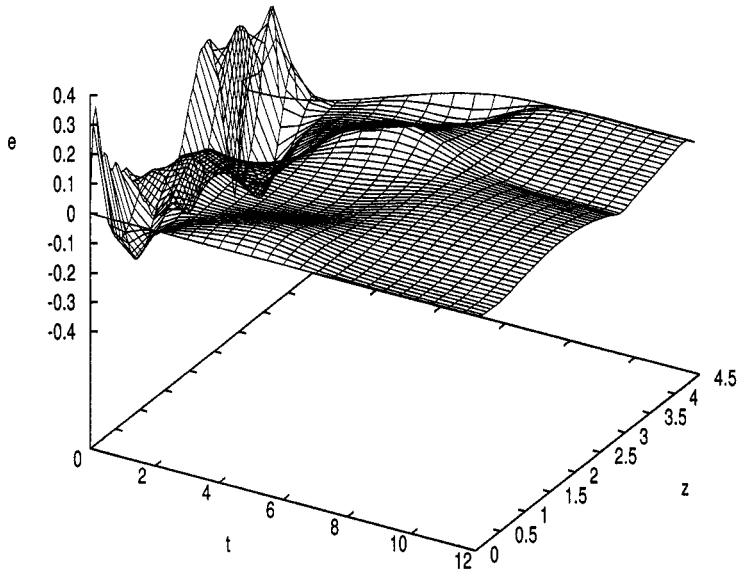


Figure 3.11: Deviation between the third-order model and the high-order discretization of the PDE ($\bar{x}_0(z) = 0.4 + 0.6sin(3\ z)$).

unstable. Therefore, the controlled outputs were defined as:

$$\begin{aligned} y_{c1}(t) &= \int_0^{l(t)} \phi_1(z,t)\bar{x}(z,t)dz, \\ y_{c2}(t) &= \int_0^{l(t)} \phi_2(z,t)\bar{x}(z,t)dz \end{aligned} \tag{3.28}$$

where $\phi_i$ denotes the i-th empirical eigenfunction. The actuator distribution functions were taken to be $b_1(z,t) = 1$ (uniform in space, distributed control action) and $b_2(z,t) = \delta(z - \frac{2}{3}l(t))$ (moving point control actuation).

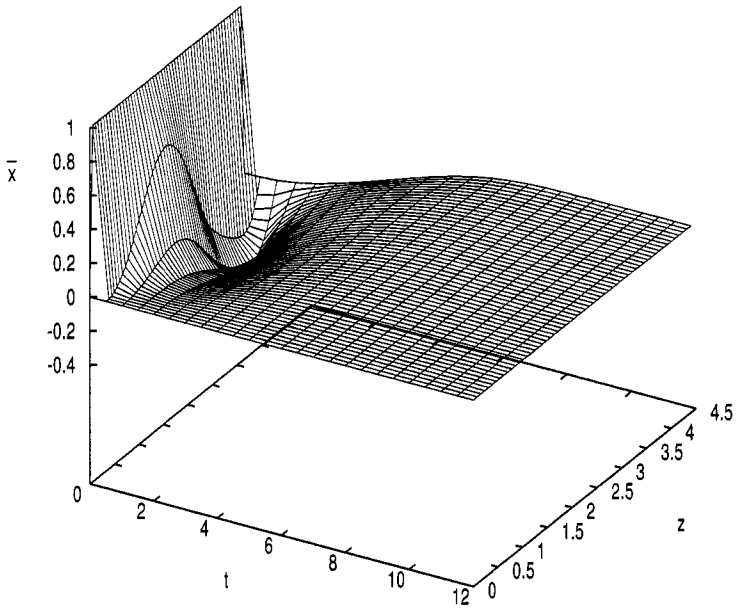


Figure 3.12: Closed-loop profile of $\bar{x}$ under nonlinear output feedback control using empirical eigenfunctions ($m = 2$).

Figure 3.12 shows the evolution of the closed-loop rod temperature profile under the nonlinear output feedback controller, while Figure 3.13 shows the corresponding manipulated input profiles. Clearly, the proposed controller achieves regulating the temperature profile at the spatially uniform steady state $\bar{x}(z,t) = 0$. For the sake of comparison, we also constructed finite-dimensional models using Galerkin's method with the analytical eigenfunctions of Eq.3.27 as basis functions, and we used the resulting models for the synthesis of nonlinear output feedback controller utilizing the result of theorem 1 in [3].

We found that the lowest-order controller that achieves stabilization of the PDE system at $\bar{x}(z,t) = 0$ is of order 4. Therefore, we observe a significant reduction on the order of the controller that stabilizes the system at the spatially uniform steady state when we use empirical eigenfunctions as basis functions. This again happens because the empirical eigenfunctions take into consideration the spatial variation of the coefficients of the process model, while the analytical eigenfunctions were derived on the basis of the spatially uniform spatial operator, and thus, they do not capture the spatially varying features of the process.

**Remark 3.1:** To illustrate the applicability of the proposed approach to parabolic PDE systems with spatially-uniform coefficients and show that its predictions are very close to the ones of models obtained by using Galerkin's method with the eigenfunctions of the spatial differential operator as basis functions, we considered the PDE system of Eq.3.19 with:

$$\beta_T = 75.0, \quad k = 1.0 \tag{3.29}$$

For this system, the steady-state $\bar{x}(z,t) = 0$ is also unstable and the eigenfunctions of the spatial operator can be computed analytically and are given in Eq.3.27. Furthermore, for this system, we constructed a representative ensemble of solutions by varying the initial conditions and the inputs and used it to construct a set of seven empirical eigenfunctions. Then, we employed Galerkin's method to construct two fifth-order models corresponding to the two different sets of basis functions (analytical and empirical). Figure 3.14 shows that the discrepancy between these two fifth-order models is extremely small, thereby implying that the use of empirical eigenfunctions leads to accurate low-order models for parabolic PDE systems with spatially-uniform coefficients as well. We finally note that the accuracy of these fifth-order models to the high-order discretization of the PDE is comparable to the one of Figure 3.4.

To illustrate the applicability of the proposed approach to construct low-order models

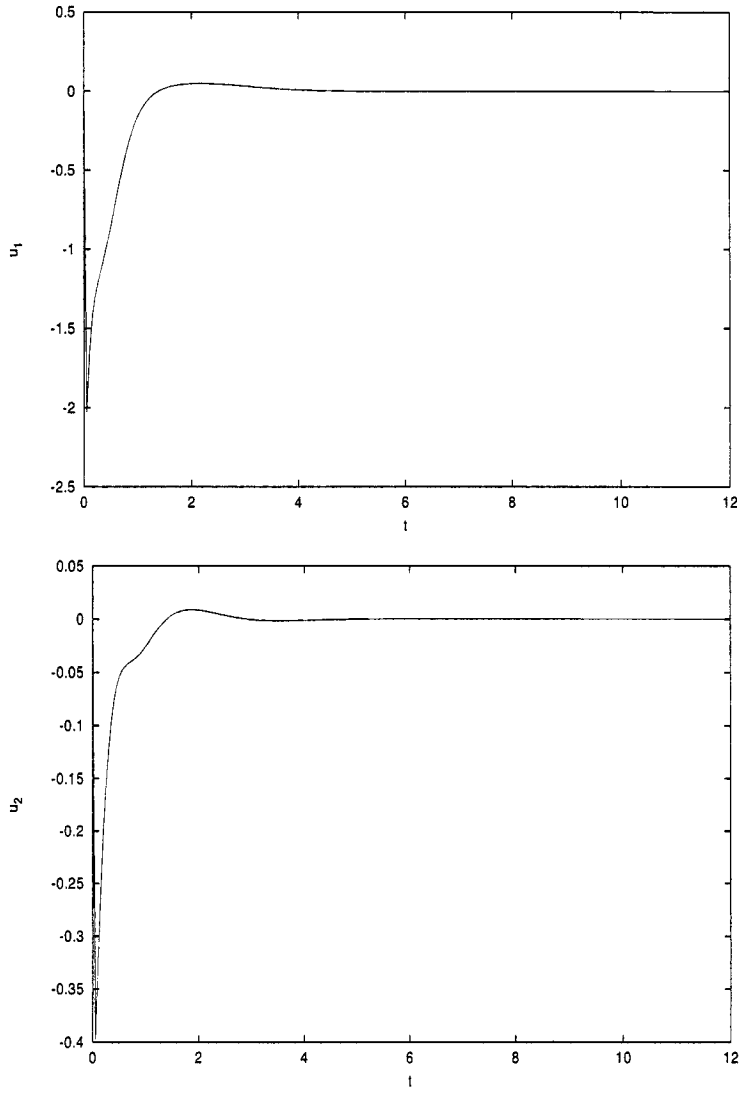


Figure 3.13: Manipulated input profiles for output feedback controller.

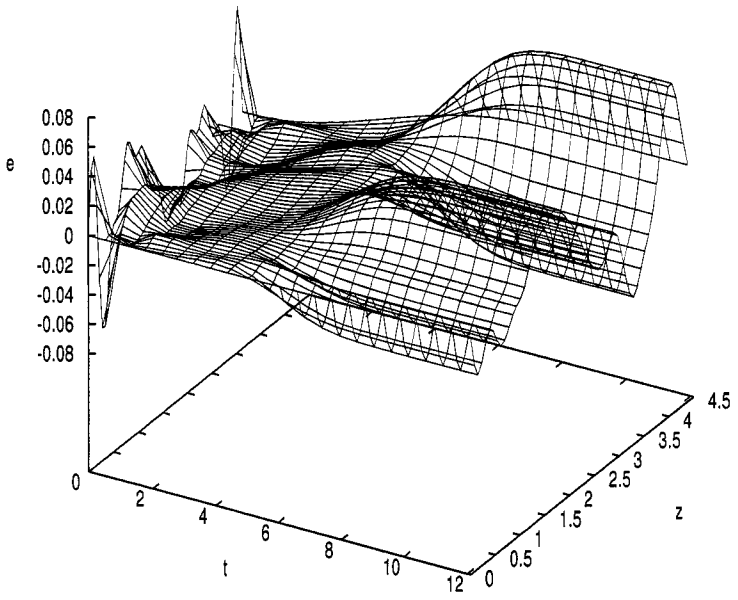


Figure 3.14: Deviation between the two fifth-order models computed by using Galerkin's method with analytical and empirical eigenfunctions, respectively ($\beta_T = 75.0$ and $k = 1.0$).

that can accurately reproduce the solution of parabolic PDE systems with time-varying inputs, we considered the PDE system of Eq.3.19 with $\beta_T = 10e^{(2.35-0.8z)}$, $k = 1.0$, $\beta_U = 2.0$, $\gamma = 4.0$, $b(z) = \delta(z - \frac{\pi}{2})$ and $l(t) = \pi$. Galerkin's method with the eigenfunctions of Eq.3.27 as basis functions was used to construct an accurate 30-th discretization of the PDE that was employed in the construction of the ensemble of solutions. Figure 3.15 shows the evolution of the state of the PDE for $u(t) = 0$ starting from initial conditions which are very close to the steady-state $\bar{x}(z,t) = 0$. We observe that the system moves to another steady-state which is characterized by a maximum, which implies that the steady state $\bar{x}(z,t) = 0$ is an unstable one, and thus, the system moves to a stable spatially non-uniform steady state.

In order to compute a set of empirical eigenfunctions, we initially constructed an ensemble of 1010 solutions of the high-order discretization of the PDE of Eq.3.25 by varying the initial conditions and the inputs to the system. The Karhunen-Loéve expansion was then applied to the developed ensemble of solutions to compute two empirical eigenfunctions that describe the dominant solution patterns embedded in the ensemble (they account for more than 99.2% of the energy included in the entire ensemble). The first

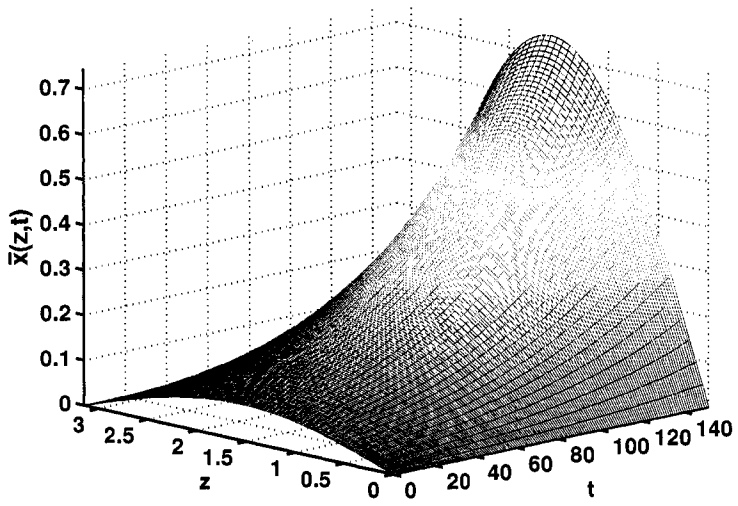


Figure 3.15: Profile of $\bar{x}$ for spatially varying $\beta_T$; $u(t) = 0$.

two of these empirical eigenfunctions are presented in Figure 3.16. We considered a time-varying input of the form $u(t) = 1.75sin(t)$. Figure 3.17 shows the evolution of the state of the PDE starting from initial conditions which are close to the stable steady-state. We observe that the state of the system changes continuously with respect to time. We applied Galerkin's method with the first two empirical eigenfunctions as basis functions to the PDE to construct a second-order model. Figure 3.18 shows the deviation between the spatiotemporal profiles of the state of the system computed by the second-order ODE model and high-order discretization of the PDE; we observe a very good agreement between the two models after a short initial transient. For the sake of comparison, we also constructed a third-order approximation of the PDE by using Galerkin's method with the first three eigenfunctions of Eq.3.27 as basis functions (this set of eigenfunctions is the result of the solution of the eigenvalue problem of the spatial operator for constant values of $k$). We observe that the error (Figure 3.19) between this third-order model and the high-order discretization of the PDE is overall larger than the one of Figure 3.18 (note that a significant error is sustained for all times); this is a result of the fact that this

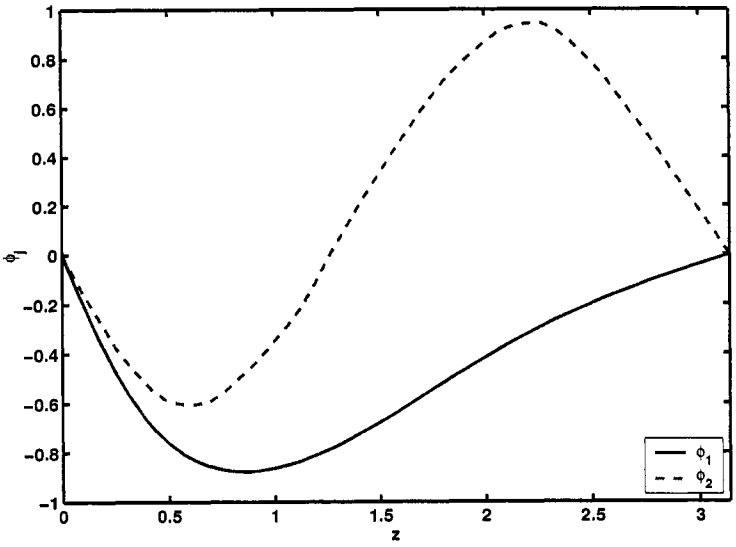


Figure 3.16: First two empirical eigenfunctions.

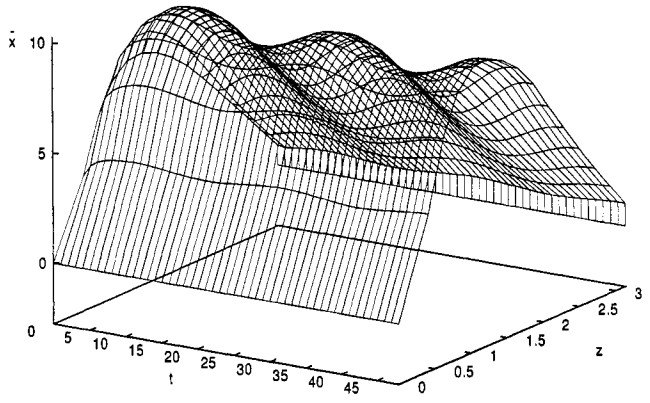


Figure 3.17: Profile of $\bar{x}$ for spatially varying $\beta_T$; $u(t) = 1.75sin(t)$.

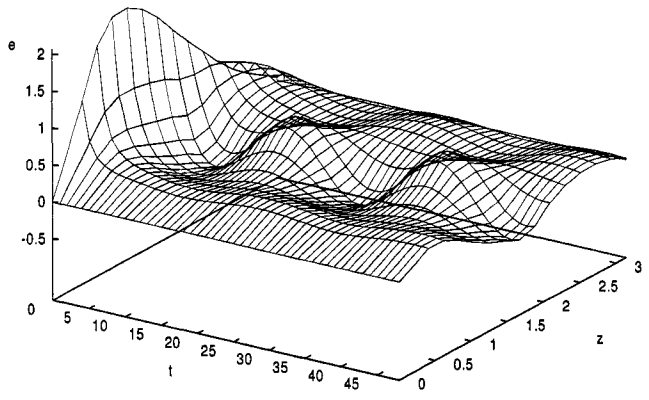


Figure 3.18: Deviation between the second-order model and the high-order discretization of the PDE - time-varying input.

approach does not account for the spatial variation of $\beta_T$.

## 3.4 Conclusion

In this chapter, we presented a technique for the construction of reduced-order models for a class of quasi-linear parabolic PDEs with spatially-varying coefficients and time-dependent spatial domain. The technique was successfully applied to a diffusion-reaction process example.

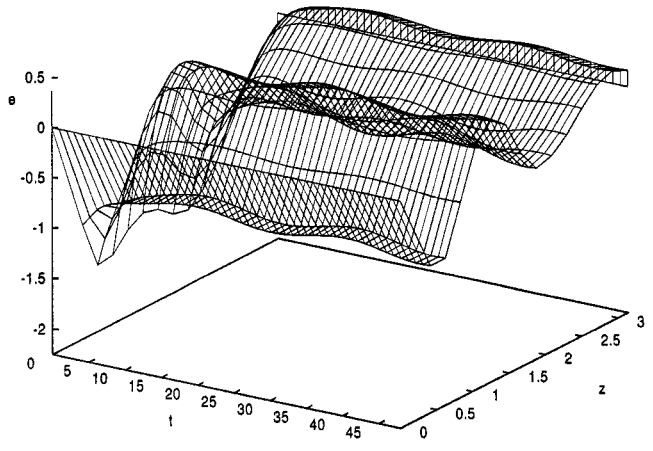


Figure 3.19: Deviation between the third-order model and the high-order discretization of the PDE (sinusoidal functions used as basis functions) - time-varying input.

# Chapter 4

# Predictive Control of Linear Parabolic PDEs with State and Control Constraints

## 4.1 Introduction

Transport-reaction processes that are characterized by significant spatial variations due to the underlying diffusion and convection phenomena. The dynamic models of transport-reaction processes over finite spatial domains typically consist of parabolic partial differential equation (PDE) systems whose spatial differential operators are characterized by a spectrum that can be partitioned into a finite (possibly unstable) slow part and an infinite stable fast complement [20]. The traditional approach to control of linear/quasi-linear parabolic PDEs involves the application of spatial discretization techniques to the PDE system to derive systems of ordinary differential equations (ODEs) that accurately describe the dynamics of the dominant (slow) modes of the PDE system. The finite-dimensional systems are subsequently used as the basis for the synthesis of finite-dimensional controllers (e.g., see [8, 50, 18]). A potential drawback of this approach, especially for quasi-linear parabolic PDEs, is that the number of modes that should be

retained to derive an ODE system that yields the desired degree of approximation may be very large, leading to complex controller design and high dimensionality of the resulting controllers.

Motivated by these considerations, significant recent work has focused on the development of a general framework for the synthesis of low-order controllers for quasi-linear parabolic PDE systems – and other highly dissipative PDE systems that arise in the modeling of spatially-distributed systems – on the basis of low-order nonlinear ODE models derived through a combination of the Galerkin method (using analytical or empirical basis functions) with the concept of inertial manifolds [14]. Using these order reduction techniques, a number of control-relevant problems, such as nonlinear and robust controller design, dynamic optimization, and control under actuator saturation have been addressed for various classes of dissipative PDE systems (e.g., see [17, 7, 5, 26] and the book [14] for results and references in this area). In addition to these works, other recent studies in control of PDE systems include [57, 22]. The approaches proposed in the above works, however, do not address the issue of state constraints in the controller design. Operation of transport-reaction processes typically requires that the state of the closed–loop system be maintained within certain bounds to achieve acceptable performance (for example, requiring reactor temperature not to exceed a certain value or requiring a product concentration not to drop below some purity requirement). Handling both state and control constraints – the latter typically arising due to the finite capacity of control actuators – in the design of the controller, therefore, is an important consideration.

Model Predictive Control (MPC), also known as receding horizon control, is a popular control method for handling constraints (both on manipulated inputs and state variables) within an optimal control setting. In MPC, the control action is obtained by solving repeatedly, on-line, a finite-horizon constrained open-loop optimal control problem. The popularity of this approach stems largely from its ability to handle, among other issues, multi-variable interactions, constraints on controls and states, and optimization require-

ments. Numerous research studies have investigated the properties of model predictive controllers and led to a plethora of MPC formulations that focus on a number of control-relevant issues, including issues of closed–loop stability, performance, implementation and constraint satisfaction (e.g., see [35, 2, 49, 45] for surveys of results and references in this area).

Most of the research in the area of predictive control, however, has focused on lumped-parameter processes modeled by ODE systems. Compared with lumped-parameter systems, the problem of designing predictive controllers for distributed parameter systems, modeled by PDEs, has received much less attention. Of the few results available on this problem, some have focused on analyzing the receding horizon control problem on the basis of the infinite-dimensional system using control Lyapunov functionals (e.g., [40]), while others have used spatial discretization techniques such as finite differences (e.g., [24]) to derive approximate ODE models (of possibly high-order) for use within the MPC design, thus leading to computationally expensive model predictive control designs that are, in general, difficult to implement on–line.

Motivated by the above considerations, we focus in this chapter on the development of a framework for the design of predictive controllers for linear parabolic PDEs with state and control constraints. The rest of the chapter is organized as follows. In section 4.2, a class of parabolic PDEs is described and formulated as an infinite-dimensional system, and the predictive control problem is formulated on the basis of the infinite-dimensional system. Then, in section 4.3, modal decomposition techniques are used to derive a finite-dimensional system that captures the dominant dynamics of the infinite-dimensional system and to express the state constraints for the infinite dimensional system in terms of the finite dimensional system state constraints. A number of MPC formulations, designed on the basis of different finite-dimensional approximations, are presented and compared. The closed–loop stability properties of the infinite dimensional system under the low order MPC controller designs are analyzed and sufficient conditions, which guarantee sta-

bilization and state constraint satisfaction for the infinite dimensional system under the reduced order MPC formulations, are derived. We also present other formulations which differ in the way the evolution of the fast eigenmodes is accounted for in the performance objective and state constraints. The impact of these differences on the ability of the predictive controller to enforce closed-loop stability and state constraints satisfaction in the infinite-dimensional system is analyzed. Finally, in section 4.4, the MPC formulations are applied, through simulations, to the problem of stabilizing the spatially-uniform unstable steady-state of a linear parabolic PDE subject to state and control constraints.

## 4.2 Preliminaries

### 4.2.1 Parabolic PDEs

To provide motivation for the class of infinite dimensional systems considered, we focus on a linear parabolic PDE with distributed control of the form:

$$\frac{\partial \bar{x}}{\partial t} = b\frac{\partial^2 \bar{x}}{\partial z^2} + c\bar{x} + w\sum_{i=1}^{m} b_i(z)u_i \tag{4.1}$$

with the following boundary and initial conditions:

$$\bar{x}(0,t) = 0, \ \bar{x}(\pi,t) = 0, \ \bar{x}(z,0) = \bar{x}_0(z) \tag{4.2}$$

subject to the following input and state constraints:

$$u_i^{min} \leq u_i \leq u_i^{max}, \ i = 1, \cdots, m \tag{4.3}$$

$$\chi^{min} \leq \int_0^{\pi} r(z)\bar{x}(z,t)dz \leq \chi^{max} \tag{4.4}$$

where $\bar{x}(z,t)$ denotes the state variable, $z \in [0,\pi]$ is the spatial coordinate, $t \in [0,\infty)$ is the time, $u_i \in \mathbb{R}$ denotes the $i$-th constrained manipulated input; $u_i^{min}$ and $u_i^{max}$ are real numbers representing the lower and upper bounds on the $i$-th input, respectively, and $\chi^{min}$ and $\chi^{max}$ are real numbers representing the lower and upper state constraints, respectively. The term $\frac{\partial^2 \bar{x}}{\partial z^2}$ denotes the second-order spatial derivative of $\bar{x}$; $b$, $c$ and $\omega$ are constant coefficients with $b > 0$, and $\bar{x}_0(z)$ is a sufficiently smooth function of $z$. The

function $b_i(z)$ is a known smooth function of $z$ that describes how the control action, $u_i(t)$, is distributed in the spatial interval $[0, \pi]$. Whenever the control action is applied to the spatial domain at a single point $z_a$, with $z_a \in [0, \pi]$ (i.e., point actuation), the function $b_i(z)$ is taken to be nonzero in a finite spatial interval of the form $[z_a - \mu, z_a + \mu]$, where $\mu$ is a small positive real number, and zero elsewhere in $[0, \pi]$. The smooth function $r(z)$ is a "state constraint distribution" function that describes how the state constraint is enforced in the spatial domain $[0, \pi]$. Throughout this chapter, the notation $|\cdot|$ will be used to denote the standard Euclidian norm in $\mathbb{R}^n$, while the notation $|\cdot|_Q$ will be used to denote the weighted norm defined by $|\hat{x}|_Q^2 = \hat{x}'Q\hat{x}$, where $Q$ is a positive-definite matrix and $\hat{x}'$ denotes the transpose of $\hat{x}$. A function $\beta(r, s) : [0, a) \times [0, \infty) \to [0, \infty)$ is said to be of class $\mathcal{KL}$ if, for each fixed $s \geq 0$, the mapping $\beta(r, s)$ is continuous, strictly increasing with respect to $r$ and satisfies $\beta(0, s) = 0$, and, for each fixed $r$, the mapping $\beta(r, s)$ is decreasing with respect to $s$ and $\beta(r, s) \to 0$, as $s \to \infty$.

To proceed with the presentation of our results, we formulate the PDE of Eqs.4.1-4.2-4.3-4.4 as an infinite dimensional system in the state space $\mathcal{H} = L_2(0, \pi)$, with inner product and norm

$$(\omega_1, \omega_2) = \int_0^\pi \omega_1(z)\omega_2(z)\, dz\,, \quad \|\omega_1\|_2 = (\omega_1, \omega_1)^{\frac{1}{2}} \tag{4.5}$$

where $\omega_1, \omega_2$ are two elements of $L_2(0, \pi)$.

Defining the state function $x(t)$ on the state-space $\mathcal{H}$ as

$$x(t) = \bar{x}(z, t), \quad t > 0, \quad 0 < z < \pi, \tag{4.6}$$

the operator $\mathcal{A}$ as

$$\mathcal{A}\phi \;=\; b\frac{d^2\phi}{dz^2} + c\phi, \quad 0 < z < \pi, \tag{4.7}$$

where $\phi(z)$ is a smooth function on $(0, \pi)$ with $\phi(0) = 0$ and $\phi(\pi) = 0$, with the following dense domain

$$\begin{aligned} \mathcal{D}(\mathcal{A}) \;=\; \{\phi(z) \in L_2(0, \pi) : \phi(z), \frac{d\phi(z)}{dz} \text{ are absolutely continuous,} \\ \mathcal{A}\phi \in L_2(0, \pi), \phi(0) = 0 \text{ and } \phi(\pi) = 0\}, \end{aligned} \tag{4.8}$$

the input operator as:

$$\mathcal{B}u = \sum_{i=1}^{m} b_i(\cdot)u_i, \tag{4.9}$$

and the state constraint as:

$$\chi^{min} \leq (r, x) \leq \chi^{max}, \tag{4.10}$$

the system of Eqs.4.1-4.2-4.3-4.4 can be written as:

$$\dot{x} = \mathcal{A}x + \mathcal{B}u\,, \quad x(0) = x_0\,, \tag{4.11}$$

$$u_i^{min} \leq u_i(t) \leq u_i^{max}\,, \tag{4.12}$$

$$\chi^{min} \leq (r, x) \leq \chi^{max} \tag{4.13}$$

The spectrum of $\mathcal{A}$ can be obtained by solving the following eigenvalue problem:

$$\mathcal{A}\phi_j = b\frac{d^2\phi_j}{dz^2} + c\phi_j = \lambda_j\phi_j \tag{4.14}$$

subject to

$$\phi_j(0) = \phi_j(\pi) = 0 \tag{4.15}$$

where $\lambda_j$ denotes an eigenvalue and $\phi_j$ denotes an eigenfunction. A direct computation of the solution of the above eigenvalue problem yields

$$\lambda_j = c - bj^2, \;\; \phi_j(z) = \sqrt{\frac{2}{\pi}}sin(j\,z), \;\; j = 1, \ldots, \infty \tag{4.16}$$

The spectrum of $\mathcal{A}$, $\sigma(\mathcal{A})$, is defined as the set of all eigenvalues of $\mathcal{A}$, i.e., $\sigma(\mathcal{A}) = \{\lambda_1, \lambda_2, \ldots\}$. From the expression for the eigenvalues, it is clear that all the eigenvalues of $\mathcal{A}$ are real, and that, for a given $b$ and $c$, only a finite number of unstable eigenvalues exist, and the distance between any two consecutive eigenvalues (i.e., $\lambda_j$ and $\lambda_{j+1}$) increases as $j$ increases. Furthermore, $\sigma(\mathcal{A})$ can be partitioned as $\sigma(\mathcal{A}) = \sigma_1(\mathcal{A}) \bigcup \sigma_2(\mathcal{A})$, where $\sigma_1(\mathcal{A}) = \{\lambda_1, \ldots, \lambda_m\}$ contains the first $m$ (with $m$ finite) "slow" eigenvalues (including all, if any, possibly unstable eigenvalues) and $\sigma_2(\mathcal{A}) = \{\lambda_{m+1}, \lambda_{m+2}, \ldots\}$ contains the remaining "fast" stable eigenvalues. This implies that the dominant dynamics of the

PDE can be described by a finite-dimensional system, and motivates the use of modal decomposition to derive a finite-dimensional system that captures the dominant (slow) dynamics of the PDE.

From the properties of $\mathcal{A}$ and its spectrum, it follows (Theorem 2.10 in [20]) that $\mathcal{A}$ generates a strongly continuous $C_0$-semigroup, $\mathcal{T}(t)$. Moreover, since $\mathcal{B}$ is a bounded operator, the system of Eq.4.11 has a mild solution (Theorem 2.31 in [20]) of the form:

$$x(t) = \mathcal{T}(t)x_0 + \int_0^t \mathcal{T}(t-\tau)\mathcal{B}u(\tau)d\tau \tag{4.17}$$

**Remark 4.1:** Note that while we use the PDE system of Eqs.4.1-4.4 to motivate and illustrate the development of the infinite dimensional system of Eq.4.11, our subsequent results are not limited to single PDEs of the form of Eqs.4.1-4.4. The results developed in this work apply to parabolic PDEs, with possibly other types of boundary condition (for example, mixed boundary condition), and also systems of parabolic PDEs, as long as they possess operators $\mathcal{A}$ for which the eigenspectrum can be partitioned into $\sigma_1(\mathcal{A})$ and $\sigma_2(\mathcal{A})$, where $\sigma_1(\mathcal{A})$ and $\sigma_2(\mathcal{A})$ possess the properties described above.

### 4.2.2 MPC formulation

Referring to the system of Eq.4.11, we consider the problem of asymptotic stabilization of the origin, subject to the control constraints of Eq.4.12 and the state constraint of Eq.4.13. The problem will be addressed within the MPC framework (see [45] for a review of various MPC algorithms for finite-dimensional systems) where the control, at state $x$ and time $t$, is conventionally obtained by solving, on-line, a finite-horizon constrained optimal control problem of the form:

$$P(x,t) : \min\{J(x,t,u(\cdot)) \mid u(\cdot) \in S\} \tag{4.18}$$

$$\begin{aligned} s.t.\ \dot{x}(\tau) &= \mathcal{A}x(\tau) + \mathcal{B}u(\tau) \\ u(\tau) &\in \mathcal{U} \\ \chi^{min} &\leq (r, x(\tau)) \leq \chi^{max},\ \tau \in [t, t+T] \end{aligned} \tag{4.19}$$

where $S = S(t,T)$ is the family of piecewise continuous functions (functions continuous from the right), with period $\Delta$, mapping $[t, t+T]$ into $\mathcal{U} := \{u \in \mathbb{R}^m : u_i^{min} \leq u_i \leq u_i^{max},\ i = 1, \cdots, m\}$, and $T$ is the specified horizon. A control $u(\cdot)$ in $S$ is characterized by the sequence $u[k]$, where $u[k] := u(k\Delta)$, and satisfies $u(t) = u[k]$ for all $t \in [k\Delta, (k+1)\Delta)$. The performance index is given by

$$J(x,t,u(\cdot)) = \int_t^{t+T} \left[q\|x^u(\tau;x,t)\|_2^2 + |u(\tau)|_R^2\right] d\tau + F(x(t+T)) \tag{4.20}$$

where $q$ is a strictly positive real number, $x^u(\tau;x,t)$ denotes the solution of Eq.4.11, due to control $u$, with initial state $x$ at time $t$, and $F(\cdot)$ denotes the terminal penalty. The minimizing control $u^0(\cdot) \in S$ is then applied to the system over the interval $[k\Delta, (k+1)\Delta]$ and the procedure is repeated indefinitely. This defines an implicit model predictive control law

$$M(x) := u^0(t;x,t) \tag{4.21}$$

The predictive controller problem of Eqs.4.18-4.19 is formulated on the basis of the infinite dimensional system, and therefore, it leads to a predictive controller that is of higher-order and can not be readily implemented in practice. To overcome this problem, in the next section, we develop computationally efficient predictive control formulations that achieve stabilization of the system of Eq.4.11 subject to the control and state constraints of Eqs.4.12-4.13.

**Remark 4.2:** It is well known that even for the finite-dimensional system the control law defined by Eqs.4.18-4.21 is not necessarily stabilizing. For finite-dimensional systems, the issue of closed-loop stability is usually addressed by means of imposing suitable penalties and constraints on the state at the end of the optimization horizon (e.g., see [2, 45] for surveys of different approaches).

## 4.3 Predictive control of infinite dimensional systems

Initially, we apply modal decomposition techniques to the system of Eq.4.11 to derive a finite-dimensional system that captures the dominant dynamics of the infinite-dimensional system. The state constraints of the infinite-dimensional system are appropriately expressed in terms of constraints on the finite-dimensional system. The finite-dimensional system is used for construction of a low-order predictive controller and the closed–loop stability properties of the infinite dimensional system are analyzed and sufficient conditions, which guarantee stabilization and state constraint satisfaction for the infinite dimensional system under the reduced-order predictive controller. Other MPC formulations, designed on the basis of the finite-dimensional approximations, that differ in the way the state constraints are handled within the optimization problem are then presented and compared in terms of their ability to enforce closed-loop stability and ensure constraint satisfaction for the state of the infinite dimensional system.

### 4.3.1 Modal decomposition

In this section, we apply standard modal decomposition to the infinite-dimensional system of Eq.4.11 to derive a finite-dimensional system. Let $\mathcal{H}_s$, $\mathcal{H}_f$ be modal subspaces of $\mathcal{A}$, defined as $\mathcal{H}_s = span\{\phi_1, \phi_2, \ldots, \phi_m\}$ and $\mathcal{H}_f = span\{\phi_{m+1}, \phi_{m+2}, \ldots\}$ (the existence of $\mathcal{H}_s$, $\mathcal{H}_f$ follows from the properties of $\mathcal{A}$). Defining the orthogonal projection operators, $P_s$ and $P_f$, such that $x_s = P_s x$, $x_f = P_f x$, the state $x$ of the system of Eq.4.11 can be decomposed as

$$x = x_s + x_f = P_s x + P_f x \tag{4.22}$$

Applying $P_s$ and $P_f$ to the system of Eq.4.11 and using the above decomposition for $x$, the system of Eq.4.11 can be re-written in the following equivalent form

$$\begin{aligned} \frac{dx_s}{dt} &= \mathcal{A}_s x_s + \mathcal{B}_s u, \quad x_s(0) = P_s x(0) = P_s x_0 \\ \frac{dx_f}{dt} &= \mathcal{A}_f x_f + \mathcal{B}_f u, \quad x_f(0) = P_f x(0) = P_f x_0 \end{aligned} \tag{4.23}$$

where $\mathcal{A}_s = P_s\mathcal{A}$, $\mathcal{B}_s = P_s\mathcal{B}$, $\mathcal{A}_f = P_f\mathcal{A}$, $\mathcal{B}_f = P_f\mathcal{B}$. In the above system, $\mathcal{A}_s$ is a diagonal matrix of dimension $m \times m$ of the form $\mathcal{A}_s = diag\{\lambda_j\}$ ($\lambda_j$ are possible unstable eigenvalues of $\mathcal{A}_s$) and $\mathcal{A}_f$ is an unbounded differential operator which is exponentially stable (following from the fact that $\lambda_{m+1} < 0$ and the selection of $\mathcal{H}_s, \mathcal{H}_f$). In the remainder of this chapter, we will refer to the $x_s$- and $x_f$-subsystems in Eq.4.23 as the slow and fast subsystems, respectively. From the properties of $\mathcal{A}_s$ and $\mathcal{A}_f$ and the fact that $\mathcal{B}_s$ and $\mathcal{B}_f$ are bounded operators, it follows (Theorem 2.10 and 2.31 in [20]) that there exist $C_0$-semigroups $\mathcal{T}_s$ and $\mathcal{T}_f$ such that the $x_s$- and $x_f$ subsystems of Eq.4.23 admit, on the interval $t \in [0, \infty)$, the following mild solutions:

$$x_s(t) = \mathcal{T}_s(t)x_s(0) + \int_0^t \mathcal{T}_s(t-\tau)\mathcal{B}_s u(\tau)d\tau \tag{4.24}$$

$$x_f(t) = \mathcal{T}_f(t)x_f(0) + \int_0^t \mathcal{T}_f(t-\tau)\mathcal{B}_f u(\tau)d\tau \tag{4.25}$$

Furthermore, since $\mathcal{A}_f$ is a stable operator, the spectrum of $\mathcal{A}_f$ satisfies $sup\ \{Re\ \sigma(\mathcal{A}_f)\} < -\gamma$, for some $\gamma > |c - b(m+1)^2|$, and thus, $\mathcal{T}_f(t)$ satisfies ([20], $p.74$):

$$\|\mathcal{T}_f(t)\|_2 \leq M_0 e^{-\gamma t}, \quad t \geq 0 \tag{4.26}$$

for some $M_0 > 0$.

### 4.3.2 MPC formulations: accounting for input and state constraints

We first present an MPC formulation, designed on the basis of the slow states of the system, that ensures stabilization of the infinite dimensional system. The MPC law in this case is obtained by solving, in a receding horizon fashion, the following optimization problem

$$\min_u \left[ \int_t^{t+T} \left[ q_s \|x_s(\tau)\|_2^2 + |u(\tau)|_R^2 \right] d\tau + F(x_s(t+T)) \right] \tag{4.27}$$

$$\begin{aligned} s.t.\ \ \dot{x}_s(\tau) &= \mathcal{A}_s x_s(\tau) + \mathcal{B}_s u(\tau) \\ u(\tau) &\in \mathcal{U} \\ \chi^{min} &\leq (r, x_s(\tau)) \leq \chi^{max}, \tau \in [t, t+T] \\ x_s(t+T) &= 0 \end{aligned} \tag{4.28}$$

To proceed, we assume that the predictive control law of Eqs.4.27-4.28, with a fixed horizon length $T$, is initially and successively feasible and achieves stabilization of the $x_s$-subsystem for all $x_s(0) \in \Omega_s \subset \mathcal{H}_s$. Note that the set $\Omega_s$ depends on the constraints on the states and inputs, the system dynamics and $T$ (see remarks 4.5 and 4.6 for discussion on this issue). This assumption is precisely stated below.

**Assumption 4.1:** *There exists a set $\Omega_s \subset \mathcal{H}_s$ such that for all $x_s(0) \in \Omega_s$, the steady-state solution $x_s(t) = 0$ of the closed-loop system of Eq.4.24 under the MPC law of Eqs.4.27-4.28 is asymptotically stable in the sense that $x_s(t) \in \Omega_s$ for all $t \geq 0$ and satisfies $||x_s(t)||_2 \leq \beta(||x_s(0)||_2, t)$, where $\beta(\cdot,\cdot)$ is a class $\mathcal{KL}$ function.*

Proposition 4.1 below establishes that a predictive control law of Eqs.4.27-4.28, for which Assumption 4.1 holds, achieves also asymptotic stability of the closed-loop infinite dimensional system.

**Proposition 4.1:** *Consider the system of Eq.4.11 subject to the input and state constraints of Eqs.4.12-4.13, under the predictive controller of Eqs.4.27-4.28 for which Assumption 4.1 holds. If the initial condition of the infinite dimensional system, $x(0)$, is such that $x_s(0) \in \Omega_s$, then $x(t) = 0$ is an asymptotically stable solution of the closed-loop infinite dimensional system.*

**Proof of Proposition 4.1**: We first note that the control law of Eqs.4.27-4.28 is only a function of the state of the slow subsystem $u = M(x_s)$ and satisfies $\lim_{t\to\infty} u(t) = 0$ (this follows from the assumption that $x(t) = 0$ is a steady-state solution of the closed-loop system of Eqs.4.24-4.27-4.28, Assumption 4.1). Using the decomposition of Eq.4.23, the closed–loop system of Eq.4.11 under the MPC of Eqs. 4.27-4.28 can therefore be written as a cascaded system of the form:

$$\frac{dx_s}{dt} = \mathcal{A}_s x_s + \mathcal{B}_s M(x_s) \tag{4.29}$$

$$\frac{dx_f}{dt} = \mathcal{A}_f x_f + \mathcal{B}_f M(x_s) \tag{4.30}$$

From Assumption 4.1, we have that since $x_s(0) \in \Omega_s$, $x_s(t)$ of Eq.4.29 satisfies $\|x_s(t)\| \leq \beta(\|x_s(0)\|_2, t)$ for all $t \geq 0$. We now show that the fast, $x_f$-subsystem of Eq.4.30, is also

asymptotically stable, and thus, the infinite-dimensional closed-loop system of Eqs.4.11-4.12-4.13 under the control of Eqs.4.27-4.28 is asymptotically stable. To this end, we first note that since $\mathcal{A}_f$ is a stable operator which generates a $C_0$-semigroup $\mathcal{T}_f$ that satisfies Eq.4.26 and $\mathcal{B}_f$ is a bounded operator (boundedness of $\mathcal{B}_f$ follows from the fact that $b(z) \in L_2(0,\pi)$), by taking the 2-norm in space of both sides of Eq.4.25, the following bound for the state of the $x_f$ subsystem of Eq.4.30 can be written:

$$\|x_f(t)\|_2 \leq Ke^{-\gamma t}\|x_f(0)\|_2 + \|\mathcal{B}_f\|_2 \left| \int_0^t e^{-\gamma(t-\tau)} u(\tau) d\tau \right| \tag{4.31}$$

where $K$ is a positive real number and $u(\tau) = M(x_s(\tau))$. Further, since $u(t)$ is bounded (i.e., $|u(t)| \leq \bar{u}$ where $\bar{u} = max\{|u^{max}|, |u^{min}|\}$) and $e^{-\gamma(t-\tau)} \geq 0$ for $0 \geq \tau \leq t$, Eq.4.31 can be written as:

$$\|x_f(t)\|_2 \leq Ke^{-\gamma t}\|x_f(0)\|_2 + \|\mathcal{B}_f\|_2 \sup_{0\leq\tau\leq t} |u(\tau)| \left| \int_0^t e^{-\gamma(t-\tau)} d\tau \right| \tag{4.32}$$

or

$$\|x_f(t)\|_2 \leq Ke^{-\gamma t}\|x_f(0)\|_2 + M_2 \sup_{0\leq\tau\leq t} |u(\tau)| \tag{4.33}$$

where $M_2 = \|\mathcal{B}_f\|_2/\gamma$. To use Eq.4.33 to prove that $\lim_{t\to\infty} \|x_f\|_2 = 0$, we need the following argument. First, we note that by taking the supremum over time of both sides of the inequality of Eq.4.33, we have:

$$\sup_{t\geq 0} \|x_f(t)\|_2 \leq K\|x_f(0)\|_2 + M_2\bar{u} =: \bar{K} \tag{4.34}$$

The fact that the inequality of Eq.4.33 holds for every initial time, $t_0$, yields that for $\forall$ $t \geq t_0$:

$$\|x_f(t)\|_2 \leq Ke^{-\gamma(t-t_0)}\|x_f(t_0)\|_2 + M_2 \sup_{\tau\geq t_0} |u(\tau)| \tag{4.35}$$

Taking $t_0 = \frac{t}{2}$ and using the bound of Eq.4.34 in Eq.4.35, we have

$$\|x_f(t)\|_2 \leq Ke^{-\gamma\frac{t}{2}}\bar{K} + M_2 \sup_{\tau\geq\frac{t}{2}} |u(\tau)| \tag{4.36}$$

Taking the limit of both sides as $t \rightarrow \infty$ and using that $\lim_{t\rightarrow\infty} \sup_{\tau\geq t} u(\tau) = 0$ (this follows directly from $\lim_{t\rightarrow\infty} u(t) = 0$), we finally have

$$\lim_{t\rightarrow\infty} \|x_f(t)\|_2 \leq \lim_{t\rightarrow\infty}(Ke^{-\gamma\frac{t}{2}}\bar{K}) + \lim_{t\rightarrow\infty}(M_2 \sup_{\tau\geq\frac{t}{2}}|u(\tau)|) = 0 \tag{4.37}$$

We therefore have that $\lim_{t\rightarrow\infty} \|x_f\|_2 = 0$, and thus, the infinite dimensional closed–loop system is asymptotically stable; this completes the proof of Proposition 4.1.

**Remark 4.3:** Note that the above formulation is designed on the basis of the slow subsystem only. The evolution of the fast states is neither accounted for in the cost function nor in the state constraints. While the resulting MPC controller enforces closed-loop stability of the infinite dimensional system, a potential drawback of this formulation is the fact that there is no guarantee that the state constraints for the infinite dimensional system will be satisfied. This may occur because the controller design neglects the dynamics of the fast modes, and, the satisfaction of $\chi^{min} \leq (r, x_s) \leq \chi^{max}$ does not guarantee that $\chi^{min} \leq (r, x_s + x_f) = (r, x) \leq \chi^{max}$. So, while the stabilization objective can be achieved independently of the fast subsystem, the additional objective of state constraints satisfaction requires that the MPC controller, even if designed on the basis of the slow subsystem, in some way accounts for the contribution of the fast states to the state of the infinite dimensional system.

We now present a modification to the MPC controller of Eqs.4.27-4.28, and a sufficient condition on the initial condition of the fast subsystem such that the resulting control law, when applied to the infinite dimensional system, achieves both the objectives of stabilization and state constraint satisfaction for the infinite dimensional system. The key idea is to revise (shrink) the state constraint enforcement in the controller design, to compensate for the contribution to the infinite dimensional system state by the fast modes. By invoking input to state boundedness of the fast subsystem, we then derive appropriate bounds on the initial conditions for the fast subsystem which ensure state constraint satisfaction for the closed–loop infinite dimensional system. Proposition 2 below formalizes the input to state boundedness property and Theorem 1 states the

necessary conditions for state constraint satisfaction of the infinite dimensional system. To this end, consider the MPC formulation of Eqs.4.27-4.28 with the states constraints $\chi^{max}$, $\chi^{min}$ replaced by $S^{max}$ and $S^{min}$ as:

$$\min_{u} \left[ \int_{t}^{t+T} \left[ q_s \|x_s(\tau)\|_2^2 + |u(\tau)|_R^2 \right] d\tau + F(x_s(t+T)) \right] \tag{4.38}$$

$$\begin{aligned} s.t.\ \dot{x}_s(\tau) &= \mathcal{A}_s x_s(\tau) + \mathcal{B}_s u(\tau) \\ u(\tau) &\in \mathcal{U} \\ S^{min} &\leq (r, x_s(\tau)) \leq S^{max}, \tau \in [t, t+T] \\ x_s(t+T) &= 0 \end{aligned} \tag{4.39}$$

where $S^{max} \leq \chi^{max} - \alpha$ and $S^{min} \geq \chi^{min} + \alpha$ where $\alpha$ is a positive real number, to be determined later. We denote the set of initial conditions for which the predictive controller of Eqs.4.38-4.39 satisfies the conditions of Assumption 4.1, as $\Omega'_s$.

**Proposition 4.2:** *Consider the system of Eq.4.11 and the input and state constraints of Eqs.4.12-4.13. There exist real numbers $M_1^*$ and $M_2^*$ such that $|(r, x_f(t))| \leq M_1^* \|x_f(0)\|_2 + M_2^* \bar{u}$, for all $t \geq 0$, where $\bar{u} = max\{|u^{max}|, |u^{min}|\}$.*

**Proof of Proposition 4.2**: First, using Hölder's inequality [52], we get

$$|\int_0^\pi r(z) f(z,\tau) dz| \ \leq \ \left( \int_0^\pi r(z)^2 dz \right)^{\frac{1}{2}} \times \left( \int_0^\pi f(z,\tau)^2 dz \right)^{\frac{1}{2}} \tag{4.40}$$

Let $M_3 = \left( \int_0^\pi |r(z)|^2 dz \right)^{\frac{1}{2}}$. Note that since $r(z)$ is a smooth function in $[0, \pi]$, $M_3$ is a positive real number. Recognizing that the term on the left hand side of the inequality is $|(r, x_f)|$, and the second term on the right hand side is $\|x_f\|_2$, we have that

$$|(r, x_f)| \ \leq \ M_3 \|x_f\|_2 \tag{4.41}$$

From Eq.4.33, using that $\sup_{0 \leq \tau \leq t} |u(\tau)| \leq \bar{u}$, it follows that

$$\|x_f(t)\|_2 \leq M_1 \|x_f(0)\|_2 + M_2 \bar{u} \tag{4.42}$$

where $M_1 = K$ and $M_2 = \|\mathcal{B}_f\|_2/\gamma$. Substituting Eq.4.42 into Eq.4.41, we have

$$|(r, x_f(t))| \leq M_1^* \|x_f(0)\|_2 + M_2^* \bar{u} \tag{4.43}$$

where $M_1^* = M_1 M_3$ and $M_2^* = M_2 M_3$. This completes the proof of Proposition 4.2.

**Theorem 4.1:** *Consider the system of Eq.4.11 subject to the input and state constraints of Eqs.4.12-4.13 under the predictive control law of Eqs.4.38-4.39 for which Assumption 4.1 holds with $x_s(0) \in \Omega_s'$. Then, given that there exists a positive real number $\delta$ such that $\chi^{max} - \chi^{min} \geq 2(M_2^* \bar{u} + \delta)$, where $M_2^*$, $\bar{u}$ were defined in Proposition 4.2, there exist positive real numbers $\alpha$ and $\beta$ such that if $x_s(0) \in \Omega_s'$ and $\|x_f(0)\|_2 \leq b$, then $x(t) = 0$ is an asymptotically stable solution of the closed-loop system and $\chi^{min} \leq (r, x(t)) \leq \chi^{max}$ for all $t \geq 0$.*

**Proof of Theorem 4.1**: Asymptotic stability of the closed-loop infinite dimensional system under the control law of Eqs.4.38-4.39 for which Assumption 4.1 holds with $x_s(0) \in \Omega_s'$ can be shown using similar arguments to the ones in the proof of Proposition 4.1. We now consider the problem of constraint satisfaction. First, we assume that there exists a positive real number $\delta$ such that $\chi^{max} - \chi^{min} \geq 2(M_2^* \bar{u} + \delta)$, where $M_2^*$, $\bar{u}$ were defined in Proposition 4.2. We also note that

$$(r, x_s + x_f) = (r, x_s) + (r, x_f) \tag{4.44}$$

and pick $\alpha = M_2^* \bar{u} + \delta$ and $\beta = \delta / M_1^*$. By picking $\|x_f(0)\|_2 \leq \beta$, we have that $-M_1^* \beta - M_2^* \bar{u} \leq (r, x_f(t)) \leq M_1^* \beta + M_2^* \bar{u}$ (Proposition 2), and moreover, $-\delta - M_2^* \bar{u} \leq (r, x_f(t)) \leq \delta + M_2^* \bar{u}$ and thus $-\alpha \leq (r, x_f(\tau)) \leq \alpha$.

Furthermore satisfaction of the constraint of $(r, x_s(\tau)) \leq S^{max} \leq \chi^{max} - \alpha$ implies $(r, x_s(\tau)) + \alpha \leq \chi^{max}$. This finally implies that $(r, x_s(\tau)) + (r, x_f(\tau)) = (r, x(\tau)) \leq \chi^{max}$ (since $\alpha \geq (r, x_f(\tau))$.

Similarly satisfaction of the constraint of $(r, x_s(\tau)) \geq S^{min} \geq \chi^{min} + \alpha$ implies

$(r, x_s(\tau)) - \alpha \geq \chi^{min}$ which implies $(r, x_s(\tau)) + (r, x_f(\tau)) \geq \chi^{min}$ (since $(r, x_f(\tau)) \geq -\alpha$) and finally $(r, x) \geq \chi^{min}$. This proves that for the above choices of $\alpha$ and $b$, the satisfaction of the constraint of $S^{min} \leq (r, x_s) \leq S^{max}$ implies $\chi^{min} \leq (r, x) \leq \chi^{max}$, which is the state constraint for the infinite dimensional system.

Note that the condition $\chi^{max} - \chi^{min} \geq 2(M_2^* \bar{u} + \delta)$ ensures that for this choice of $\alpha$, we get $S^{max} \geq S^{min}$, which is necessary for the optimization problem to be feasible. This completes the proof the Theorem 1.

**Remark 4.4:** Note that the conditions imposed on the initial conditions, and the revision of the state constraints in the controller design, are 'worst case' corrections, and are therefore only sufficient conditions. It may happen, for instance, that the controller design of Theorem 1, when implemented in the closed–loop may achieve infinite dimensional state constraint satisfaction, even if the fast modes of the infinite dimensional system do not satisfy the required condition ($\|x_f(0)\|_2 \leq \beta$). Satisfaction of the revised state constraints in the controller design, however, when done according to Theorem 4.1, guarantees state constraint satisfaction for the infinite dimensional system.

**Remark 4.5:** Note that the set of initial conditions for which a given MPC formulation is guaranteed to be initially and successively feasible is in general a complex function of the inherent dynamics of the system ($\mathcal{A}$, $\mathcal{B}$), the constraints on the input and the states ($u^{min}, u^{max}, \chi^{min}, \chi^{max}, r(\cdot)$) and the controller parameters ($T, Q, R$). Within the MPC framework, it is in general hard to come up with an explicit characterization of this set, and/or compare, for instances the sets $\Omega_s$ (of Proposition 4.1) and $\Omega_s'$ (of Theorem 4.1) or of the sets we subsequently define and this is not the focus of this work. What Theorem 1, and other formulations that follow do, is only to provide sufficient conditions that need to be incorporated in the reduced order MPC formulation that, upon satisfaction, guarantee state constraint satisfaction and stabilization for the infinite dimensional system.

**Remark 4.6:** The problem of implementing various MPC formulations within a hybrid

predictive control structure that provides an explicit characterization of the closed–loop stability region for linear systems with input constraints has been addressed in [27]. A similar approach can be utilized to provide an explicit characterization for the closed–loop stability region for finite dimensional input and state constrained systems. The use of the reduced order MPC formulations allows the use of these approaches because the set $\Omega_s$ only pertains to the set of initial conditions for a finite number of states, and can be obtained using the approach in [27]. Note that the initial conditions for the fast states only need to satisfy a bound, and hence are also characterized by a finite (in this case, one) number of conditions.

### 4.3.3 Higher-order MPC formulations

Since the MPC formulation of Theorem 4.1, instead of explicitly accounting for the fast mode dynamics, accounts, in some sense, for the 'worst case' dynamics, the formulation may be conservative in terms of restricting the set of initial conditions for which stabilization and state constraint satisfaction for the infinite dimensional system is accomplished. To alleviate this conservatism, we present two MPC formulations which explicitly account for the evolution of the $x_f$-subsystem.

One way to account for the effect of the fast states on the state constraints of the infinite dimensional system, is incorporating the fast states explicitly into the state constraints equation. The control action in this case is computed by solving the following optimization problem

$$\min_u \left[ \int_t^{t+T} \left[ q_s \|x_s(\tau)\|_2^2 + |u(\tau)|_R^2 \right] d\tau + F(x_s(t+T)) \right] \tag{4.45}$$

$$\begin{aligned} s.t.\ \ \dot{x}_s(\tau) &= \mathcal{A}_s x_s(\tau) + \mathcal{B}_s u(\tau) \\ \dot{x}_f(\tau) &= \mathcal{A}_f x_f(\tau) + \mathcal{B}_f u(\tau) \\ u(\tau) &\in \mathcal{U} \\ \chi^{min} &\leq (r, x_s(\tau) + x_f(\tau)) \leq \chi^{max} \\ x_s(t+T) &= 0,\ \tau \in [t, t+T] \end{aligned} \tag{4.46}$$

Note that for the set of initial conditions defined by $\Omega_i'$, for which this formulation is

initially and successively feasible, stabilization and state constraints satisfaction for the infinite dimensional system is achieved. Stabilization of the closed–loop system infinite-dimensional system under the formulation of Eqs.4.45-4.46 can be proved using a similar argument to the one in the proof of proposition 4.1. The implementation of the above controller, however, will require computation of the fast mode dynamics, which can only be done approximately in practice. The key feature of this formulation is that it underscores the fact that even when using a sufficiently high number of modes to simulate the dynamics of the fast modes, the fast modes need not be a part of the cost function, thereby keeping the computation requirement low.

**Remark 4.7:** The formulation of Eqs.4.45-4.46 represents a more straightforward approach to enforcing state constraint satisfaction, that of incorporating them exactly as constraints in the optimization problem. The drawback of doing this, though, is that the set of initial conditions for which this problem is feasible is infinite dimensional, and impossible to compute or even estimate. The realization that the stability of the slow states is sufficient to enforce stabilization of the infinite dimensional system allows the use of only the slow modes in the cost function and the stability constraint, thereby substantially reducing the computational requirement. In practice, the evolution of fast modes can be accounted for in the state constraint satisfaction by including a sufficiently high, but finite, number of fast modes.

In the formulation of Eq.4.46, the fast modes dynamics have been accounted exactly in the state constraints, which requires that the predictive controller integrates the dynamics of the fast modes, which might be computationally intensive. We now present another formulation that approximates the effect of the fast dynamics by exploiting the two time-scale separation between the slow and fast subsystems and deriving an approximate model that describes the evolution of the fast subsystem. We define $\epsilon := \frac{|Re\{\lambda_1\}|}{|Re\{\lambda_{m+1}\}|}$ and

multiply the $x_f$-subsystem of Eq.4.23 by $\epsilon$ to obtain the following system [14]:

$$\begin{aligned} \frac{dx_s}{dt} &= \mathcal{A}_s x_s + \mathcal{B}_s u \\ \epsilon\frac{dx_f}{dt} &= \mathcal{A}_{f\epsilon} x_f + \epsilon\mathcal{B}_f u \end{aligned} \tag{4.47}$$

where $\mathcal{A}_{f\epsilon}$ is an unbounded differential operator defined as $\mathcal{A}_{f\epsilon} = \epsilon\mathcal{A}_f$. Introducing the fast time scale $\bar{\tau} = \frac{t}{\epsilon}$, the system of Eq.4.47 takes the form:

$$\begin{aligned} \frac{dx_s}{d\bar{\tau}} &= \epsilon(\mathcal{A}_s x_s + \mathcal{B}_s u) \\ \frac{dx_f}{d\bar{\tau}} &= \mathcal{A}_{f\epsilon} x_f + \epsilon B_f u \end{aligned} \tag{4.48}$$

Setting $\epsilon = 0$, we get

$$\begin{aligned} \frac{d\bar{x}_s}{d\bar{\tau}} &= 0 \\ \frac{d\bar{x}_f}{d\bar{\tau}} &= \mathcal{A}_{f\epsilon}\bar{x}_f \end{aligned} \tag{4.49}$$

From the properties of $\mathcal{A}_{f\epsilon}$, we have that the solution of $x_f$-subsystem of Eq.4.23 can be approximated by $\bar{x}_f(t) = e^{\mathcal{A}_f t}\bar{x}_f(0)$ (note that from the properties of $\mathcal{A}_f$, it follows that $\mathcal{T}_f(t) = e^{\mathcal{A}_f t}$, [19]- p.153). Based on this two-time-scale analysis, we consider the following MPC formulation:

$$\min_u \left[\int_t^{t+T} \left[q_s\|x_s(\tau)\|_2^2 + |u(\tau)|_R^2\right] d\tau + F(x_s(t+T))\right] \tag{4.50}$$

$$\begin{aligned} s.t.\ \dot{x}_s(\tau) &= \mathcal{A}_s x_s(\tau) + \mathcal{B}_s u(\tau) \\ u(\tau) &\in \mathcal{U} \\ \bar{S}^{min} &\leq (r, x_s(\tau) + e^{\mathcal{A}_f(\tau-t)}x_f(t)) \leq \bar{S}^{max} \end{aligned} \tag{4.51}$$

where $\tau \in [t, t+T]$, and constraints are given as $\bar{S}^{min} = \chi^{min} + M_2^*\bar{u}$ and $\bar{S}^{max} = \chi^{max} - M_2^*\bar{u}$, where $M_2^*$, $\bar{u}$ were defined in Proposition 4.2. Once again we denote the set of initial conditions for which the predictive controller of Eqs.4.50-4.51 achieves stabilization of the $x(t) = 0$ solution of the closed-loop infinite dimensional systems by $\Omega'$. Note that, as opposed to Theorem 4.1, the set of initial conditions include the slow as well as the fast states because the fast states appear explicitly (even though 'approximately') in the constraints in the optimization problem. State constraint satisfaction for the infinite

dimensional system is achieved by revising the state constraints in the controller formulation by the worst case error (induced due to neglecting the effect of the input on the evolution of the fast modes) in the prediction of the fast state dynamics. We formalize this idea in the following theorem.

**Theorem 4.2:** *Consider the system of Eq.4.11, the input and state constraints of Eqs.4.12-4.13, under the control law of Eqs.4.50-4.51. Then, if* $x(0) \in \Omega'$, *the* $x(t) = 0$ *is an asymptotically stable solution of the closed-loop system of Eqs.4.11-4.50-4.51 and* $\chi^{min} \leq (r, x(t)) \leq \chi^{max}$ *for all* $t \geq 0$.

**Proof of Theorem 4.2**: The fact that the control law of Eqs.4.50-4.51 achieves stabilization of the closed–loop infinite dimensional system can be proved using similar arguments to the one in the proof of Proposition 4.1. We focus on constraint satisfaction.

Satisfaction of the constraint $(r, x_s + e^{\mathcal{A}_f(\tau-t)}x_f(t)) \leq \bar{S}^{max} = \chi^{max} - M_2^*\bar{u}$ implies $(r, x_s(\tau)) + (r, e^{\mathcal{A}_f(\tau-t)}x_f(t)) + M_2^*\bar{u} \leq \chi^{max}$. Note that $(r, x_s(\tau)) + (r, x_f(\tau))) \leq (r, x_s(\tau)) + (r, e^{\mathcal{A}_f(\tau-t)}x_f(t)) + M_2^*\bar{u}$ (see proof of proposition 2). Hence, $(r, x_s(\tau)) + (r, e^{\mathcal{A}_f(\tau-t)}x_f(t)) + M_2^*\bar{u} \leq \chi^{max}$ implies $(r, x(\tau)) \leq \chi^{max}$.

Similarly, satisfaction of the constraint $(r, x_s(\tau) + e^{\mathcal{A}_f(\tau-t)}x_f(t)) \geq \bar{S}^{min} = \chi^{min} + M_2^*\bar{u}$ implies $(r, x_s(\tau)) + (r, e^{\mathcal{A}_f(\tau-t)}x_f(t)) - M_2^*\bar{u} \geq \chi^{min}$. Note, once again that $(r, x_f(\tau)) \geq (r, e^{\mathcal{A}_f(\tau-t)}x_f(t)) - M_2^*\bar{u}$ (see proof of proposition 2). Therefore, $(r, x_s(\tau)) + (r, e^{\mathcal{A}_f(\tau-t)}x_f(t)) - M_2^*\bar{u} \geq \chi^{min}$ implies $(r, x(\tau)) \geq \chi^{min}$. This completes the proof of Theorem 2.

## 4.4 Simulation example

In this section, we demonstrate and compare, through computer simulations, the implementation of the various MPC formulations discussed in the previous section. To this end, we consider the parabolic PDE of Eq.4.1 with $b = 1$, $c = 1.66$, $w = 2$ and two control actu-

ators ($m = 2$) with the following distribution functions $b_i(z) = 1/\mu$ for $z \in [z_{ai} - \mu, z_{ai} + \mu]$ and $b_i(z) = 0$ elsewhere in $[0, \pi]$, where $\mu = 0.005$ is a small positive real number and $z_{a1} = \pi/3$ and $z_{a2} = 2\pi/3$. For these values, it was verified that the operating steady-state, $\bar{x}(z,t) = 0$, is an unstable one. The control objective is to stabilize the state profile at the unstable zero steady-state by manipulating $u_i(t)$ subject to the input and state constraints of Eqs.4.12-4.13 with $u_i^{min} = -3$, $u_i^{max} = 3$, for $i = 1, 2$, $\chi^{min} = -3.0$, $\chi^{max} = 3.0$. $r(z)$ is the state constraint distribution function, chosen to be $r(z) = 1/m$ for $z \in [z_c - \nu, z_c + \nu]$, with $m = 0.0035$, $\nu = 0.0018$ and $z_c = 1.156$, and zero elsewhere. The solution of the eigenvalue problem of the spatial differential operator of Eq.4.14 is:

$$\lambda_j = 1.66 - j^2, \ \phi_j(z) = \sqrt{\frac{2}{\pi}} sin(j\ z), \ \ j = 1, \ldots, \infty \tag{4.52}$$

For this system, we consider the first two eigenmodes to be the dominant ones. To simplify the presentation of the results, we will work with the amplitudes of the eigenmodes of the PDE of Eq.4.11. Specifically, using standard modal decomposition, we derive the following high-order ODE system that describes the temporal evolution of the amplitudes of the first $l$ eigenmodes:

$$\begin{aligned} \dot{a}_s(t) &= A_s a_s(t) + B_s u(t) \\ \dot{a}_f(t) &= A_f a_f(t) + B_f u(t) \end{aligned} \tag{4.53}$$

where $a_s(t) = [a_1(t) \ \ a_2(t)]'$, $a_f(t) = [a_3(t) \ \ a_4(t) \ \cdots \ a_l(t)]'$, $a_i(t) \in \mathbb{R}$ is the modal amplitude of the $i$-th eigenmode, the notation $a_s'$ denotes the transpose of $a_s$, $l$ is chosen to be 50, $u(t) = [u_1(t) \ \ u_2(t)]'$, the matrices $A_s$ and $A_f$ are diagonal matrices, given by $A_s = diag\{\lambda_i\}$, for $i = 1, 2$ and $A_f = diag\{\lambda_i\}$, for $i = 3, \cdots, l$. $B_s$ and $B_f$ are a $2 \times 2$ and $(l-2) \times m$ matrices, respectively whose $(i,j)$-th element is given by $B_{ij} = (b_j(z), \phi_i(z))$. Note that $\bar{x}(z,t) = \sum_{i=1}^{l} a_i(t)\phi_i(z)$, $x_s(t) = a_1(t)\phi_1 + a_2(t)\phi_2$, $x_f(t) = \sum_{i=3}^{50} a_i(t)\phi_i$ and that $(x(t), \phi_i) = a_i(\phi_i, \phi_i)$. Using these projections, the state constraints of Eq.4.13 can be expressed as constraints on the modal amplitudes as follows:

$$\chi^{min} \leq \sum_{i=1}^{2} a_i(t)\phi_i(z_c) + \sum_{i=3}^{l} a_i(t)\phi_i(z_c) \leq \chi^{max} \tag{4.54}$$

We now proceed with the design and implementation of the different predictive control formulations presented in the previous section. In the first scenario, we use the $a_s$-subsystem

in Eq.4.53 as the basis for the predictive controller design (the $a_f$-subsystem is neglected). For this case, we consider an MPC formulation of the form of Eqs.4.27-4.28 with the following objective function and constraints:

$$\min_u \left[ \int_t^{t+T} \left[ q_s |a_s(\tau)|^2 + |u(\tau)|_R^2 \right] d\tau \right] \tag{4.55}$$

$$\begin{aligned} s.t.\ \dot{a}_s(\tau) &= A_s a_s(\tau) + B_s u(\tau) \\ u_{min} &\leq u_i(\tau) \leq u_{max},\ i = 1,2 \\ \chi^{min} &\leq C_s a_s(\tau) \leq \chi^{max},\quad \tau \in [t, t+T] \end{aligned} \tag{4.56}$$

where $C_s = [\phi_1(z_c)\ \phi_2(z_c)]$ is a row vector, $q_s = 8.79$, $R = rI$, with $r = 0.01$, and $T = 0.007$. To ensure stability, we also impose a terminal equality constraint of the form $a_s(t+T) = 0$ on the optimization problem. The resulting quadratic program is solved using the MATLAB subroutine QuadProg. The control action is then implemented on the 50-th order model of Eq.4.53. Figure 5.1 shows the closed-loop state under the implementation of the MPC Eqs.4.55-4.56 stabilizes the PDE state at the unstable zero steady-state starting from the initial condition $\bar{x}(z,0) = 0.02\sin(z) + 0.01\sin(2z) + 3.15\sin(3z) + 3.15\sin(4z)$, By examining Figure 5.3 (solid line), we observe that the integral constraint $R(z_c,t) = \int_0^\pi r(z)\bar{x}(z,t)dz$ violates the lower constraint for some time. The violation of the state constraint is a consequence of neglecting the contribution of the $a_f$ states to the state of the PDE in the MPC formulation.

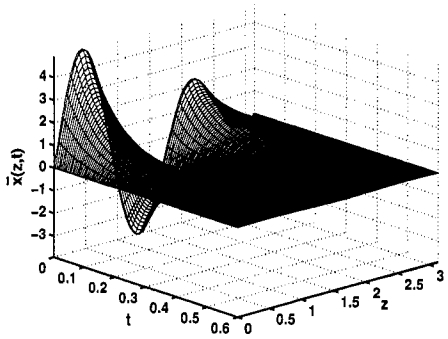


Figure 4.1: Closed-loop state profile under the MPC formulation of Eqs.4.55-4.56 with $\bar{x}(z,0) = 0.02\sin(z) + 0.01\sin(2z) + 3.15\sin(3z) + 3.15\sin(4z)$.

We now revise the constraints in the previous MPC formulation, and consider the following objective function and constraints (analyzed in Theorem 4.1):

$$\min_u \left[ \int_t^{t+T} \left[ q_s |a_s(\tau)|^2 + |u(\tau)|_R^2 \right] d\tau \right] \tag{4.57}$$

$$\begin{aligned} s.t.\ \dot{a}_s(\tau) &= A_s a_s(\tau) + B_s u(\tau) \\ u_{min} &\leq u_i(\tau) \leq u_{max},\ i = 1,2 \\ S^{min} &\leq C_s a_s(\tau) \leq S^{max},\ \tau \in [t, t+T] \end{aligned} \tag{4.58}$$

where $C_s = [\phi_1(z_c)\ \phi_2(z_c)]$ is a row vector, and $q_s$, $R$,$r$ and $T$ are the same to the ones used in the first scenario, and $S^{max} = 3 - \alpha$ and $S^{min} = -3 + \alpha$. Following the result of Theorem 1, we have verified that $\delta = 1$ satisfies $\chi^{max} - \chi^{min} \geq 2(M_2^* \bar{u} + \delta)$ where $\bar{u} = 3$ and $M_2^* = M_2 M_3 = M_3 \|\mathcal{B}_f\|_2 / \gamma = 0.477$, and pick $\alpha = M_2^* \bar{u} + \delta = 2.43$ and $\beta = \delta / M_1^* = 1.0/1.003 = 0.99$

Picking the initial condition $\bar{x}(z,0) = 0.02\sin(z) + 0.01\sin(2z) + 0.95\sin(3z)$ which satisfies $\|x_f(0)\|_2 \leq 0.99$, implementation of the predictive controller of Eqs.4.57-4.58 results in stabilization and satisfaction of the state constraint of the closed-loop system (Figure 5.2 and dashed lines in Figures 5.3-5.5). Note that, since the control action is computed on the basis of the slow states – and since the initial conditions for the slow states are the same as in the previous scenario – the controller implements the same control action as before (i.e., the solid and the dashed lines overlap in Figure 5.5). The closed-loop state profile, however, stays within the constraints because of appropriate initialization of the fast modes and modification of the state constraint in the predictive controller of Eqs.4.57-4.58.

We now consider higher-order MPC formulations. First, we demonstrate the implementation of the MPC formulation of Eqs.4.45-4.46 where the PDE state constraints are exactly accounted for in the controller design. In this case, the objective function and constraints are given by

$$\min_u \left[ \int_t^{t+T} \left[ q_s |a_s(\tau)|^2 + |u(\tau)|_R^2 \right] d\tau \right] \tag{4.59}$$

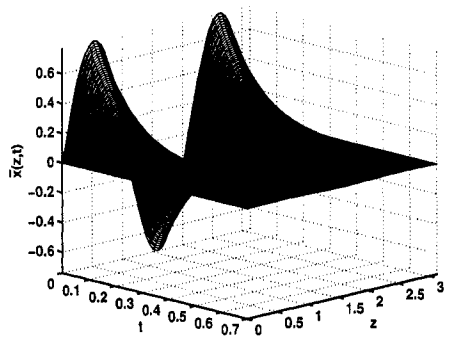


Figure 4.2: Closed-loop state profile under the MPC formulation of Eqs.4.57-4.58 with $\bar{x}(z,0) = 0.02\sin(z) + 0.01\sin(2z) + 0.95\sin(3z)$.

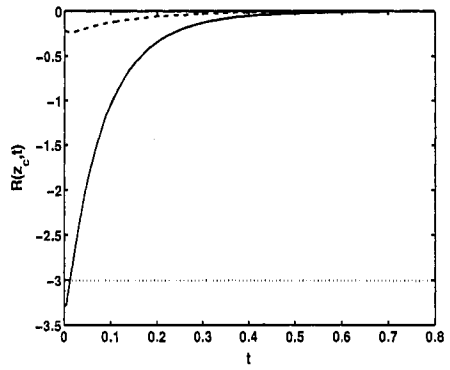


Figure 4.3: $R(z_c,t) = \int_0^\pi r(z)\bar{x}(z,t)dz$ under the MPC formulation of Eqs.4.55-4.56 (solid line) and under the MPC formulation of Eqs.4.57-4.58 (dashed line). The dotted line represents the lower state constraint.

$$\begin{aligned} s.t.\ \dot{a}_s(\tau) &= A_s a_s(\tau) + B_s u(\tau) \\ \dot{a}_f(\tau) &= A_f a_s(\tau) + B_f u(\tau) \\ u_{min} &\leq u_i(\tau) \leq u_{max},\ i = 1,2 \\ \chi^{min} &\leq C_s a_s(\tau) + C_f a_f(\tau) \leq \chi^{max} \end{aligned} \tag{4.60}$$

where $\tau \in [t, t+T]$, $C_f = [\phi_3(z_c) \ \cdots \ \phi_{50}(z_c)]$ is a row vector and the MPC tuning parameters have the same values used in the previous two cases. The results are shown in Figure 5.7 and Figure 4.7 (dashed lines), where we see that starting from the initial condition $\bar{x}(z,0) = 0.02\sin(z) + 0.01\sin(2z) + 2.8\sin(3z) + 2.85\sin(4z)$ the predictive controller of Eqs.4.59-4.60 successfully stabilizes the system at the zero steady-state and

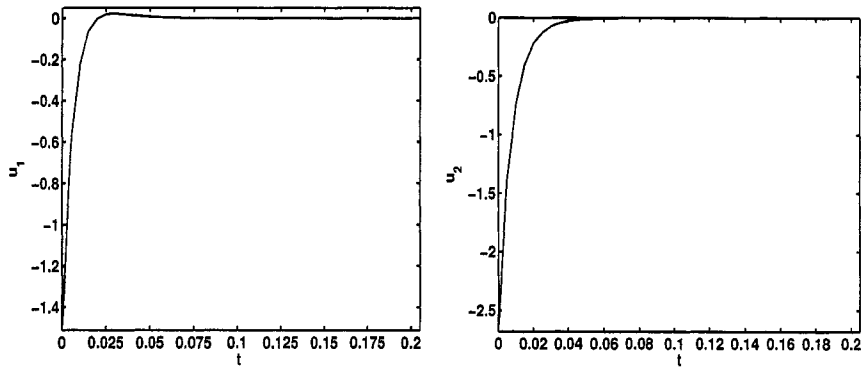


Figure 4.4: Manipulated input profiles for the first and second control actuators applied at $z_{a_1} = \pi/3$ and $z_{a_2} = 2\pi/3$ under the MPC formulation of Eqs.4.55-4.56 (solid line) and under the MPC formulation of Eqs.4.57-4.58 (dashed line); note that the dashed and solid line coincide because of the same initial conditions of the $a_s$-states.

the PDE state constraints is satisfied for all times. The corresponding manipulated input profiles are given in Figure 4.8.

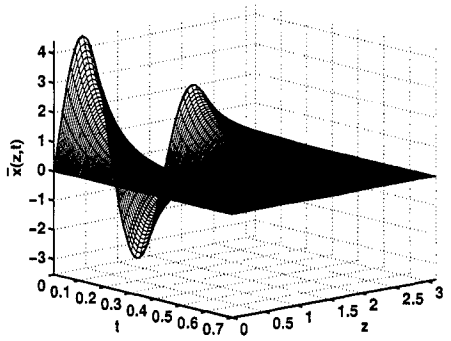


Figure 4.5: Closed-loop state profile under the MPC formulation of Eqs.4.59-4.60 with $\bar{x}(z,0) = 0.02\sin(z) + 0.01\sin(2z) + 2.8\sin(3z) + 2.85\sin(4z)$.

Finally, we demonstrate the implementation of the MPC formulation of Eqs.4.50-4.51 (analyzed in Theorem 2). Using the approximation of Eq.4.49 in the formulation of Eqs.4.59-4.60 yields the following objective function and constraints:

$$\min_{u} \left[ \int_{t}^{t+T} \left[ q_s |a_s(\tau)|^2 + |u(\tau)|_R^2 \right] d\tau \right] \tag{4.61}$$

$$
\begin{aligned}
s.t.\ \ \dot{a}_s(\tau) &= A_s a_s(\tau) + B_s u(\tau) \\
u_{min} \leq u_i(\tau) &\leq u_{max},\ \ i = 1, 2 \\
\bar{S}^{min} \leq C_s a_s(\tau) + C_f \exp\left(A_f(\tau - t)\right) a_f(t) &\leq \bar{S}^{max}
\end{aligned}
\tag{4.62}
$$

where $\tau \in [t, t+T]$. $\bar{S}^{max}$ and $\bar{S}^{min}$ are calculated by using the value $M_2^* \bar{u} = 1.431$, as follows $\bar{S}^{max} = \chi^{max} - M_2^* \bar{u} = 1.569$ and $\bar{S}^{min} = \chi^{min} + M_2^* \bar{u} = -1.569$. The above formulation does not require solving the state evolution equation for the $a_f$-subsystem at each time step; instead it uses an explicit (approximate) expression, $a_f(\tau) = e^{A_f(\tau - t)} a_f(t)$, to account for the dynamics of the fast subsystem which contribute to the PDE state constraints. The initial conditions in this scenario are picked as $(\bar{x}(z,0) = 0.02\sin(z) + 0.01\sin(2z) + 1.45\sin(3z) + 1.5\sin(4z))$; note that for the initial condition $\bar{x}(z,0) = 0.02\sin(z) + 0.01\sin(2z) + 2.8\sin(3z) + 2.85\sin(4z)$, the formulation of Eqs.4.61-4.62 is not feasible. The receding horizon implementation of the predictive controller implies that for subsequent computations, this expression is used with the updated value of $a_f(t)$. Note, however, that this does not imply that the optimization problem needs to solve the fast mode dynamics; it only means that at the new initial condition, the optimization problem in the predictive controller is solved starting from this updated system state, in line with the standard receding horizon implementation of predictive controllers. The resulting predictive controller, when implemented on the system of Eq.4.1 successfully stabilizes the zero steady-state and enforces PDE state constraints satisfaction (see Figure 4.6 and solid lines Figures 4.7-4.8).

**Remark 4.8:** As a final note, we want to demonstrate that even if $\bar{x}(z,0)$ does not violate the state constraints, these constraints can be violated for some time $t \geq 0$. To this end, we pick $\chi^{min} = -0.035$ and $\chi^{max} = 2$, and $u_i^{min} = -10$, $u_i^{max} = 10$, and use the $a_s$-subsystem in Eq.4.53 as the basis for the predictive controller design (the $a_f$-subsystem is neglected). For this case, we consider the predictive controller of Eqs.4.55-4.62 where $C_s = [\phi_1(z_c)\ \phi_2(z_c)]$ is a row vector, $q_s = 8.79$, $R = rI$, with $r = 0.01$, and $T = 0.007$. To ensure stability, we impose a terminal equality constraint of the form $a_s(t+T) = 0$ on the optimization problem. The control action is then implemented on the 50-th order model

of Eq.4.53. Figure 4.9 shows state constraint profile starting from the initial condition $\bar{x}(z,0) = 0.04\sin(z)+0.0005\sin(2z)+0.07\sin(3z)$, that does not violates state constraints. It is clear that the predictive controller successfully stabilizes the state at the zero steady-state and that the state violates the lower constraint for some time.

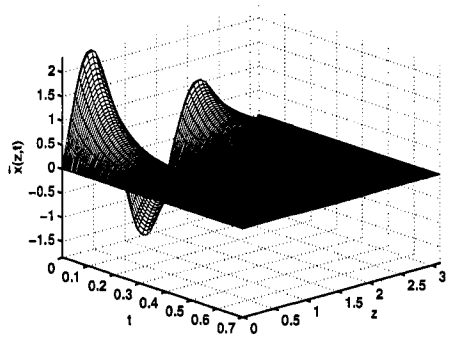


Figure 4.6: Closed-loop state profile under the MPC formulation of Eqs.4.61-4.62 with $\bar{x}(z,0) = 0.02\sin(z) + 0.01\sin(2z) + 1.45\sin(3z) + 1.5\sin(4z)$.

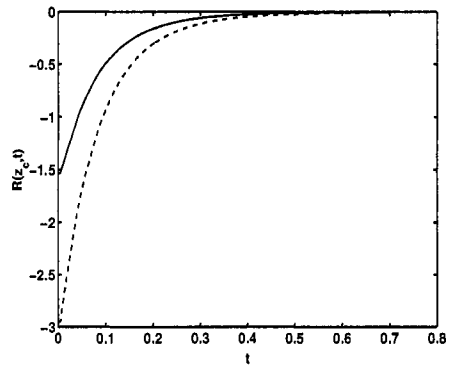


Figure 4.7: $R(z_c,t) = \int_0^\pi r(z)\bar{x}(z,t)dz$ under the MPC formulation of Eqs.4.59-4.60, (dashed line) and under the MPC formulation of Eqs.4.61-4.62 (solid line).

## 4.5 Conclusions

In this chapter, we focused on linear parabolic PDEs with state and control constraints and developed predictive control strategies on the basis of lower-order ODE models obtained

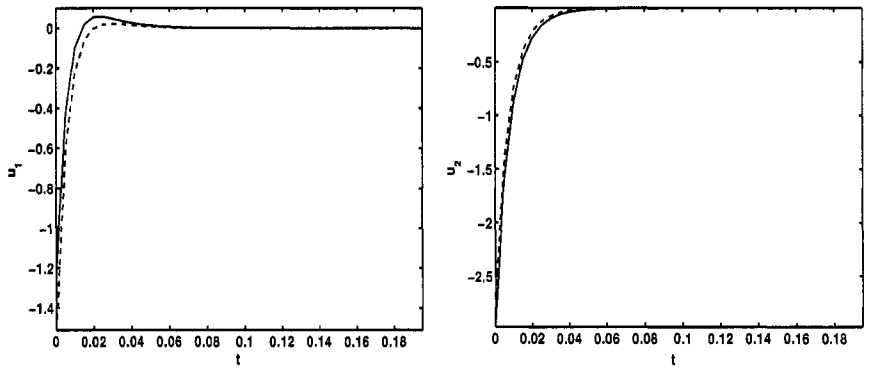


Figure 4.8: Manipulated input profiles for the first and second control actuators applied at $z_{a_1} = \pi/3$ and $z_{a_1} = 2\pi/3$ under the MPC formulation of Eqs.4.59-4.60 (dashed line) and under the MPC formulation of Eqs.4.61-4.62 (solid line).

through application of appropriate order reduction techniques to the infinite-dimensional system. In order to account for the effect of both the slow and fast modes of the PDE in the cost function of the optimal control problem and the state constraints, we developed various MPC formulations which are distinct with respect to the number of modal states employed in the cost function and/or state constraints formulation. Namely, the number of modal states utilized in the cost function and number of modal states utilized in the state constraints may differ in the various MPC formulations which affects the performance of the proposed formulation and point out to trade-offs which are necessary to be made with respect to state constraints satisfaction and number of modal states accounted for in the formulation. The developed predictive control algorithms were numerically validated using a linearized diffusion-reaction example.

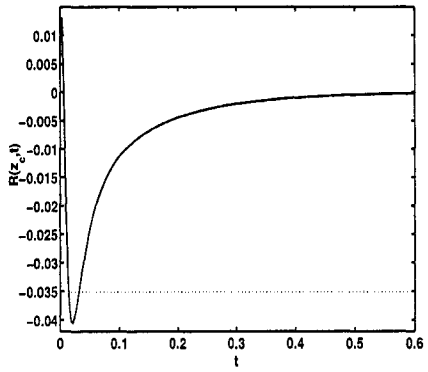


Figure 4.9: $R(z_c,t) = \int_0^\pi r(z)\bar{x}(z,t)dz$ under the MPC formulation of Eqs.4.55-4.56 with $\bar{x}(z,0) = 0.04\sin(z) + 0.0005\sin(2z) + 0.07\sin(3z)$ and state constraints $-0.035 \leq R(z_c,t) \leq 2$ with $[u_{max}, u_{min}] = [-10, 10]$.

# Chapter 5

# Predictive Control of Transport-Reaction Processes

## 5.1 Introduction

In this part of the thesis, we focus on the development of computationally efficient predictive control algorithms for nonlinear parabolic and hyperbolic PDEs with state and control constraints arising in the context of transport-reaction processes. The rest of this chapter is organized as follows: in section 5.2, we consider a diffusion-reaction process described by a nonlinear parabolic PDE and address the problem of stabilization of an unstable steady-state subject to input and state constraints. Galerkin's method is used to derive finite-dimensional systems that capture the dominant dynamics of the parabolic PDE, which are subsequently for controller design. Various MPC formulations are constructed on the basis of the finite dimensional approximations and are demonstrated, through simulation, to achieve the control objectives. Next, in section 5.3, we consider a convection-reaction process example described by a set of hyperbolic PDEs and address the problem of stabilization of the desired steady-state subject to input and state constraints, in the presence of disturbances. An easily implementable predictive controller based on a finite dimensional approximation of the PDE obtained by the finite difference

method is derived and demonstrated, via simulation, to achieve the control objective.

## 5.2 Predictive control of diffusion-reaction processes

**Motivating example.** In this section, we consider a representative example of a diffusion-reaction system described by a parabolic PDE of the following form:

$$\begin{aligned} \frac{\partial \bar{x}}{\partial t} &= \frac{\partial^2 \bar{x}}{\partial z^2} + \beta_T (e^{-\frac{\gamma}{1+\bar{x}}} - e^{-\gamma}) - \beta_U \bar{x} + \beta_U \sum_{i=1}^{m} b_i(z) u_i(t) \\ \bar{x}(0,t) &= 0, \quad \bar{x}(\pi,t) = 0, \quad \bar{x}(z,0) = x_0(z) \end{aligned} \tag{5.1}$$

where $\bar{x}$ denotes the dimensionless state of the system, $\beta_T$ denotes a dimensionless heat of reaction, $\gamma$ denotes a dimensionless activation energy, $\beta_U$ denotes a dimensionless heat transfer coefficient, $u_i(t)$ denotes the manipulated input and $b_i(z)$ is the actuator distribution function of the $i$-th actuator, chosen to be $b_i(z) = 1/\mu$ for $z \in [z_{ai} - \mu, z_{ai} + \mu]$ and $b_i(z) = 0$ elsewhere in $[0, \pi]$, where $\mu$ is a small positive real number and $z_{ai}$ is the center of the interval where actuation is applied. The following typical values are given to the process parameters: $\beta_T = 50$, $\beta_U = 2$ and $\gamma = 4$. For these values, it was verified that the operating steady-state, $\bar{x}(z,t) = 0$, is an unstable one, as can be seen from Figure 5.1. The control objective is to stabilize the state profile at the unstable zero steady-state

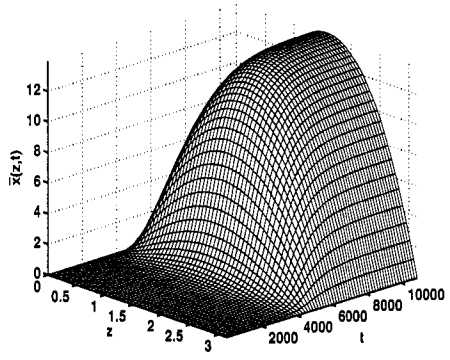


Figure 5.1: Open-loop profile showing the instability of the $\bar{x}(z,t) = 0$ steady-state.

subject to the following input and state constraints

$$u_i^{min} \leq u_i \leq u_i^{max} \tag{5.2}$$

$$\chi^{min} \leq \int_0^{\pi} r(z)\bar{x}(z,t)dz \leq \chi^{max} \tag{5.3}$$

where $u_i^{min} = -10$, $u_i^{max} = 10$, for $i = 1, 2$, $\chi^{min} = -0.035$, $\chi^{max} = 2$. The state constraints distribution function, $r(\cdot)$, is chosen to be $r(z) = \delta(z - z_c)$ for $z \in [0, \pi]$ and $z_c = 1.156$. This choice of $r(z)$ implies that the state constraints are to be enforced only at a single point in the spatial domain, i.e., $-0.035 \leq \bar{x}(z_c, t) \leq 2$. For this system, we consider the first two eigenvalues as the dominant ones and use two point control actuators ($m = 2$), with finite support, centered at $z_{a1} = \pi/3$ and $z_{a2} = 2\pi/3$, to achieve the control objective subject to the constraints of Eqs.5.2-5.3.

**Galerkin's method.** To present our results, we first formulate the PDE of Eq.4.1 as an infinite dimensional system in the Hilbert space $\mathcal{H}([0, \pi]; \mathbb{R})$, with $\mathcal{H}$ being the space of measurable functions defined on $[0, \pi]$, with inner product and norm:

$$(\omega_1, \omega_2) = \int_0^{\pi} (\omega_1(z), \omega_2(z))_{\mathbb{R}^n} dz, ||\omega_1||_2 = (\omega_1, \omega_1)^{\frac{1}{2}} \tag{5.4}$$

where $\omega_1, \omega_2$ are two elements of $\mathcal{H}([0, \pi]; \mathbb{R}^n)$ and the notation $(\cdot, \cdot)_{\mathbb{R}^n}$ denotes the standard inner product in $\mathbb{R}^n$. Defining the state function $x$ on $\mathcal{H}([0, \pi]; \mathbb{R})$ as:

$$x(t) = \bar{x}(z, t), \quad t > 0, \quad z \in [0, \pi], \tag{5.5}$$

the operator $\mathcal{A}$ in $\mathcal{H}([0, \pi]; \mathbb{R})$ as:

$$\begin{aligned} \mathcal{A}x &= \frac{\partial^2 \bar{x}}{\partial z^2}, \\ x \in D(\mathcal{A}) &= \{x \in \mathcal{H}([0, \pi]; \mathbb{R}^n) : \bar{x}(0, t) = 0, \ \bar{x}(\pi, t) = 0\} \end{aligned} \tag{5.6}$$

and the input operators as:

$$\mathcal{B}u = \sum_{i=1}^{m} b_i u_i, \tag{5.7}$$

the system of Eq.5.1 takes the form:

$$\dot{x} = \mathcal{A}x + \mathcal{F}(x) + \mathcal{B}u, \quad x(0) = x_0 \tag{5.8}$$

where $x_0 = x_0(z)$. For the operator $\mathcal{A}$, the eigenvalue problem takes the form

$$\frac{d^2\phi_j}{dz^2} = \lambda_j \phi_j \tag{5.9}$$

subject to

$$\phi_j(0) \;=\; \phi_j(\pi) \;=\; 0 \tag{5.10}$$

The above eigenvalue problem can be solved analytically and its solution yields

$$\lambda_j \;= -j^2, \quad \phi_j(z) = \sqrt{\frac{2}{\pi}} sin(j\ z), \quad j = 1, \ldots, \infty \tag{5.11}$$

Throughout the rest of the chapter, the notation $|\cdot|$ will be used to denote the standard Euclidian norm in $\mathbb{R}^n$, while the notation $|\cdot|_Q$ will be used to denote the weighted norm defined by $|x|_Q^2 = x'Qx$, where $Q$ is a positive-definite matrix and $x'$ denotes the transpose of $x$. Finally the notation $\|\cdot\|_2$ will be used to denote the $L_2$ norm (as defined in Eq.5.4 above) associated with a finite or infinite dimensional Hilbert space.

Next, we apply standard Galerkin's method to the infinite-dimensional system of Eq.5.8 to derive a finite-dimensional system. Let $\mathcal{H}_s$, $\mathcal{H}_f$ be modal subspaces of $\mathcal{A}$, defined as $\mathcal{H}_s = span\{\phi_1, \phi_2, \ldots, \phi_m\}$ and $\mathcal{H}_f = span\{\phi_{m+1}, \phi_{m+2}, \ldots\}$ (the existence of $\mathcal{H}_s$, $\mathcal{H}_f$ follows from the properties of $\mathcal{A}$). Defining the orthogonal projection operators, $P_s$ and $P_f$, such that $x_s = P_s x$, $x_f = P_f x$, the state $x$ of the system of Eq.5.8 can be decomposed as

$$x \;=\; x_s + x_f \;=\; P_s x + P_f x \tag{5.12}$$

Applying $P_s$ and $P_f$ to the system of Eq.5.8 and using the above decomposition for $x$, the system of Eq.5.8 can be re-written in the following equivalent form

$$\begin{aligned}
\frac{dx_s}{dt} &= \mathcal{A}_s x_s + \mathcal{F}_s(x_s, x_f) + \mathcal{B}_s u, \\
\frac{dx_f}{dt} &= \mathcal{A}_f x_f + \mathcal{F}_f(x_s, x_f) + \mathcal{B}_f u \\
x_s(0) \;&=\; P_s x(0) \;=\; P_s x_0 \\
x_f(0) \;&=\; P_f x(0) \;=\; P_f x_0
\end{aligned} \tag{5.13}$$

where $\mathcal{A}_s = P_s\mathcal{A}$, $\mathcal{B}_s = P_s\mathcal{B}$, $\mathcal{A}_f = P_f\mathcal{A}$, $\mathcal{B}_f = P_f\mathcal{B}$. In the above system, $\mathcal{A}_s$ is a diagonal matrix of dimension $m \times m$ of the form $\mathcal{A}_s = diag\{\lambda_j\}$ ($\lambda_j$ are possible unstable

eigenvalues of $\mathcal{A}_s$) and $\mathcal{A}_f$ is an unbounded differential operator which is exponentially stable (following from the fact that $\lambda_{m+1} < 0$ and the selection of $\mathcal{H}_s, \mathcal{H}_f$). In the remainder of the chapter, we will refer to the $x_s$- and $x_f$-subsystems in Eq.5.13 as the slow and fast subsystems, respectively.

**Control problem formulation.** Referring to the system of Eq.5.8, we consider the problem of asymptotic stabilization of the origin, subject to the following control and state constraints:

$$\dot{x}(t) = \mathcal{A}x(t) + \mathcal{F}(x(t)) + \mathcal{B}u(t), \quad x(0) = x_0 \tag{5.14}$$

$$u_i^{min} \leq u_i(t) \leq u_i^{max} \tag{5.15}$$

$$\chi^{min} \leq (r, x(t)) \leq \chi^{max} \tag{5.16}$$

This problem will be addressed within an MPC framework where the control, at state $x$ and time $t$, is conventionally obtained by solving, on-line, a finite-horizon constrained optimal control problem of the form

$$P(x,t) : \min\{J(x,t,u(\cdot)) \mid u(\cdot) \in S\} \tag{5.17}$$

$$\begin{aligned} s.t.\ \dot{x}(\tau) &= \mathcal{A}x(\tau) + \mathcal{F}(x(\tau)) + \mathcal{B}u(\tau) \\ \chi^{min} &\leq (r, x(\tau)) \leq \chi^{max}, \quad \tau \in [t, t+T] \end{aligned} \tag{5.18}$$

where $S = S(t,T)$ is the family of piecewise continuous functions (functions continuous from the right), with period $\Delta$, mapping $[t, t+T]$ into $\mathcal{U} := \{u \in \mathbb{R}^m : u_i^{min} \leq u_i \leq u_i^{max},\ i = 1, \cdots, m\}$, and $T$ is the specified horizon. A control $u(\cdot)$ in $S$ is characterized by the sequence $u[k]$, where $u[k] := u(k\Delta)$, and satisfies $u(t) = u[k]$ for all $t \in [k\Delta, (k+1)\Delta)$. The performance index is given by

$$\int_t^{t+T} \left[ q\|x^u(\tau; x, t)\|_2^2 + |u(\tau)|_R^2 \right] d\tau + F(x(t+T)) \tag{5.19}$$

where $q > 0$, $R$ is a strictly positive definite matrix, $x^u(\tau) = x(\tau; x, t)$ denotes the solution of Eq.5.8, due to control $u$, with initial state $x$ at time $t$, and $F(\cdot)$ denotes the terminal penalty. The minimizing control $u^0(\cdot) \in S$ is then applied to the system over the interval

$[k\Delta, (k+1)\Delta]$ and the procedure is repeated indefinitely. This defines an implicit model predictive control law

$$M(x) \;:=\; u^0(t; x, t) \tag{5.20}$$

**Remark 5.1:** It is well known that the control law defined by Eqs.5.17-5.20 is not necessarily stabilizing (even for the finite-dimensional system). For finite-dimensional systems, the issue of closed-loop stability is usually addressed by means of imposing suitable penalties and constraints on the state at the end of the optimization horizon (e.g., see [2, 10, 45] for surveys of different approaches). For the simulation example presented here, and for the choice of MPC parameters and initial conditions, the closed–loop system under MPC was found to be stabilizing; we therefore do not impose stability constraints in the optimization problem, but focus on the task of state constraint satisfaction.

One possible way to formulate the constrained nonlinear MPC problem is to design it on the basis of the full system of Eq.5.13. The control action is then obtained by solving the following optimization problem:

$$\min_u \int_t^{t+T} [q_s \|x_s(\tau)\|_2^2 + q_f \|x_f(\tau)\|_2^2 + |u(\tau)|_R^2]\, d\tau \tag{5.21}$$

$$\begin{aligned} s.t.\ \dot{x}_s(\tau) &= \mathcal{A}_s x_s(\tau) + \mathcal{F}_s(x_s(\tau), x_f(\tau)) + \mathcal{B}_s u(\tau) \\ \dot{x}_f(\tau) &= \mathcal{A}_f x_f(\tau) + \mathcal{F}_f(x_s(\tau), x_f(\tau)) + \mathcal{B}_f u(\tau) \\ u(\tau) &\in \mathcal{U} \\ \chi^{min} &\leq (r, x(\tau)) \leq \chi^{max}, \tau \in [t, t+T] \end{aligned} \tag{5.22}$$

where $q_s$, $q_f$ are positive real numbers and $R$ is a positive definite matrix. The above formulation includes penalties on both the slow and fast states and uses models that describe their evolution for prediction purposes. The infinite dimensional nature of the controller, however, renders it unsuitable for the purpose of online implementation. We now present and compare nonlinear MPC formulations that differ in the way the state constraints are enforced and in the construction of the performance functional in the optimization problem.

### 5.2.1 Low-order predictive control formulation.

In this formulation, the predictive controller is designed on the basis of the low-order, finite-dimensional slow subsystem describing the evolution of the $x_s$ states (the fast subsystem is neglected). Specifically, the nonlinear MPC law is obtained by solving, in a receding horizon fashion, the following optimization problem:

$$\min_u \int_t^{t+T} \left[ q_s \|x_s(\tau)\|_2^2 + |u(\tau)|_R^2 \right] d\tau \tag{5.23}$$

$$\begin{aligned} s.t.\ \dot{x}_s(\tau) &= \mathcal{A}_s x_s(\tau) + \mathcal{F}_s(x_s(\tau), 0) + \mathcal{B}_s u(\tau) \\ u(\tau) &\in \mathcal{U} \\ \chi^{min} &\leq (r, x_s(\tau)) \leq \chi^{max}, \tau \in [t, t+T] \end{aligned} \tag{5.24}$$

To simplify the presentation of the results, we will work with the amplitudes of the eigenmodes of the PDE of Eq.5.1. Specifically, using Galerkin's method, we derive the following high-order ODE system that describes the temporal evolution of the amplitudes of the first $l$ eigenmodes:

$$\begin{aligned} \dot{a}_s(t) &= A_s a_s(t) + F_s(a_s(t), a_f(t)) + B_s u(t) \\ \dot{a}_f(t) &= A_f a_f(t) + F_f(a_s(t), a_f(t)) + B_f u(t) \end{aligned} \tag{5.25}$$

where $a_s(t) = [a_1(t)\ a_2(t)]'$, $a_f(t) = [a_3(t)\ a_4(t)\ \cdots\ a_l(t)]'$, $a_i(t) \in \mathbb{R}$ is the modal amplitude of the $i$-th eigenmode, the notation $a_s'$ denotes the transpose of $a_s$, $u(t) = [u_1(t)\ \ u_2(t)]'$, the matrices $A_s$ and $A_f$ are diagonal matrices, given by $A_s = diag\{\lambda_i\}$, for $i = 1, 2$ and $A_f = diag\{\lambda_i\}$, for $i = 3, \cdots, l$. $B_s$ and $B_f$ are a $2 \times 2$ and $(l-2) \times m$ matrices, respectively whose $(i,j)$-th element is given by $B_{ij} = (b_j(z), \phi_i(z))$. Note that $\bar{x}(z,t) = \sum_{i=1}^{l} a_i(t)\phi_i(z)$, $x_s(t) = a_1(t)\phi_1 + a_2(t)\phi_2$, $x_f(t) = \sum_{i=3}^{l} a_i(t)\phi_i$ and that $(x_s(t), \phi_i) = a_i(\phi_i, \phi_i)$. Using these projections, the state constraints of Eq.5.3 can be expressed as constraints on the modal amplitudes as follows:

$$\chi^{min} \leq \sum_{i=1}^{2} a_i(t)\phi_i(z_c) + \sum_{i=3}^{l} a_i(t)\phi_i(z_c) \leq \chi^{max} \tag{5.26}$$

The MPC formulation of Eq.5.24, when written in terms of the amplitudes of the eigenmodes takes the following form:

$$\min_u \int_t^{t+T} \left[ q_s |a_s(\tau)|^2 + |u(\tau)|_R^2 \right] d\tau \tag{5.27}$$

$$
\begin{aligned}
s.t.\ \dot{a}_s(\tau) &= A_s a_s(\tau) + F_s(a_s, 0) + B_s u(\tau) \\
u_{min} &\leq u_i(\tau) \leq u_{max},\ i = 1, 2 \\
\chi^{min} &\leq C_s a_s(\tau) \leq \chi^{max},\ \tau \in [t, t+T]
\end{aligned} \tag{5.28}
$$

where $C_s = [\phi_1(z_c)\ \phi_2(z_c)]$ is a row vector. We now proceed with the implementation of the predictive control formulation of Eqs.5.27-5.28 and choose $q_s = 1000$, $R = rI$, with $r = 0.001$, and $T = 0.011$. In all simulation runs, we considered the following initial condition: $\bar{x}(z,0) = 0.08sin(z) + 0.001sin(2z)$ and $l$ is chosen to be 30. The resulting program is solved using the MATLAB subroutine fmincon. The control action is then implemented on the 30-th order model of Eq.5.25. The closed-loop state and manipulated input profiles under the MPC controller of Eqs.5.23-5.24 are shown in Figure 5.2 and Figures 5.6-5.7 (solid lines), respectively. It is clear that the controller successfully stabilizes the state at the zero steady-state. However, by examining Figure 5.5 (solid line), we observe that the state at $z_c = 1.156$ violates the lower constraint for some time. The violation of the state constraint is a consequence of neglecting the contribution of the $a_f$ states to the full state of the PDE in the MPC formulation.

**Remark 5.2:** Note that while the controller is designed only on the basis of the slow modes, the stabilization of the slow modes of the system leads to the stabilization of the infinite dimensional system, since the remaining fast modes are open loop stable (for a similar result in the context of linear parabolic PDE systems, see [23]).

**Remark 5.3:** For linear parabolic PDEs, low order predictive controller formulations can be derived, which, upon being feasible, guarantee stabilization and state constraint satisfaction of the infinite dimensional system (see, [23]). The inherent coupling between the fast and slow subsystems through the terms $F_s(x_s, x_f)$, $F_f(x_s, x_f)$, however, significantly complicates the derivation of similar results in the nonlinear setting.

### 5.2.2 Higher-order predictive control formulation.

In order to account for the evolution of the fast states in the optimization problem, we consider the following MPC formulation with the objective function and constraints given

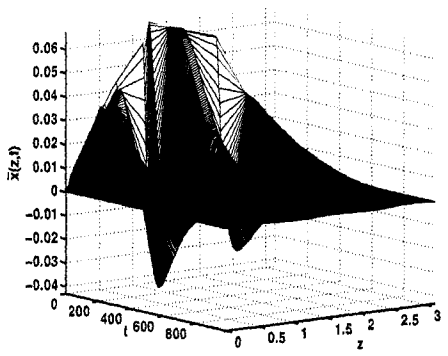


Figure 5.2: Closed-loop state profile under the MPC formulation of Eqs.5.23-5.24 without accounting for the fast modal states in the constraints.

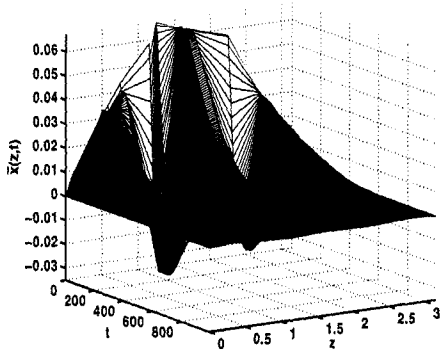


Figure 5.3: Closed-loop state profile under the MPC formulation of Eqs.5.31-5.32 accounting for the fast modes in the state constraints.

by:

$$\min_{u} \int_{t}^{t+T} \left[ q_s \|x_s(\tau)\|_2^2 + |u(\tau)|_R^2 \right] d\tau \tag{5.29}$$

$$\begin{aligned} s.t.\ \dot{x}_s(\tau) &= \mathcal{A}_s x_s(\tau) + \mathcal{F}_s(x_s(\tau), x_f(\tau)) + B_s u(\tau) \\ \dot{x}_f(\tau) &= \mathcal{A}_f x_s(\tau) + \mathcal{F}_f(x_s(\tau), x_f(\tau)) + B_f u(\tau) \\ u_{min} &\leq u_i(\tau) \leq u_{max},\ i = 1, 2 \\ \chi^{min} &\leq (r, x_s(\tau) + x_f(\tau)) \leq \chi^{max} \end{aligned} \tag{5.30}$$

where $\tau \in [t, t+T]$. Note that even though the fast modes appear explicitly in the state constraint equation, they do not appear in the cost function, keeping the computational requirement relatively low.

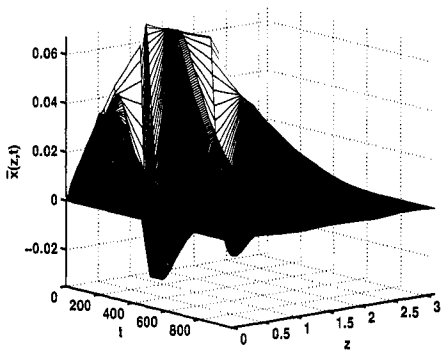


Figure 5.4: Closed-loop state profile under the MPC formulation of Eqs.5.33-5.34 accounting for the fast modes in the state constraints.

The MPC formulation above, when written using modal amplitudes, takes the following form:

$$\min_{u} \int_{t}^{t+T} \left[ q_s |a_s(\tau)|^2 + |u(\tau)|_R^2 \right] d\tau \tag{5.31}$$

$$\begin{aligned} s.t.\ \dot{a}_s(\tau) &= A_s a_s(\tau) + F_s(a_s(\tau), a_f(\tau)) + B_s u(\tau) \\ \dot{a}_f(\tau) &= A_f a_s(\tau) + F_f(a_s(\tau), a_f(\tau)) + B_f u(\tau) \\ u_{min} &\leq u_i(\tau) \leq u_{max},\ i = 1, 2 \\ \chi^{min} &\leq C_s a_s(\tau) + C_f a_f(\tau) \leq \chi^{max} \end{aligned} \tag{5.32}$$

where $\tau \in [t, t+T]$, $C_f = [\phi_3(z_c) \ \cdots \ \phi_{50}(z_c)]$ is a row vector and the MPC tuning parameters have the same values used in the previous formulation.

Figure 5.3 and Figure 5.5 (dotted lines) demonstrate that the MPC formulation of Eqs.5.31-5.32 successfully stabilizes the state profile at the zero steady-state and that the state constraints are satisfied for all times. The corresponding manipulated input profiles are given in Figures 5.6-5.7.

**Remark 5.4:** Note that even though the optimization problem is nonconvex, and the solution obtained may only represent a local minimum, it does not detrimentally affect the task of state constraint satisfaction, because state constraints are posed as explicit constraints in the optimization problem. Even if a solution is not a global minimum (which, in general it will not be), the feasibility of the constraints in the optimization problem ensure that upon implementation of this control action, the state constraints will

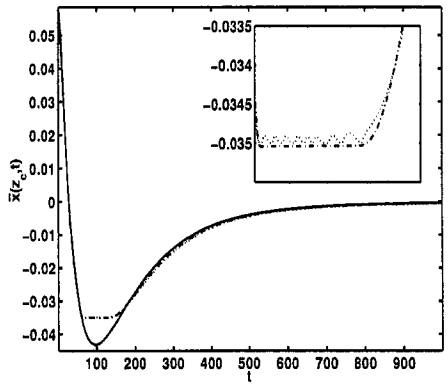


Figure 5.5: Closed-loop state profile at $z_c = 1.156$ under the MPC formulation of Eqs.5.23-5.24 without accounting for the evolution of fast modes (solid), under the MPC formulation of Eqs.5.31-5.32 accounting for the fast modes in the state constraints (dotted), and under the MPC formulation of Eqs.5.33-5.34 using linearization approximation for the evolution of modal states in the constraints (dashed-dotted).

be satisfied for the infinite dimensional system.

### 5.2.3 High-order predictive control formulation based on two-time-scale approximation.

As evidenced by the examples shown before, accounting for the evolution of the fast modes is important for the purpose of satisfying state constraints. The computational complexity associated with accounting for the fast modes could be eased by approximating the dynamics of the fast modes, while retaining the nonlinear dynamics of the slow modes (so as to not adversely effect the task of stabilization). One possible way of approximation is to neglect the nonlinearity in the equations describing the evolution of the fast modes. This is because the term $A_f$ behaves like $1/\epsilon$, where $\epsilon$ is a small parameter, and therefore, $A_f$ is much larger than $F_f$ and thus $F_f$ can be neglected from the equation (see [14] for more discussion and analysis of this approximation). Using this approximation, the predictive control formulation takes the following form:

$$\min_{u} \int_0^{t_f} \left[ q_s |a_s(\tau)|^2 + |u(\tau)|_R^2 \right] d\tau \tag{5.33}$$

$$\begin{aligned} s.t.\ \dot{a}_s(\tau) &= A_s a_s + F_s(a_s(\tau), a_f(\tau)) + B_s u(\tau) \\ \dot{a}_f(\tau) &= A_f a_f(\tau) + B_f u(\tau) \\ u_{min} &\leq u_i(\tau) \leq u_{max},\ i = 1,2 \\ \chi^{min} &\leq C_s a_s(\tau) + C_f a_f(\tau) \leq \chi^{max} \end{aligned} \tag{5.34}$$

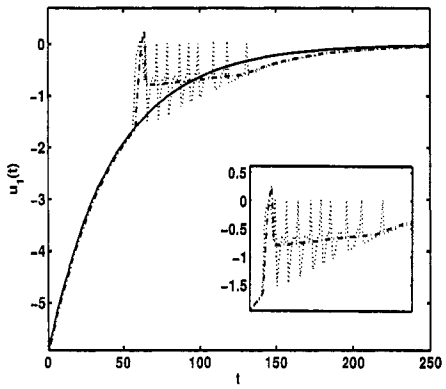


Figure 5.6: Manipulated input profiles for the first control actuator applied at $z_{a_1} = \pi/3$ under the MPC formulation of Eqs.5.23-5.24 (solid), under the MPC formulation of Eqs.5.31-5.32 (dotted), and under the MPC formulation of Eqs.5.33-5.34 (dashed-dotted).

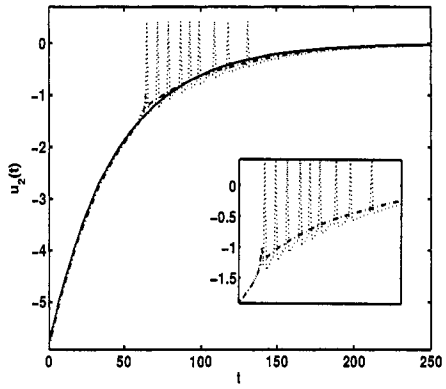


Figure 5.7: Manipulated input profiles for the second control actuator applied at $z_{a_2} = 2\pi/3$ under the MPC formulation of Eqs.5.23-5.24 (solid), under the MPC formulation of Eqs.5.31-5.32 (dotted), and under the MPC formulation of Eqs.5.33-5.34 (dashed-dotted).

Figure 5.4 and Figure 5.5 (dotted lines) demonstrate that the MPC formulation of

Eqs.5.33-5.34 successfully stabilizes the state profile at the zero steady-state and that the state constraints are satisfied for all times. The corresponding manipulated input profiles are given in Figures 5.6-5.7. Note also, that using the approximations leads to substantial ease in the computational burden and the time required for the computation of the control moves decreases by about 50 %.

## 5.3 Predictive control of convection-reaction processes

We consider a convection-reaction process example described by the following hyperbolic first-order PDE system:

$$\begin{aligned}
\frac{\partial x_1}{\partial t} &= -\frac{\partial x_1}{\partial z} + Da(1-x_1)e^{\frac{x_2}{1+x_2/\gamma}} \\
\frac{\partial x_2}{\partial t} &= -\frac{\partial x_2}{\partial z} + BDa(1-x_1)e^{\frac{x_2}{1+x_2/\gamma}} + \beta_U(\chi_{w,n}-x_2) + \beta_U\sum_{i=1}^{m} b_i(z)u_i(t) \\
x_1(0,t) &= x_1(t),\ x_2(0,t) = x_2(t),\ x_1(z,0) = \bar{x}_1(z),\ x_2(z,0) = \bar{x}_2(z)
\end{aligned} \tag{5.35}$$

where $x_1$ denotes a dimensionless conversion, and $x_2$ denotes a dimensionless temperature, $D_a$ is the Damköhler number, $\gamma$ is a dimensionless activation energy, $\chi_{w,n}$ is the nominal dimensionless wall temperature, $B$ is a dimensionless heat of reaction, $\beta_U$ denotes a dimensionless heat transfer coefficient, $u_i(t)$ denotes change in wall temperature from the nominal value and is the manipulated input, and $b_i(z)$ is the distribution function of the $i$-th actuator, chosen to be $b_i(z) = [H(z-z_i) - H(z-z_{i+1})]$ where $H(z)$ is the standard Heaviside function. The following typical values are given to the process parameters: $Da = 0.25$, $B = 10.5$, $\beta_U = 5.4$, $\chi_{w,n} = 0.1$ and $\gamma = 8$. The initial conditions chosen were $\bar{x}_1(z) = \bar{x}_2(z) = 0$, and the boundary conditions were chosen to be $x_1(t) = 0.05$ and $x_2(t) = 4.0$. For these values, it was verified that the operating steady-state profile is stable (solid lines in Figure 5.8 depict the steady state profile of the temperature $T$ in the reactor). The dashed lines represent constraints on the temperature in the reactor and correspond to the constraints in the dimensionless state variable given by $x_2^{max} = x_{2s} + 0.25$, $x_2^{min} = x_{2s} - 0.25$.

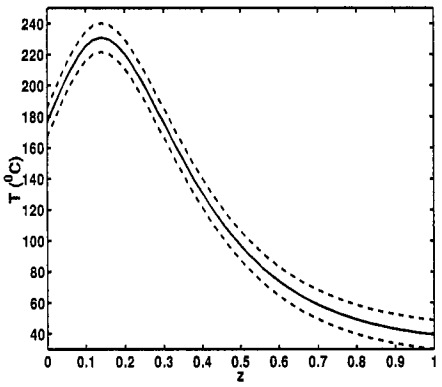


Figure 5.8: Open-loop profile showing the steady-state temperature profile (solid lines). The dashed lines denote the upper and lower constraints on the temperature.

Due to the exothermic nature of the reaction, a small increase/decrease in the inlet concentration may result (by changing the net reaction, and therefore, the net heat generation) in a significant change in the peak of the temperature profile in the reactor (see dash-dotted line in Figure 5.9 for the steady-state profile in the reactor under the presence of a negative disturbance of magnitude 0.03 in both $x_1(t)$ and $x_2(t)$). Note that reducing the value of $x_1(t)$ implies greater inlet reactant concentration, increased reaction and heat generation in the reactor, that subsequently leads to violation of the state constraints in the reactor.

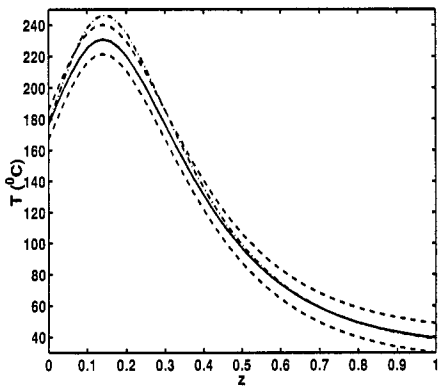


Figure 5.9: The steady-state temperature profile (dash-dotted lines) induced by a negative disturbance of magnitude 0.03 in the dimensionless inlet temperature and concentration.

We therefore consider the control objective of maintaining the desired steady-state profile along the reactor within the bounds of allowed temperature variation in the presence of disturbances. A predictive control algorithm, designed to achieve the aforementioned control objective takes the following form:

$$
\begin{aligned}
\min_{u(\tau)} \quad & \int_t^{t+T} \left[ \left\{ \int_Z e(z,\tau)^2 q dz \right\} + u' R u \right] d\tau \\
s.t. \quad & \frac{\partial x_1}{\partial t} = -\frac{\partial x_1}{\partial z} + Da(1-x_1) e^{\frac{x_2}{1+x_2/\gamma}} \\
& \frac{\partial x_2}{\partial t} = -\frac{\partial x_2}{\partial z} + BDa(1-x_1) e^{\frac{x_2}{1+x_2/\gamma}} + \beta_U(\chi_{w,n} - x_2) + \beta_U \sum_{i=1}^{m} b_i(z) u_i(t) \\
& x_1(0,t) = x_1(t), \; x_2(0,t) = x_2(t), \; x_1(z,0) = \bar{x}_1(z), \; x_2(z,0) = \bar{x}_2(z) \\
& u_i^{min} \leq u_i \leq u_i^{max}, \; i = 1, \cdots, m \\
& x_{2min} \leq x_2(z, t+\tau) \leq x_{2max} \; \forall \; z \in Z, \; \tau \in [t, \; t+T]
\end{aligned}
\tag{5.36}
$$

where $e(z,\tau) = x_{2ss} - x_2(z,\tau)$, $u_i^{max}, u_i^{min}$, $i = 1, \cdots, m$ represent constraints on the manipulated variables, and $x_2^{min}$, $x_2^{max}$ represent state constraints. The above optimization problem may be solved off-line or solved in a receding horizon fashion and implemented online in order to achieve robustness of the closed–loop system with respect to unknown disturbances.

The PDE system being hyperbolic, however, prevents the use of low-order approximations that can be used for the purpose of controller design, and renders the task of real-time implementation of the controller design of Eq.5.36 very difficult. To come up with a controller design that can be readily implemented in real time, we make the following simplifications: first, we exploit the fact that for the system under consideration, the transients are very fast, and both the control objective, and the state constraint satisfaction can be required to hold at the steady-state. Then, to reduce the complexity of the computation, the decision variable is chosen as a feedback gain, instead of the manipulated inputs themselves. Finally, instead of requiring the constraints to hold over the entire spatial domain, we restrict it to a zone, and furthermore, divide the zone into a number of subzones, such that in each subzone, a different value of the control action can

be implemented. Specifically, we solve the following optimization problem:

$$
\begin{aligned}
\min_{K} \quad & \left[\left\{\int_{\triangle Z} q e_s(z)^2 dz\right\} + u_s' R u_s\right] \\
s.t. \quad & 0 = -\frac{\partial x_{1s}'}{\partial z} + Da(1 - x_{1s}')e^{\frac{x_{2s}'}{1 + x_{2s}'/\gamma}} \\
& 0 = -\frac{\partial x_{2s}'}{\partial z} + BDa(1 - x_{1s}')e^{\frac{x_{2s}'}{1 + x_{2s}'/\gamma}} + \beta_U(\chi_{w,n} - x_{2s}') + \beta_U \sum_{i=1}^{2} b_i(z) u_{is} \\
& x_{1s}'(0) = x_{1d}, \;\; x_{2s}'(0) = x_{2d} \\
& u_{i,s} = K_i \frac{\int_{\triangle Z_i} e_s(z) dz}{\triangle Z_i} \\
& u_i^{min} \leq u_{is} \leq u_i^{max}, \; i = 1, \cdots, m \\
& x_2^{min} \leq x_{2s}'(z) \leq x_2^{max} \forall \; z \in \triangle Z
\end{aligned}
\tag{5.37}
$$

where $K = [K_i]$, $i = 1, \cdots, m$, are the gains that multiply the error, $e_s(z) = x_{2s}' - x_{2s}$, where $x_{2s}$ is the 'unperturbed', open–loop steady-state profiles, $x_{2s}'$ is the closed–loop steady-state profiles, and $\triangle Z_i, i = 1, \cdots, m$ denote the subzones within the control zone, $x_{1d}$ and $x_{1d}$ represent the steady-state inlet concentration and temperature, respectively.

In the simulation results, the control zone is chosen to be $\triangle Z \in [0.04, 0.3]$ and divided into three subzones. The finite-difference method is used for the integration of the hyperbolic PDE with discretization in space $\delta z = 0.02$, and with explicit Newton integration in time with $\delta t = 0.0001$. The parameters in the objective function of Eq.5.37 were chosen as $q = 20$, $R = rI$, $r = 0.001$, $x_2^{max} = x_{2s} + 0.25$, $x_2^{min} = x_{2s} - 0.25$, $u^{min} = -2$ and $u^{max} = 2$. Figures 5.10–5.11 demonstrate that the controller successfully achieves state constraint satisfaction and drives the closed–loop state profile (dash-dotted lines) close to the desired state profile. Note that in the absence of control, the state constraints are violated in the presence of disturbance (see Figure 5.9).

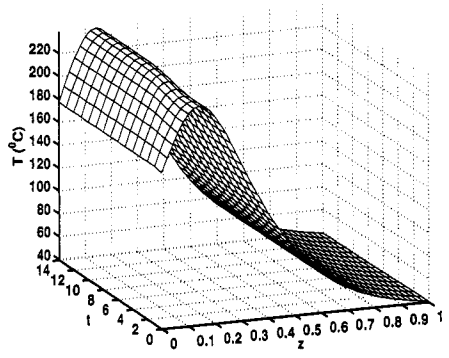


Figure 5.10: Closed–loop evolution of the temperature profile in the presence of disturbance.

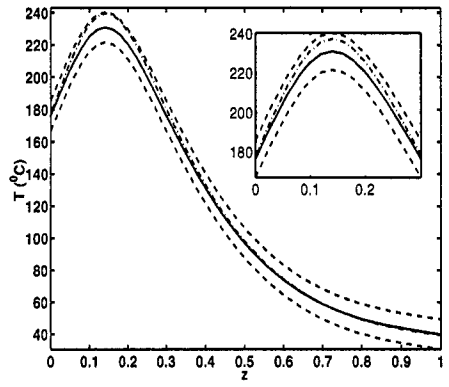


Figure 5.11: Steady state closed–loop profile (dash-dotted line) in the presence of disturbance.

## 5.4 Conclusions

This chapter focused on the development of computationally-efficient predictive control algorithms for nonlinear parabolic and hyperbolic PDEs with state and control constraints arising in the context of diffusion-reaction and convection-reaction processes, respectively. Specifically, we initially considered a diffusion-reaction process described by a nonlinear parabolic PDE and addressed the problem of stabilization of an unstable steady-state subject to input and state constraints. Galerkin's method was used to derive finite-dimensional systems that capture the dominant dynamics of the parabolic PDE, which were subsequently used for controller design. Various MPC formulations were constructed

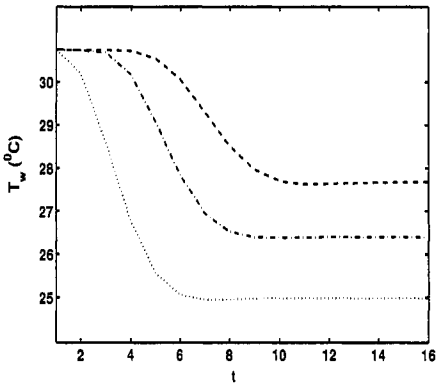


Figure 5.12: Dotted, dash-dotted, and dashed lines represent the evolution of the wall temperature, $T_{w,c}$, in the control zones 1, 2 and 3, respectively

on the basis of the finite dimensional approximations that differ in the way the evolution of the fast eigenmodes is accounted for in the performance objective and state constraints. The impact of these differences on the ability of the predictive controller to enforce state constraints satisfaction in the infinite-dimensional system was analyzed. The MPC formulations were applied, through simulation, to the problem of stabilizing an unstable steady-state of a nonlinear model of a diffusion-reaction process subject to state and control constraints. Finally, a predictive control scheme was developed for hyperbolic PDEs and applied to a convection-reaction process.

# Chapter 6

# Conclusions

Nonlinear distributed process systems abound in the modeling of semiconductor manufacturing processes, and chemical and biological systems and have attracted a great deal of attention in terms of analysis and control over the last ten years. Examples include temperature profile control in the Czochralski crystallization of high-purity crystals and deposition uniformity control in the chemical vapor deposition of thin films, as well as control of size distribution in the crystallization of proteins and the aerosol-based production of nanoparticles. From a control point of view, the distinguishing feature of complex distributed processes is that they give rise to nonlinear control problems that involve the regulation of highly distributed control variables by using spatially-distributed control actuators and measurement sensors. Thus, complex distributed processes cannot be effectively controlled with control methods which assume that the state, manipulated and to-be-controlled variables exhibit lumped behavior or with linear control algorithms derived on the basis of linear/linearized distributed models.

Motivated by these considerations, over the last decade, research has led to the development of a general framework for the synthesis of practically implementable nonlinear feedback controllers for complex distributed processes based on fundamental models that accurately predict their behavior. The approaches proposed in these works, however, do not address two important issues: a) the availability of actuation and sensing technologies

which make possible the use of large numbers of actuators and sensors to control spatially distributed processes, and b) the direct incorporation of state variables and manipulated input constraints in the controller design.

Motivated by the possibility of using finely spatially distributed actuation/sensing, the first part of this thesis focused on the extension of the traditional control formulation for spatially-distributed processes to an 'infinite sensing' - 'infinite actuation' formulation. Using an infinite-dimensional formulation for the actuator/sensor spaces, the control problem was formulated as the one of designing a feedback control system which provides the link between actuation and sensing, so that the closed-loop system exhibits the desirable spatio-temporal behavior. Under the assumption that the target complex spatio-temporal behavior is described by a "target nonlinear PDE", we used a combination of Galerkin's method and nonlinear control techniques to design nonlinear state and static output feedback controllers to address this problem. In addition to controller design, we provided lower-bounds on the number of actuators/sensors needed to enforce a given spatio-temporal behavior in the closed-loop system. We used several examples of diffusion-reaction processes to demonstrate the formulation of the control problem and the effectiveness of the proposed systematic approach to creating complex spatio-temporal behavior. Using these illustrative examples, we demonstrated that both (a) large number of actuators/sensors, and (b) nonlinear control laws are necessary to achieve this goal.

In the second part of the thesis, we focused on the development and application of predictive-based strategies for control of distributed processes with state and control constraints. The predictive control strategies were developed on the basis of lower-order ODE models obtained through application of appropriate order reduction techniques to the infinite-dimensional distributed models. To illustrate the design methodology, we considered transport-reaction processes, modeled by linear/nonlinear parabolic PDE systems with state and control constraints. The model predictive controller was designed on the basis of lower-order ODE models obtained through application of Galerkin's method

to the PDE system. Both input and state constraints are handled in the optimization problem; the input constraints directly as a bound of the feasible control input, while the state constraints are handled by being translated into appropriate constraints on the modal states of the low - order model. In order to account for the effect of both the slow and fast modes of the PDE in the cost function of the optimal control problem and the state constraints, we developed various MPC formulations which are distinct with respect to the number of modal states employed in the cost function and/or state constraints formulation. Namely, the number of modal states utilized in the cost function and number of modal states utilized in the state constraints may differ in the various MPC formulations which affects the performance of the proposed formulation and point out to trade-offs which are necessary to be made with respect to state constraints satisfaction and number of modal states accounted for in the formulation. We presented applications of the developed algorithms to several diffusion-reaction processes.

# Bibliography


[1] H. Aling, S. Benerjee, A. K. Bangia, V. Cole, J. Ebert, A. Emani-Naeini, K. F. Jensen, I. G. Kevrekidis, and S. Shvartsman. Nonlinear model reduction for simulation and control of rapid thermal processing. In *Proceedings of American Control Conference*, pages 2233–2238, Albuquerque, NM, 1997.

[2] F. Allgower and H. Chen. Nonlinear model predictive control schemes with guaranteed stability. In : R. Berber and C. Kravaris (Eds.), *NATO ASI on Nonlinear Model Based Process Control*, pages 465–494, Dordrecht: Kluwer, 1998.

[3] A. Armaou and P. D. Christofides. Finite-dimensional control of nonlinear parabolic pde systems with time-dependent spatial domains using empirical eigenfunctions. *Appl. Math. & Comp. Sci.*, **11**:287–317, 1999.

[4] A. Armaou and P. D. Christofides. Wave suppression by nonlinear finite-dimensional control. *Chem. Eng. Sci.*, 55:2627–2640, 2000.

[5] A. Armaou and P. D. Christofides. Dynamic optimization of dissipative PDE systems using nonlinear order reduction. *Chem. Eng. Sci.*, 57:5083–5114, 2002.

[6] Bamieh B., F. Paganini, and M. A. Dahleh. Distributed control of spatially invariant systems. *IEEE Trans. Autom. Contr.*, 47:1091–1107, 2002.

[7] J. Baker and P. D. Christofides. Finite dimensional approximation and control of nonlinear parabolic PDE systems. *Int. J. Contr.*, 73:439–456, 2000.

[8] M. J. Balas. Feedback control of linear diffusion processes. *Int. J. Contr.*, 29:523–533, 1979.

[9] A. K. Bangia, P. F. Batcho, I. G. Kevrekidis, and G. E. Karniadakis. Unsteady 2-D flows in complex geometries: Comparative bifurcation studies with global eigenfunction expansion. *SIAM J. Sci. Comp.*, 18:775–805, 1997.

[10] A. Bemporad and M. Morari. Robust model predictive control: A survey. In : A. Garulli, A. Tesi and A. Vicino (Eds.), *Robustness in Identification and Control, Lecture Notes in Control and Information Sciences* vol. 245, pages 207–266, Berlin: Springer, 1999.

[11] D. M. Boskovic and M. Kristc. Backstepping control of chemical tubular reactors. *Comp. & Chem. Eng.*, 26:1077–1085, 2002.

[12] J. A. Burns and B. B. King. A reduced basis approach to the design of low-order feedback controllers for nonlinear continuous systems. *Journal of Vibration and Control*, 4:297–323, 1998.

[13] C. I. Byrnes, I. G. Lauko, D. S. Gilliam, and V. I. Shubov. Output regulation for linear distributed parameter systems. *IEEE Trans. Autom. Contr.*, 2:170–194, 2000.

[14] P. D. Christofides. *Nonlinear and Robust Control of PDE Systems: Methods and Applications to Transport-Reaction Processes.* Birkhäuser, Boston, 2001.

[15] P. D. Christofides and J. Baker. Robust output feedback control of quasi-linear parabolic PDE systems. *Syst. & Contr. Lett.*, 36:307–316, 1999.

[16] P. D. Christofides and P. Daoutidis. Finite-dimensional control of parabolic PDE systems using approximate inertial manifolds. *J. Math. Anal. Appl.*, 216:398–420, 1997.

[17] P. D. Christofides and P. Daoutidis. Finite-dimensional control of parabolic PDE systems using approximate inertial manifolds. *J. Math. Anal. Appl.*, 216:398–420, 1997.

[18] R. F. Curtain. Finite-dimensional compensator design for parabolic distributed systems with point sensors and boundary input. *IEEE Trans. Automat. Contr.*, 27:98–104, 1982.

[19] R. F. Curtain and A. J. Pritchard. *Functional Analysis in Modern Applied Mathematics*, volume 132 of *Mathematics in Science and Engineering*. Academic Press, New York, New York, 1977.

[20] R. F. Curtain and A. J. Pritchard. *Infinite dimensional linear systems theory*, volume 9 of *Lecture Notes in Control and Information Sciences*. Springer-Verlag, Berlin, Germany, 1978.

[21] M. A. Demetriou. Numerical investigation on optimal actuator/sensor location of parabolic pde's. In *Proceedings of the 1999 American Control Conference*, pages 1722–1726, San Diego, CA, 1999.

[22] M. A. Demetriou and N. Kazantzis. A new actuator activation policy for performance enhancement of controlled diffusion processes. *Automatica*, 40:415–421, 2004.

[23] S. Dubljevic, N. H. El-Farra, P. Mhaskar, and P. D. Christofides. Predictive control of parabolic PDEs with state and control constraints. *IEEE Trans. Automat. Contr.*, provisionaly accepted, 2005.

[24] P. Dufour, Y. Touré, D. Blanc, and P. Laurent. On nonlinear distributed parameter model predictive control strategy: on-line calculation time reduction and application to an experimental drying process. *Comp. & Chem. Eng.*, 27:1533–1542, 2003.

[25] C.G. Economou, M. Morari, and B. Pallsson. Internal model control: 5. Extension to nonlinear systems. *Ind. Eng. Chem. Processs Des. Dev.*, **25**:403, 1986.

[26] N. H. El-Farra, A. Armaou, and P.D. Christofides. Analysis and control of parabolic PDE systems with input constraints. *Automatica*, 39:715–725, 2003.

[27] N. H. El-Farra, P. Mhaskar, and P. D. Christofides. Uniting bounded control and MPC for stabilization of constrained linear systems. *Automatica*, 40:101–110, 2004.

[28] C. Foias, M.S. Jolly, I.G. Kevrekidis, G.R. Sell, and E.S. Titi. On the computation of inertial manifolds. *Phys. Lett. A*, 131:433–437, 1989.

[29] C. Foias, G.R. Sell, and E.S. Titi. Exponential tracking and approximation of inertial manifolds for dissipative equations. *J. Dynamics and Differential Equations*, 1:199–244, 1989.

[30] B. A. Francis. Linear multivariable regulator problem. *SIAM J. Contr. & Optim.*, 15:486–505, 1977.

[31] B. A. Francis and W. M. Wonham. The internal model principle for linear multivariable regulators. *Appl. Math. & Optim.*, 2:170–194, 1975.

[32] K. Fukunaga. *Introduction to Statistical Pattern Recognition.* Academic Press, San Diego, USA, 1990.

[33] Papathanasiou A. G., J. Wolff, I. G. Kevrekidis, H. H. Rotermund, and G. Ertl. Some twists and turns in the path of improving surface activity. *Chemical Physics Letters*, 358:407–412, 2002.

[34] C.E. Garcia and M. Morari. Internal model control:1. A unifying review and some new results. *Ind. Eng. Chem. Process Des. Dev.*, **21**:308, 1982.

[35] C.E. Garcia, D.M. Prett, and M. Morari. Model predictive control: Theory and practice - a survey. *Automatica*, **25**:335–348, 1989.

[36] M. D. Graham and I. G. Kevrekidis. Alternative approaches to the Karhunen-Loève decomposition for model reduction and data analysis. *Comp. & Chem. Eng.*, 20:495–506, 1996.

[37] M.A. Henson and D. E. Seborg. An internal model control strategy for nonlinear systems. *AIChE J.*, **37**:1065–1081, 1993.

[38] C. M. Ho and Y. C. Tai. Micro-electro-mechanical-systems (MEMS) and fluid flows. *Ann. Rev. Fluid Mech.*, 30:579–612, 1998.

[39] B.R. Holt and M. Morari. Design of resilient processing plants V. The effect of deadtime on dynamic resilience. *Chemical Engineering Science*, **40**:1229–1237, 1985.

[40] K. Ito and K. Kunisch. Receding horizon optimal control for infinite dimensional systems. *ESIAM: Control, Optimization and Calculus of Variations*, 8:741–760, 2002.

[41] Wolff J., A. G. Papathanasiou, I. G. Kevrekidis, H. H. Rotermund, and G. Ertl. Spatiotemporal addressing of surface activity. *Science*, 294:134–137, 2001.

[42] Wolff J., A. G. Papathanasiou, H.H. Rotermund, G. Ertl, X. Li, and I. G. Kevrekidis. Local manipulation of catalytic surface reactivity. *Journal of catalysis*, 216, 2003.

[43] N. Mahadevan and K. A. Hoo. Wavelet-based model reduction of distributed parameter systems. *Chemical Engineering Science*, 55:4271–4290, 2000.

[44] N. Mahadevan, K. A. Hoo, and K. Adzievski. Model reduction and control of a class of distributed parameter processes. In *Proceedings of American Control Conference*, pages 1593–1597, San Diego, CA, 1999.

[45] D. Q. Mayne, J. B. Rawlings, C. V. Rao, and P. O. M. Scokaert. Constrained model predictive control: Stability and optimality. *Automatica*, 36:789–814, 2000.

[46] H. Michalska and D. Q. Mayne. Robust receding horizon control of constrained nonlinear systems. *IEEE Trans. Auto. Contr.*, AC-38:1623, 1993.

[47] A. Palazoglu and A. Karakas. Control of nonlinear distributed parameter systems using generalized invariants. *Automatica*, 36:697–703, 2000.

[48] H. M. Park and D.H. Cho. The use of the Karhunen-Loeve decomposition for the modeling of distributed parameter systems. *Chem. Eng. Sci.*, 51:81–98, 1996.

[49] J. B. Rawlings. Tutorial overview of model predictive control. *IEEE Control Systems Magazine*, 20:38–52, 2000.

[50] W. H. Ray. *Advanced Process Control.* McGraw-Hill, New York, 1981.

[51] J. Richalet, A. Rault, J.L. Testud, and J. Papon. Model predictive heuristic control:aplication to industrial processes. *Automatica*, **14**:413–428, 1978.

[52] F. Riesz and B. Sz.-Nagy. *Functional analysis.* Dover Publications, New York, U.S.A., 1990.

[53] S. Y. Shvartsman and I. G. Kevrekidis. Nonlinear model reduction for control of distributed parameter systems: A computer assisted study. *AIChE J.*, 44:1579–1595, 1998.

[54] L. Sirovich. Turbulence and the dynamics of coherent structures: part i: Coherent structures. *Quart. Appl. Math.*, XLV:561–590, 1987.

[55] L. Sirovich. Turbulence and the dynamics of coherent structures: part ii: Symmetries and transformations. *Quart. Appl. Math.*, XLV:573–582, 1987.

[56] L. Sirovich. Turbulence and the dynamics of coherent structures: part iii: Dynamics and scalling. *Quart. Appl. Math.*, XLV:583–590, 1987.

[57] A. Smyshlyaev and M. Krstic. Explicit formulae for boundary control of parabolic PDEs. *Lecture Notes In Control & Information Sciences*, 301:231–249, 2004.

[58] R. Temam. *Infinite-Dimensional Dynamical Systems in Mechanics and Physics.* Springer-Verlag, New York, 1988.

[59] A. Theodoropoulou, R. Adomaitis, and E. Zafiriou. Model reduction for optimization of rapid thermal chemical vapor deposition systems. *IEEE Trans. Sem. Manuf.*, **11**:85–98, 1998.

[60] A. Theodoropoulou, R. Adomaitis, and E. Zafiriou. Inverse model based real-time control for temperature uniformity of rtcvd. *IEEE Trans. Sem. Manuf.*, **12**:87–101, 1999.

[61] Justh E. W. and P. S. Krishnaprasad. Pattern-forming systems for control of large arrays of actuators. *J. Nonlinear Sci.*, 11:239–277, 2001.

[62] E. B. Ydstie and A. A. Alonso. Process systems and passivity via the Clausius-Planck inequality. *Syst. & Contr. Lett.*, 30:253–264, 1997.